Stony Brook University

OFFICIAL COPY

The official electronic file of this thesis or dissertation is maintained by the University Libraries on behalf of The Graduate School at Stony Brook University.

© All Rights Reserved by Author.

Understanding Structure and Response in Thermally Responsive Block Copolymer Assemblies

A Dissertation Presented

by

Zhe Sun

to

The Graduate School

in Partial Fulfillment of the

Requirements

for the Degree of

Doctor of Philosophy

in

Chemistry

Stony Brook University

August 2016

Stony Brook University

The Graduate School

Zhe Sun

We, the dissertation committee for the above candidate for the

Doctor of Philosophy degree, hereby recommend

acceptance of this dissertation.

Robert B. Grubbs – Dissertation Advisor
Associate Professor of the Chemistry Department

Stephen A. Koch - Chairperson of Defense
Professor of the Chemistry Department

Benjamin S. Hsiao – Third Member
Distinguished Professor of the Chemistry Department

Agostino Pietrangelo– Outside Member
Assistant Professor of the Chemistry Department
Rutgers University-Newark

This dissertation is accepted by the Graduate School

Nancy Goroff

Interim Dean of the Graduate School

Abstract of the Dissertation

Understanding Structure and Response in Thermally Responsive Block Copolymer Assemblies

by

Zhe Sun

Doctor of Philosophy

in

Chemistry

Stony Brook University

2016

There has been considerable and growing interest in the field of stimulus-responsive polymers over the last two decades, as they can be exploited in many applications including biomedicine, sensing, and separations. Temperature remains the most extensively investigated physical stimulus due to its ease of application and monitoring. In this dissertation, a new class of thermally responsive ABC poly(ethylene oxide)-*block*-poly(*N*,*N*-diethylacrylamide)-*block*-poly(*N*,*N*-dibutylacrylamide) (PEO-*b*-PDEAm-*b*-PDBAm) triblock copolymers has been synthesized by reversible addition−fragmentation chain-transfer (RAFT) polymerization. In aqueous solution, PEO-*b*-PDEAm-*b*-PDBAm copolymers self-assemble into a wide range of different aggregated structures including spherical micelles, cylindrical micelles, vesicles and large compound micelles. The precise morphology mainly depends on the relative volume fractions of the hydrophilic and hydrophobic blocks. The fast rate (within 10 minutes) of reversible thermally induced change in triblock copolymer morphologies was confirmed by dynamic light

scattering (DLS) and transmission electron microscopy (TEM). The enhanced rate further supports the hypothesis that the absence of strong interchain hydrogen bonding in the central thermally responsive block will accelerate the rearrangement. Moreover, we also designed a novel rapidly reversible thermoresponsive ABC triblock copolymer worm gel, resulting from a sphere-to-worm transition at temperatures above the lower critical solution temperature (LCST) of the PDEAm block. A preliminary experiment was also conducted, confirming the successful encapsulation of a hydrophilic dye Rhodamine B into the large compound micelles formed upon heating.

Table of Contents

List of Figures

List of Tables

List of Abbreviations

AIBN	2 2'-azobis(2-methylpropionitrile)
Boc	t-Butyloxycarbonyl
DCC	*N*, *N*-Dicyclohexylcarbodiimide
DBA	*N*, *N*-Dibutylacrylamide
DEA	*N*, *N*-Diethylacrylamide
DLS	Dynamic light scattering
DMF	*N*, *N*-Dimethylformamide
EDC	1-(3-Dimethylaminopropyl)-3-ethylcarbodiimide
GPC	Gel permeation chromatography
LCST	Lower critical solution temperature
MWCO	Molecular weight cutoff
NASI	*N*-Acryloxysuccinimide
NHS	*N*-Hydroxysuccinimide
NMR	Nuclear magnetic resonance
PDBAm	Poly(*N*,*N*-dibutylacrylamide)
PDEAm	Poly(*N*,*N*-diethylacrylamide)

PEO	Poly(ethylene oxide)
PLA	Poly(lactic acid)
RAFT	Reversible addition−fragmentation chain-transfer
SAXS	Small angle X-ray scattering
SEC	Size exclusion chromatography
TEM	Transmission electron microscopy
UCST	Upper critical solution temperature

Acknowledgments

I would like to thank everyone who helped me during my Ph.D. study.

First, I want to thank my research advisor, Professor Robert B. Grubbs, for the opportunity of working in his lab, which enabled me to learn a lot of aspects of polymer chemistry. Without his guidance, support, and encouragement, the work presented here could not have been done. I would also like to thank my thesis committee, Professor Stephen Koch, Professor Benjamin Hsiao and Professor Agostino Pietrangelo for spending their valuable time reviewing my thesis and attending my defense.

I am grateful to the following individuals: Dr. Ye Tian at the CFN, BNL, for helping me in the TEM experiment; Professor Surita Bhatia and her student Wendy Hom, for rheology experiment and data analysis; Dr. James Marecek, for NMR training and troubleshooting.

I would like to acknowledge the past and present members of the RBG group for always being helpful, friendly. Special thanks go to Dr. Yu Cai, Dr. Tianyuan Wu, Dr. Bingyin Jiang, Dr. Anna Flach, Daniel Yi, Deokkyu Choi, Menglan Jiang, Bing Qian, Fengyang Shih and David Hewitt.

Finally, I owe the greatest thanks to my parents for their continual love, support, and encouragement during my Ph.D. study.

Chapter 1 General Introduction

1.1 Stimuli-responsive polymers (smart polymers)

There has been considerable and growing interest in the field of stimulus-responsive polymers, as they can be exploited in many applications including bioconjugate chemistry, biomedicine, sensors, molecular actuators, and separation technology.[1-12] Stimuli-responsive polymers, often referred to as "smart" polymers, can respond to different external stimuli (Figure 1-1) including physical stimuli (temperature[11, 13-15], light[16-20], magnetic[21-22] and electrical[23]), chemical stimuli (pH[24-26], redox[27-29] and solvent[30-31]) and biological stimuli (glucose[32-33] and enzymes[34-35]).[36]

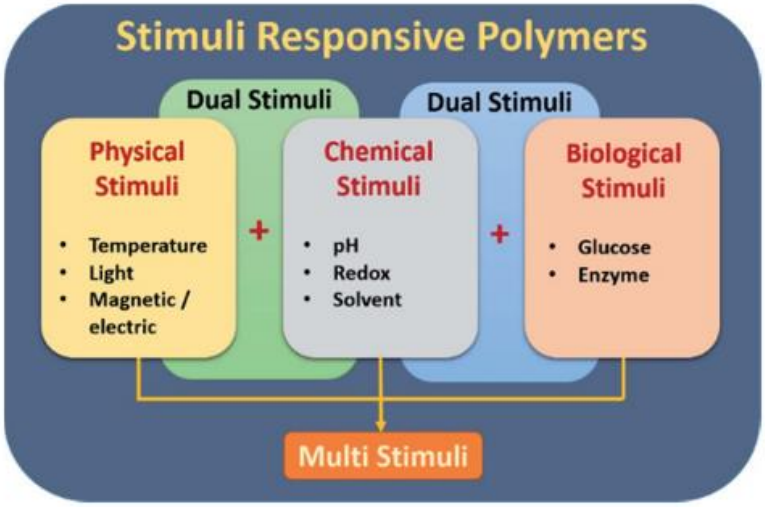

Figure 1-1. Classification of stimuli-responsive polymers. Reprinted from reference[36], with permission from Royal Society of Chemistry.

These stimuli-responsive polymers are capable of forming different nanostructured architectures including two dimensional thin films (homopolymer brush, mixed brush, layer-by-layer film, hybrid film/brush, crosslinked film and membrane) and three dimensional colloidal nanoparticles (micelle, nanogel, capsule, core-shell particle, core-hybrid shell particle, Pickering emulsion and other aggregates) , depending on their phase behaviors as shown in Figure 1-2. [12]

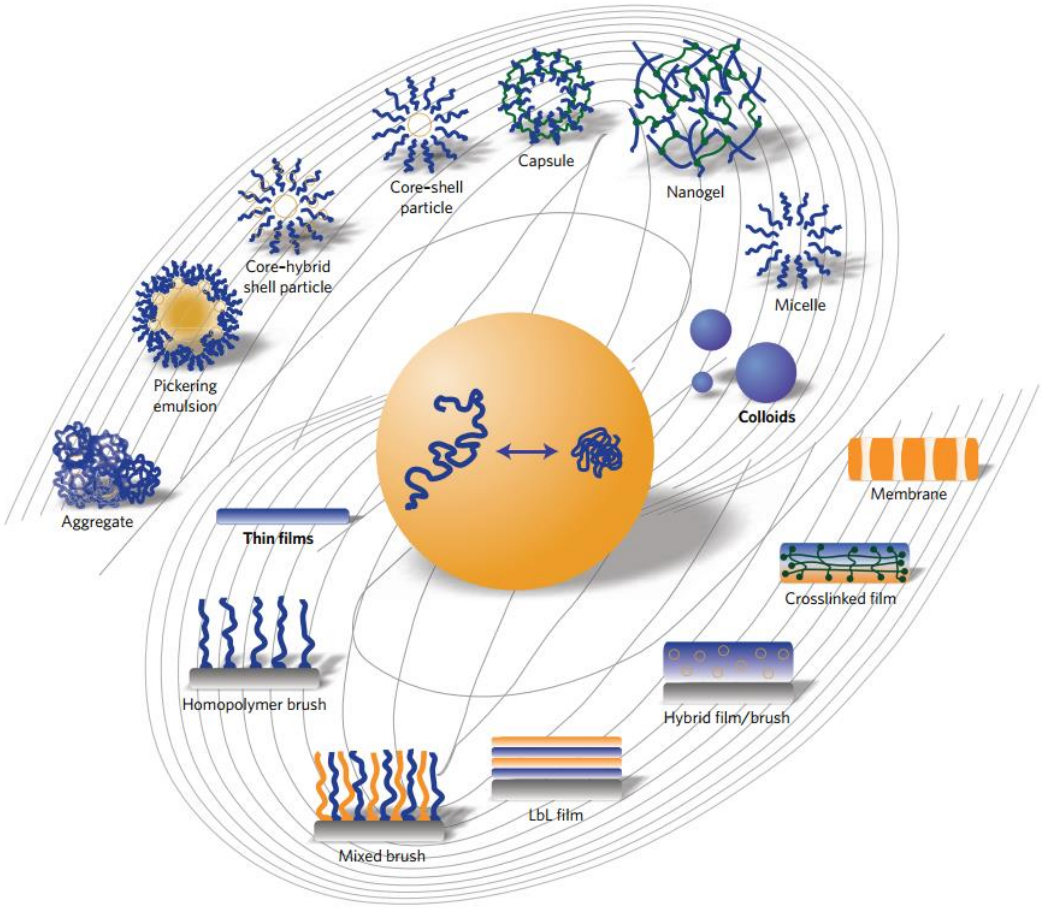

Figure 1-2. 'Galaxy' of nanostructured stimuli-responsive polymer materials. Reprinted from reference[12], with permission from Nature Publishing Group.

1.2 Thermally responsive polymers

Thermally responsive polymers that can respond to temperature are one of the most studied stimuli-responsive polymers. Figure 1-3 shows that thermally responsive polymers, which become insoluble upon heating, have a so-called LCST (lower critical solution temperature); polymers which become soluble upon heating, have a UCST (upper critical solution temperature).[37] LCST and UCST behavior are not restricted to aqueous environments, but the aqueous systems are of particular interest since water is inexpensive, environmentally benign and biologically relevant.

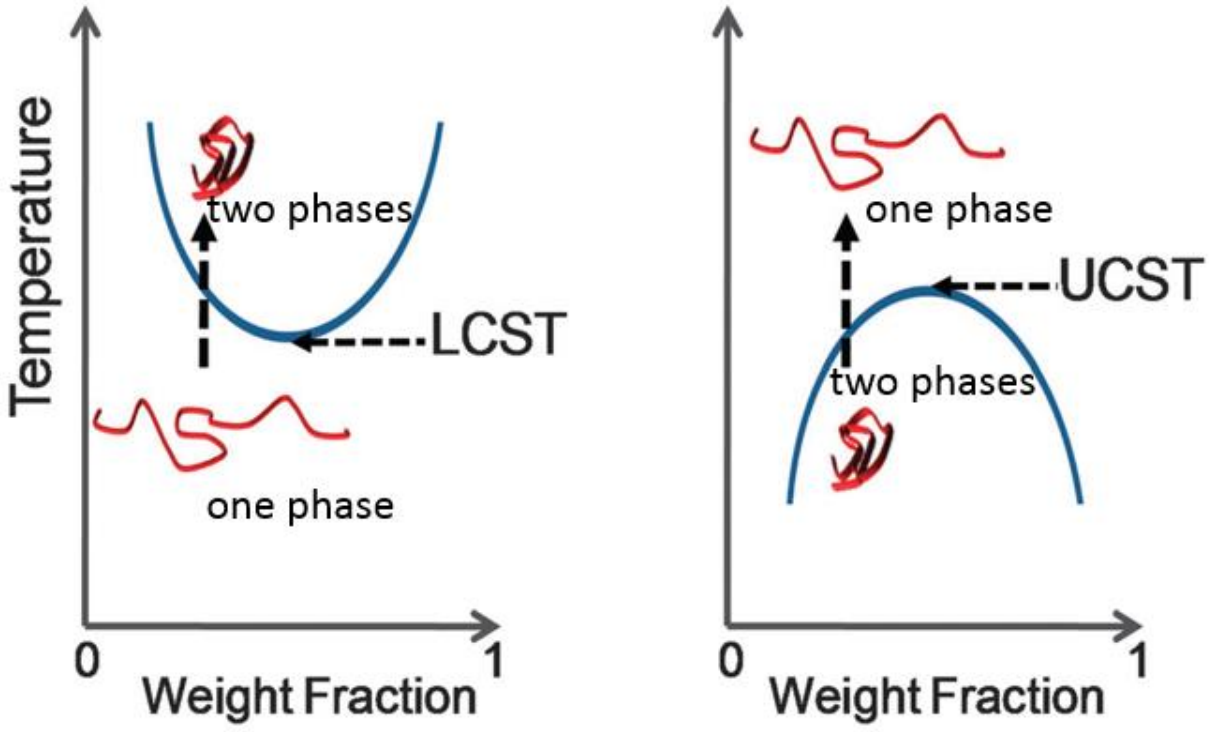

Figure 1-3. Phase transitions associated with LCST and UCST behavior. Adapted from reference[37], with permission from Royal Society of Chemistry.

The majority of thermally responsive polymers display an LCST-type transition in aqueous solution.[38] Poly(*N*-isopropylacrylamide) (PNIPAM) with a reported LCST in water around 32 °C, has been the most studied LCST-type thermally responsive polymer in bioapplications, because not only is the LCST of PNIPAM in the physiological range of body temperature but also its LCST is relatively insensitive to environmental conditions.[39-41] Many studies have shown that the critical solution temperature depends on the concentration, molecular weight and tacticity of the polymers. Additives and salt can also influence this transition temperature.[42] Below the LCST, PNIPAM is soluble in aqueous solution because of strong hydrogen bonding interaction with the surrounding water molecules. Upon heating, hydrogen bonding with water is weakened, but intra- and intermolecular hydrogen bonding/hydrophobic interactions become the dominating forces, which results in insolubility in water. The LCST is quite widespread for polymers that contain hydrogen bonding with water molecules and the related polymer used in this thesis, poly(*N*, *N*-diethylacrylamide) (PDEAm), also exhibits an LCST although with a much broader range of 29–33 °C.[42-44] Amongst the other important polymers in this class (Figure 1-4) are poly(*N*-vinylcaprolactam) (PVCL), poly(ethylene glycol) (PEG) or poly(ethylene oxide) (PEO) and poly(propylene oxide) (PPO).[38]

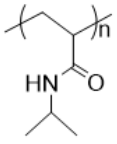

LCST ≈ 32 °C

Poly(*N*-isopropylacrylamide) (PNIPAM)

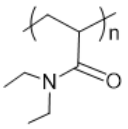

LCST ≈ 33 °C

Poly(*N*,*N*-diethylacrylamide) (PDEAM)

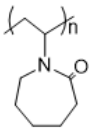

LCST ≈ 32 °C

Poly(*N*-vinylcaprolactam) (PVCL)

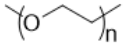

LCST ≈ 85 °C

Poly(ethylene oxide) (PEO)
Poly(ethylene glycol) (PEG)

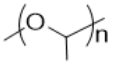

LCST ≈ 0-50 °C (M.W. 1000-400 g/mol)

Poly(propylene oxide) (PPO)
Poly(propylene glycol) (PPG)

Figure 1-4. Structures of commonly used LCST-type thermally responsive polymer systems.

Poly(*N*-vinylcaprolactam) (PVCL) is hydrophilic and water soluble at room temperature, becoming hydrophobic and insoluble around 32 °C .[45] Poly(ethylene oxide) (PEO) polymers are highly soluble in water up to temperature of around 85 °C, while poly(propylene oxide) (PPO) is hydrophobic, but co-polymers of these two materials can be prepared with a wide range of solubility and phase transition temperatures. A large number of PEO and PPO block co-polymers known as Pluronics, Poloxamers and Tetronics are commercially available and exhibit phase transitions varying from 20 °C to 85 °C.[46]

On the other hand, only a small number of UCST-type thermally responsive polymers involving phase separation upon cooling have been reported compared to their LCST counterparts. Most studies on UCST-type polymers have focused on zwitterionic (charged) polymers with a UCST sensitive to electrolytes (ions), which limits their potential utility in bioapplications. In recent years, progress has been made on the discovery of some uncharged UCST-type thermal responsive polymers, for example, poly(methacrylamide) and poly(*N*-acryloylasparaginamide) (PNAAAM),[47-48] whose thermal sensitivity is not affected significantly by the presence of ions and salts, thereby making them more suitable for biomedical applications.

1.3 Self-assemblies of amphiphilic copolymers

It is well-known that amphiphilic block copolymers are able to self-assemble into a wide range of different aggregated structures in water, including spherical micelles, cylindrical micelles, vesicles and large compound micelles.[49-58] The precise morphologies of these self-assembled block copolymers mainly depends on the relative volume fractions of the hydrophilic and hydrophobic

blocks and the interfacial energy associated with the block junction.[59-60] The morphology of these self-assemblies can be predicted by the packing parameter, p, which is defined in Equation 1-1 below

$$p = \frac{v}{al} \qquad (1\text{-}1)$$

Where v is the volume of the hydrophobic block, a is the effective interfacial area of the block junction, and l is the length of the hydrophobic block. For a given molecule, the packing parameter can be used to predict its most likely self-assembled morphology. As a general rule, spherical micelles are formed when $p \leq 1/3$, cylindrical micelles when $1/3 \leq p \leq 1/2$, and enclosed membrane structures (vesicles, also known as polymersomes) when $1/2 \leq p \leq 1$ (Figure 1).[59]

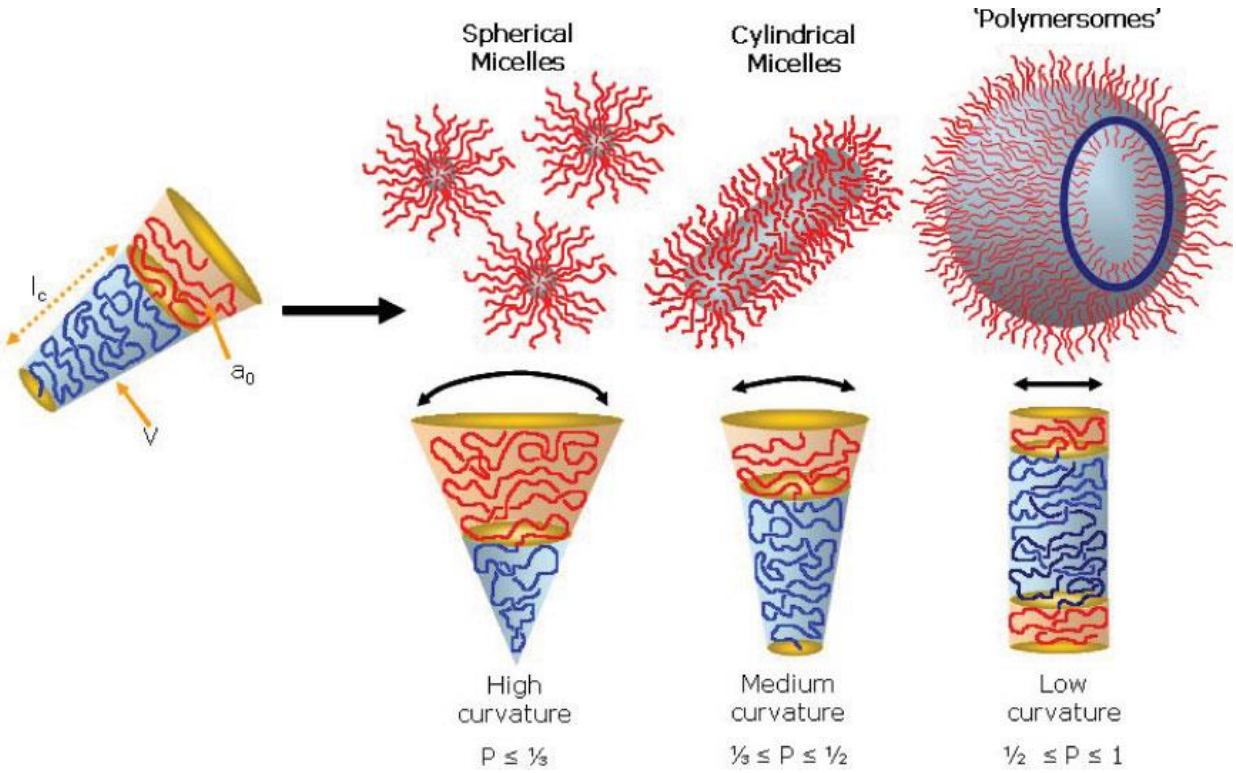

Figure 1-5. Various self-assembled structures formed by amphiphilic block copolymers in a block-selective solvent. The type of structure formed is due to the inherent curvature of the molecule,

which can be estimated through calculation of its dimensionless packing parameter, *p*. Reprinted from reference[59], with permission from John Wiley & Sons.

Recently, Discher and Ahmed reported a simplified model to predict the morphology of amphiphilic block copolymer assemblies, using the hydrophilic mass fraction *f*. On the basis of many investigated amphiphilic block copolymers, one unifying rule (or at least a starting point) for formation of vesicles in water is the ratio of hydrophilic to total mass (25 %< f < 40%). Polymers with f > 50 % can be expected to form micelles, 40 %< f < 50% form wormlike micelles and f < 25% form inverted microstructures.[61]

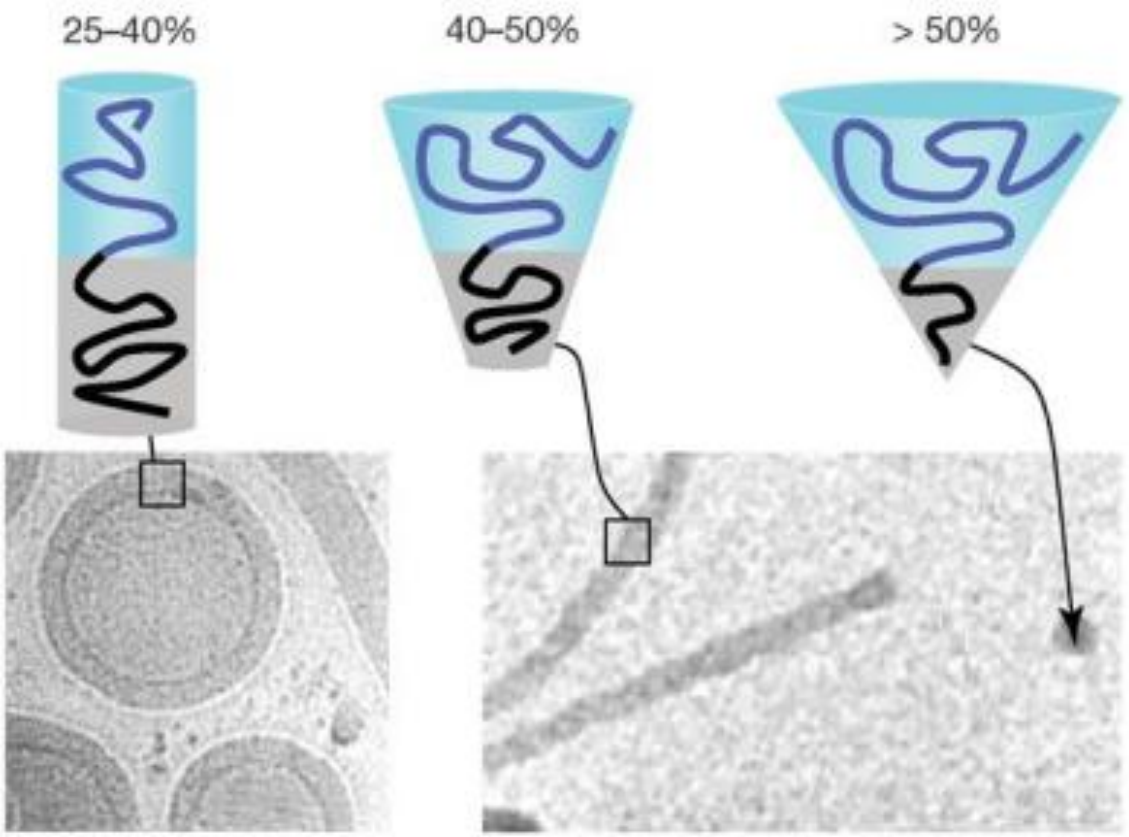

Figure 1-6. Schematics of block copolymer fractions with respective cryogenic transmission electron microscopy images showing vesicles or worm micelles and spherical micelles. Reprinted from reference[61], with permission from Annual Reviews.

1.4 Controlled/Living Radical Polymerization

A controlled/living radical polymerization (CRP/LRP) is a free-radical polymerization displaying living character in that the occurrence of typical radical termination and transfer reactions is minimized. Like conventional radical polymerization (RP), controlled/living radical polymerizations proceed via the same radical mechanism comprised of initiation, propagation, transfer, and termination steps. It can be exploited to polymerize a similar range of monomers. However, there are some significant advantages in controlled/living radical polymerization (CRP/LRP), for example, faster initiation, longer lifetime of growing chains with slower termination rate and near instantaneous growth of all chains, which are able to provide control over the molecular weight and the molecular weight distribution of polymerization.[62-63]

1.5 Reversible Addition-Fragmentation Chain Transfer polymerization

A number of CRP methods including nitroxide-mediated polymerization (NMP)[64], atom transfer radical polymerization (ATRP)[65], and reversible addition-fragmentation-chain transfer (RAFT) polymerization[66-68] have been developed. Among these controlled/living polymerization techniques, RAFT polymerization is one of the most powerful synthetic tools for polymer chemists because of tolerance to a wide range of functional groups (e.g. –OH, -COOH, -$CONR_2$). In

addition, it is compatible with both organic solution and aqueous solution, and can be used over a wide temperature range (20-150 ˚C).

Reversible addition-fragmentation-chain transfer (RAFT) polymerization, first introduced by Moad and Thang in 1998,[66] proceeds via a degenerative transfer process and relies on the use of RAFT chain-transfer agents (CTAs) which possess a thiocarbonylthio moiety.

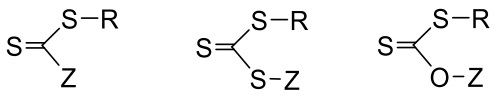

The R group initiates the growth of polymeric chains, and the Z group activates the thiocarbonyl bond towards radical addition and stabilizes the resultant adduct radical.

The generally accepted mechanism for a RAFT polymerization is shown in Figure 1-6. It starts with an initiator-derived radical (I·) that reacts with monomer (M) to give a polymeric radical (P_m·) (Step I Initiation). And then P_m· reacts with the RAFT CTA agent **1** after which the intermediate radical **2** fragments to give the RAFT macro-RAFT agent **3** and the reinitiating radical (R·)(Step ii Initial equilibrium). Following re-initiation, polymer chains grow by adding monomer (Step iii Reinitiation), and they rapidly exchange between existing growing radicals and the species capped with a thiocarbonylthio group (Step iv Main equilibrium). In the end, as in conventional radical polymerization, termination reactions can still occur with low frequency via combination or disproportionation mechanisms (Step v Termination).

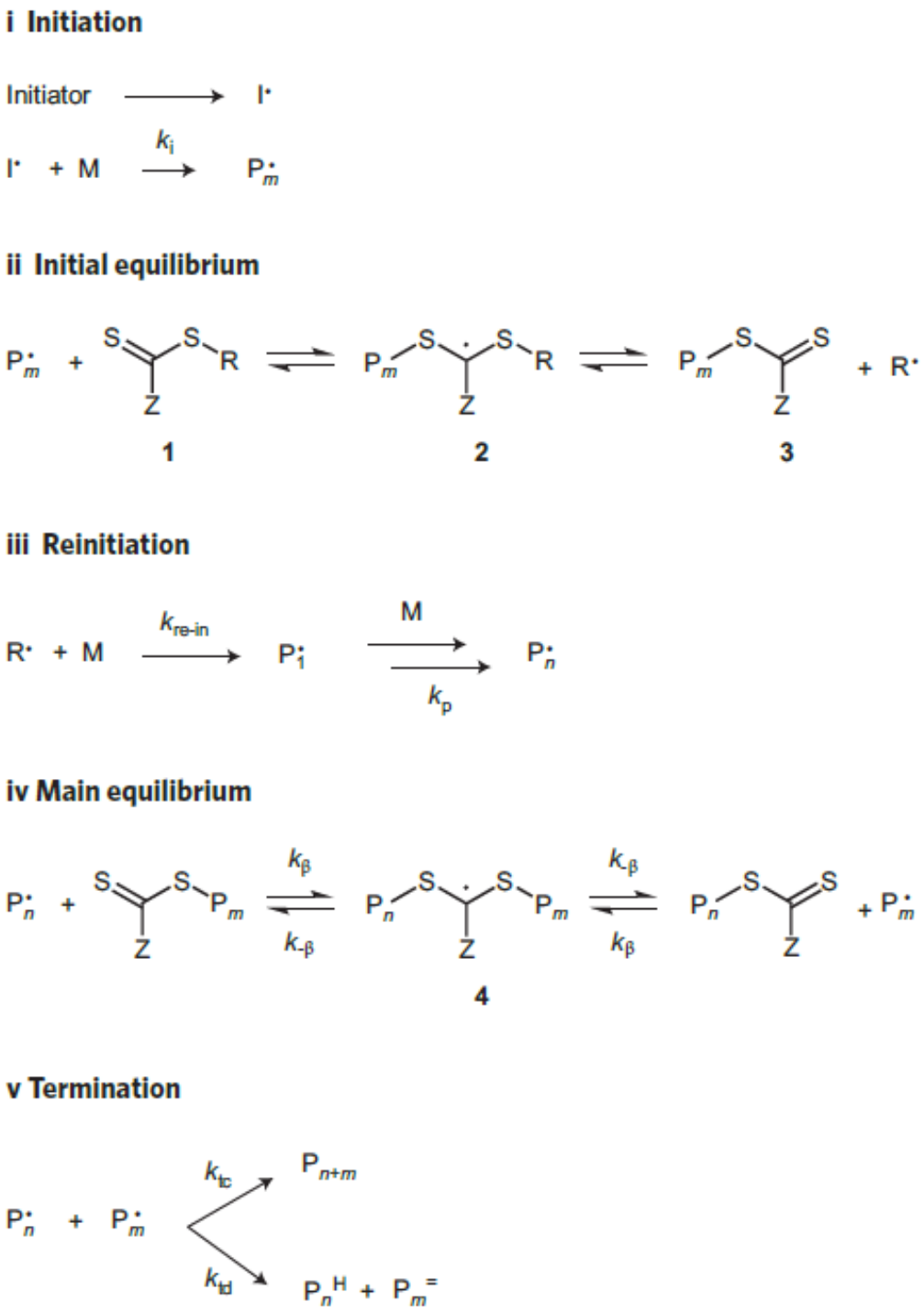

Figure 1-7. Generally accepted mechanism for RAFT polymerization. Reprinted from reference[69], with permission from Nature Publishing Group.

1.6 Scope of the Thesis

The research in this thesis was focused on the synthesis and characterization of thermally responsive ABC triblock copolymers, as well as their self-assembly in aqueous solution at 25 °C and higher temperature above the lower critical solution temperature (LCST) of the thermally responsive block.

Chapter 2 describes the use of reversible addition-fragmentation-chain transfer (RAFT) polymerization to synthesize a new class of thermally responsive ABC triblock copolymers, poly(ethylene oxide)-*block*-poly(*N*,*N*-diethylacrylamide)-*block*-poly(*N*,*N*-dibutylacrylamide) (PEO-*b*-PDEAm-*b*-PDBAm). A series of triblock copolymers with different block lengths has been synthesized and characterized by proton nuclear magnetic resonance (^{1}HNMR) and gel permeation chromatography (GPC).

Chapter 3 describes on the formation of nanostructures from the self-assembly of PEO-*b*-PDEAm-*b*-PDBAm triblock copolymers with different hydrophilic/hydrophobic block ratios in water. Dynamic light scattering (DLS) and transmission electron microscopy (TEM) were used to characterize the size and morphologies of these nanostructures at 25 °C and higher temperature above the LCST of thermally responsive PDEAm block. Moreover, at a higher polymer concentration of 5.0 w/w%, the PEO_{45}-*b*-$PDEAm_{41}$-*b*-$PDBAm_{12}$ polymer solution was found to form a free-standing physical gel after heating at 55 °C for 10 min due to a thermally induced sphere-to-worm transition and interworm entanglements, as confirmed and characterized by rheology. In contrast, the PEO_{45}-*b*-$PDEAm_{89}$-*b*-$PDBAm_{12}$ copolymer solution was found to undergo phase separation after heating at 55 °C for 10 min as a result of sedimentation of large compound micelles. A preliminary experiment was also conducted, confirming the successful

encapsulation of a hydrophilic dye Rhodamine B into the large compound micelles formed by PEO_{45}-*b*-$PDEAm_{89}$-*b*-$PDBAm_{13}$ upon heating.

Chapter 4 describes the attempted synthesis of a nonlinear tri-arm poly(ethylene oxide)-*block*-poly(*N*,*N*-diethylacrylamide)-*block*-polylactide (PEO-*b*-PDEAm-*b*-PLA). However, we have some problems about the characterization of the targeted tri-arm star block polymers.

Chapter 5 contains conclusions and suggestions for future work.

References (Chapter 1)

1. Wei, H.; Cheng, S. X.; Zhang, X. Z.; Zhuo, R. X., Thermo-sensitive polymeric micelles based on poly(N-isopropylacrylamide) as drug carriers. *Prog. Polym. Sci.* **2009,** *34* (9), 893-910. (doi: 10.1016/j.progpolymsci.2009.05.002)

2. Pietsch, C.; Hoogenboom, R.; Schubert, U. S., PMMA based soluble polymeric temperature sensors based on UCST transition and solvatochromic dyes. *Polymer Chemistry* **2010,** *1* (7), 1005-1008. (doi: 10.1039/c0py00162g)

3. Pietsch, C.; Hoogenboom, R.; Schubert, U. S., Soluble polymeric dual sensor for temperature and pH value. *Angew. Chem. Int. Ed. Engl.* **2009,** *48* (31), 5653-5656. (doi: 10.1002/anie.200901071)

4. Uchiyama, S.; Kawai, N.; de Silva, A. P.; Iwai, K., Fluorescent polymeric AND logic gate with temperature and pH as inputs. *J. Am. Chem. Soc.* **2004,** *126* (10), 3032-3033. (doi: 10.1021/ja039697p)

5. de Las Heras Alarcon, C.; Pennadam, S.; Alexander, C., Stimuli responsive polymers for biomedical applications. *Chem. Soc. Rev.* **2005,** *34* (3), 276-285. (doi: 10.1039/b406727d)

6. Ganta, S.; Devalapally, H.; Shahiwala, A.; Amiji, M., A review of stimuli-responsive nanocarriers for drug and gene delivery. *J Control Release* **2008,** *126* (3), 187-204. (doi: 10.1016/j.jconrel.2007.12.017)

7. Gil, E. S.; Hudson, S. M., Stimuli-reponsive polymers and their bioconjugates. *Prog. Polym. Sci.* **2004,** *29* (12), 1173-1222. (doi: 10.1016/j.progpolymsci.2004.08.003)

8. Li, C.; Gunari, N.; Fischer, K.; Janshoff, A.; Schmidt, M., New perspectives for the design of molecular actuators: thermally induced collapse of single macromolecules from

cylindrical brushes to spheres. *Angew. Chem. Int. Ed. Engl.* **2004,** *43* (9), 1101-1104. (doi: 10.1002/anie.200352845)

9. Meng, F.; Zhong, Z.; Feijen, J., Stimuli-responsive polymersomes for programmed drug delivery. *Biomacromolecules* **2009,** *10* (2), 197-209. (doi: 10.1021/bm801127d)

10. Mori, T.; Umeno, D.; Maeda, M., Sequence-specific affinity precipitation of oligonucleotide using poly(N-isopropylacrylamide)-oligonucleotide conjugate. *Biotechnol. Bioeng.* **2001,** *72* (3), 261-268. (doi: Doi 10.1002/1097-0290(20010205)72:3<261::Aid-Bit2>3.0.Co;2-7)

11. Schmaljohann, D., Thermo- and pH-responsive polymers in drug delivery. *Adv Drug Deliv Rev* **2006,** *58* (15), 1655-1670. (doi: 10.1016/j.addr.2006.09.020)

12. Stuart, M. A.; Huck, W. T.; Genzer, J.; Muller, M.; Ober, C.; Stamm, M.; Sukhorukov, G. B.; Szleifer, I.; Tsukruk, V. V.; Urban, M.; Winnik, F.; Zauscher, S.; Luzinov, I.; Minko, S., Emerging applications of stimuli-responsive polymer materials. *Nat Mater* **2010,** *9* (2), 101-113. (doi: 10.1038/nmat2614)

13. Chung, J. E.; Yokoyama, M.; Yamato, M.; Aoyagi, T.; Sakurai, Y.; Okano, T., Thermo-responsive drug delivery from polymeric micelles constructed using block copolymers of poly(N-isopropylacrylamide) and poly(butylmethacrylate). *J. Controlled Release* **1999,** *62* (1-2), 115-127. (doi: Doi 10.1016/S0168-3659(99)00029-2)

14. Zhang, N.; Salzinger, S.; Rieger, B., Poly(vinylphosphonate)s with Widely Tunable LCST: A Promising Alternative to Conventional Thermoresponsive Polymers. *Macromolecules* **2012,** *45* (24), 9751-9758. (doi: 10.1021/ma3019014)

15. Xue, B.; Gao, L.; Hou, Y.; Liu, Z.; Jiang, L., Temperature controlled water/oil wettability of a surface fabricated by a block copolymer: application as a dual water/oil on-off switch. *Adv. Mater.* **2013,** *25* (2), 273-277. (doi: 10.1002/adma.201202799)

16. Jiang, J.; Tong, X.; Zhao, Y., A new design for light-breakable polymer micelles. *J. Am. Chem. Soc.* **2005,** *127* (23), 8290-8291. (doi: 10.1021/ja0521019)

17. Jochum, F. D.; Theato, P., Temperature and light sensitive copolymers containing azobenzene moieties prepared via a polymer analogous reaction. *Polymer* **2009,** *50* (14), 3079-3085. (doi: 10.1016/j.polymer.2009.05.041)

18. Jochum, F. D.; zur Borg, L.; Roth, P. J.; Theato, P., Thermo- and Light-Responsive Polymers Containing Photoswitchable Azobenzene End Groups. *Macromolecules* **2009,** *42* (20), 7854-7862. (doi: 10.1021/ma901295f)

19. Zhao, Y., Light-Responsive Block Copolymer Micelles. *Macromolecules* **2012,** *45* (9), 3647-3657. (doi: 10.1021/ma300094t)

20. Jochum, F. D.; Theato, P., Temperature- and light-responsive smart polymer materials. *Chem. Soc. Rev.* **2013,** *42* (17), 7468-7483. (doi: 10.1039/c2cs35191a)

21. Yu, X.; Zhou, S.; Zheng, X.; Guo, T.; Xiao, Y.; Song, B., A biodegradable shape-memory nanocomposite with excellent magnetism sensitivity. *Nanotechnology* **2009,** *20* (23), 235702. (doi: 10.1088/0957-4484/20/23/235702)

22. Golbang, A.; Kokabi, M., Temporary shape development in shape memory nanocomposites using magnetic force. *Eur. Polym. J.* **2011,** *47* (8), 1709-1719. (doi: 10.1016/j.eurpolymj.2011.06.008)

23. Mendes, P. M., Stimuli-responsive surfaces for bio-applications. *Chem. Soc. Rev.* **2008,** *37* (11), 2512-2529. (doi: 10.1039/b714635n)

24. Nunes, S. P.; Behzad, A. R.; Hooghan, B.; Sougrat, R.; Karunakaran, M.; Pradeep, N.; Vainio, U.; Peinemann, K. V., Switchable pH-responsive polymeric membranes prepared via block copolymer micelle assembly. *ACS Nano* **2011,** *5* (5), 3516-3522. (doi: 10.1021/nn200484v)

25. Liu, R.; Liao, P.; Liu, J.; Feng, P., Responsive polymer-coated mesoporous silica as a pH-sensitive nanocarrier for controlled release. *Langmuir* **2011,** *27* (6), 3095-3099. (doi: 10.1021/la104973j)

26. Plunkett, K. N.; Moore, J. S., Patterned dual pH-responsive core-shell hydrogels with controllable swelling kinetics and volumes. *Langmuir* **2004,** *20* (16), 6535-6537. (doi: 10.1021/la049453y)

27. Nagel, B.; Warsinke, A.; Katterle, M., Enzyme activity control by responsive redoxpolymers. *Langmuir* **2007,** *23* (12), 6807-6811. (doi: 10.1021/la700331w)

28. Phillips, D. J.; Gibson, M. I., Degradable thermoresponsive polymers which display redox-responsive LCST behaviour. *Chem Commun (Camb)* **2012,** *48* (7), 1054-1056. (doi: 10.1039/c1cc16323j)

29. Logtenberg, H.; Browne, W. R., Electrochemistry of dithienylethenes and their application in electropolymer modified photo- and redox switchable surfaces. *Org Biomol Chem* **2013,** *11* (2), 233-243. (doi: 10.1039/c2ob26723c)

30. Chen, J. K.; Hsieh, C. Y.; Huang, C. F.; Li, P. M.; Kuo, S. W.; Chang, F. C., Using Solvent Immersion to Fabricate Variably Patterned Poly(methyl methacrylate) Brushes on Silicon Surfaces. *Macromolecules* **2008,** *41* (22), 8729-8736. (doi: 10.1021/ma801127m)

31. Chen, J. K.; Hsieh, C. Y.; Huang, C. F.; Li, P. M., Characterization of patterned poly(methyl methacrylate) brushes under various structures upon solvent immersion. *J. Colloid Interface Sci.* **2009,** *338* (2), 428-434. (doi: 10.1016/j.jcis.2009.06.040)

32. Cerritelli, S.; Velluto, D.; Hubbell, J. A., PEG-SS-PPS: reduction-sensitive disulfide block copolymer vesicles for intracellular drug delivery. *Biomacromolecules* **2007,** *8* (6), 1966-1972. (doi: 10.1021/bm070085x)

33. Koo, A. N.; Lee, H. J.; Kim, S. E.; Chang, J. H.; Park, C.; Kim, C.; Park, J. H.; Lee, S. C., Disulfide-cross-linked PEG-poly(amino acid)s copolymer micelles for glutathione-mediated intracellular drug delivery. *Chem Commun (Camb)* **2008,** (48), 6570-6572. (doi: 10.1039/b815918a)

34. Sinha, V. R.; Kumria, R., Polysaccharides in colon-specific drug delivery. *Int. J. Pharm.* **2001,** *224* (1-2), 19-38. (doi: 10.1016/S0378-5173(01)00720-7)

35. Chambin, O.; Dupuis, G.; Champion, D.; Voilley, A.; Pourcelot, Y., Colon-specific drug delivery: Influence of solution reticulation properties upon pectin beads performance. *Int. J. Pharm.* **2006,** *321* (1-2), 86-93. (doi: 10.1016/j.ijpharm.2006.05.015)

36. Ganesh, V. A.; Baji, A.; Ramakrishna, S., Smart functional polymers - a new route towards creating a sustainable environment. *Rsc Advances* **2014,** *4* (95), 53352-53364. (doi: 10.1039/c4ra10631h)

37. Gibson, M. I.; O'Reilly, R. K., To aggregate, or not to aggregate? considerations in the design and application of polymeric thermally-responsive nanoparticles. *Chem. Soc. Rev.* **2013,** *42* (17), 7204-7213. (doi: 10.1039/c3cs60035a)

38. Roy, D.; Brooks, W. L.; Sumerlin, B. S., New directions in thermoresponsive polymers. *Chem. Soc. Rev.* **2013,** *42* (17), 7214-7243. (doi: 10.1039/c3cs35499g)

39. Schild, H. G., Poly (N-Isopropylacrylamide) - Experiment, Theory and Application. *Prog. Polym. Sci.* **1992,** *17* (2), 163-249. (doi: Doi 10.1016/0079-6700(92)90023-R)

40. Vihola, H.; Laukkanen, A.; Valtola, L.; Tenhu, H.; Hirvonen, J., Cytotoxicity of thermosensitive polymers poly(N-isopropylacrylamide), poly(N-vinylcaprolactam) and amphiphilically modified poly(N-vinylcaprolactam). *Biomaterials* **2005,** *26* (16), 3055-3064. (doi: 10.1016/j.biomaterials.2004.09.008)

41. Lutz, J. F.; Akdemir, O.; Hoth, A., Point by point comparison of two thermosensitive polymers exhibiting a similar LCST: is the age of poly(NIPAM) over? *J. Am. Chem. Soc.* **2006,** *128* (40), 13046-13047. (doi: 10.1021/ja065324n)

42. Lessard, D. G.; Ousalem, M.; Zhu, X. X.; Eisenberg, A.; Carreau, P. J., Study of the phase transition of poly(N,N-diethylacrylamide) in water by rheology and dynamic light scattering. *J Polym Sci Pol Phys* **2003,** *41* (14), 1627-1637. (doi: 10.1002/polb.10517)

43. Rieger, J.; Grazon, C.; Charleux, B.; Alaimo, D.; Jerome, C., Pegylated Thermally Responsive Block Copolymer Micelles and Nanogels via In Situ RAFT Aqueous Dispersion Polymerization. *J Polym Sci Pol Chem* **2009,** *47* (9), 2373-2390. (doi: 10.1002/pola.23329)

44. Watanabe, R.; Takaseki, K.; Katsumata, M.; Matsushita, D.; Ida, D.; Osa, M., Characterization of poly(N,N-diethylacrylamide) and cloud points in its aqueous solutions. *Polym. J.* **2016,** *48* (5), 621-628. (doi: 10.1038/pj.2015.120)

45. Maeda, Y.; Nakamura, T.; Ikeda, I., Hydration and phase behavior of poly(N-vinylcaprolactam) and poly(N-vinylpyrrolidone) in water. *Macromolecules* **2002,** *35* (1), 217-222. (doi: 10.1021/ma011034+)

46. Alexandridis, P.; Alan Hatton, T., Poly(ethylene oxide)・poly(propylene oxide)・poly(ethylene oxide) block copolymer surfactants in aqueous solutions and at interfaces:

thermodynamics, structure, dynamics, and modeling. *Colloids and Surfaces A: Physicochemical and Engineering Aspects* **1995,** *96* (1-2), 1-46. (doi: 10.1016/0927-7757(94)03028-x)

47. Glatzel, S.; Laschewsky, A.; Lutz, J. F., Well-Defined Uncharged Polymers with a Sharp UCST in Water and in Physiological Milieu. *Macromolecules* **2011,** *44* (2), 413-415. (doi: 10.1021/ma102677k)

48. Seuring, J.; Agarwal, S., First Example of a Universal and Cost-Effective Approach: Polymers with Tunable Upper Critical Solution Temperature in Water and Electrolyte Solution. *Macromolecules* **2012,** *45* (9), 3910-3918. (doi: 10.1021/ma300355k)

49. Antonietti, M.; Forster, S., Vesicles and liposomes: A self-assembly principle beyond lipids. *Adv. Mater.* **2003,** *15* (16), 1323-1333. (doi: 10.1002/adma.200300010)

50. Cui, H.; Chen, Z.; Zhong, S.; Wooley, K. L.; Pochan, D. J., Block copolymer assembly via kinetic control. *Science* **2007,** *317* (5838), 647-650. (doi: 10.1126/science.1141768)

51. Discher, B. M.; Won, Y. Y.; Ege, D. S.; Lee, J. C. M.; Bates, F. S.; Discher, D. E.; Hammer, D. A., Polymersomes: Tough vesicles made from diblock copolymers. *Science* **1999,** *284* (5417), 1143-1146. (doi: DOI 10.1126/science.284.5417.1143)

52. Discher, D. E.; Eisenberg, A., Polymer vesicles. *Science* **2002,** *297* (5583), 967-973. (doi: 10.1126/science.1074972)

53. Jain, S.; Bates, F. S., On the origins of morphological complexity in block copolymer surfactants. *Science* **2003,** *300* (5618), 460-464. (doi: 10.1126/science.1082193)

54. Jenekhe, S. A.; Chen, X. L., Self-assembly of ordered microporous materials from rod-coil block copolymers. *Science* **1999,** *283* (5400), 372-375. (doi: 10.1126/science.283.5400.372)

55. Luo, L.; Eisenberg, A., One-step preparation of block copolymer vesicles with preferentially segregated acidic and basic corona chains. *Angew. Chem. Int. Ed. Engl.* **2002,** *41* (6), 1001-1004. (doi: 10.1002/1521-3773(20020315)41:6<1001::AID-ANIE1001>3.0.CO;2-Q)

56. Wang, X.; Guerin, G.; Wang, H.; Wang, Y.; Manners, I.; Winnik, M. A., Cylindrical block copolymer micelles and co-micelles of controlled length and architecture. *Science* **2007,** *317* (5838), 644-647. (doi: 10.1126/science.1141382)

57. Won, Y. Y.; Davis, H. T.; Bates, F. S., Giant wormlike rubber micelles. *Science* **1999,** *283* (5404), 960-963. (doi: 10.1126/science.283.5404.960)

58. Zhang, L.; Eisenberg, A., Multiple Morphologies of "Crew-Cut" Aggregates of Polystyrene-b-poly(acrylic acid) Block Copolymers. *Science* **1995,** *268* (5218), 1728-1731. (doi: 10.1126/science.268.5218.1728)

59. Blanazs, A.; Armes, S. P.; Ryan, A. J., Self-Assembled Block Copolymer Aggregates: From Micelles to Vesicles and their Biological Applications. *Macromol. Rapid Commun.* **2009,** *30* (4-5), 267-277. (doi: 10.1002/marc.200800713)

60. Israelachvili, J. N., *Intermolecular and Surface Forces Preface to the Third Edition*. 2011; p Xvii-+.

61. Discher, D. E.; Ahmed, F., Polymersomes. *Annual Review of Biomedical Engineering* **2006,** *8*, 323-341. (doi: 10.1146/annurev.bioeng.8.061505.095838)

62. Matyjaszewski, K.; Spanswick, J., Controlled/living radical polymerization. *Mater. Today* **2005,** *8* (3), 26-33. (doi: 10.1016/s1369-7021(05)00745-5)

63. Braunecker, W. A.; Matyjaszewski, K., Controlled/living radical polymerization: Features, developments, and perspectives. *Prog. Polym. Sci.* **2007,** *32* (1), 93-146. (doi: 10.1016/j.progpolymsci.2006.11.002)

64. Hawker, C. J.; Bosman, A. W.; Harth, E., New polymer synthesis by nitroxide mediated living radical polymerizations. *Chem. Rev.* **2001,** *101* (12), 3661-3688. (doi: 10.1021/cr990119u)

65. Matyjaszewski, K.; Xia, J., Atom transfer radical polymerization. *Chem. Rev.* **2001,** *101* (9), 2921-2990. (doi: 10.1021/cr940534g)

66. Chiefari, J.; Chong, Y. K.; Ercole, F.; Krstina, J.; Jeffery, J.; Le, T. P. T.; Mayadunne, R. T. A.; Meijs, G. F.; Moad, C. L.; Moad, G.; Rizzardo, E.; Thang, S. H., Living Free-Radical Polymerization by Reversible Addition−Fragmentation Chain Transfer: The RAFT Process. *Macromolecules* **1998,** *31* (16), 5559-5562. (doi: 10.1021/ma9804951)

67. Chong, Y. K.; Le, T. P. T.; Moad, G.; Rizzardo, E.; Thang, S. H., A more versatile route to block copolymers and other polymers of complex architecture by living radical polymerization: The RAFT process. *Macromolecules* **1999,** *32* (6), 2071-2074. (doi: 10.1021/ma981472p)

68. Moad, G.; Chiefari, J.; Chong, Y. K.; Krstina, J.; Mayadunne, R. T. A.; Postma, A.; Rizzardo, E.; Thang, S. H., Living free radical polymerization with reversible addition-fragmentation chain transfer (the life of RAFT). *Polym. Int.* **2000,** *49* (9), 993-1001. (doi: Doi 10.1002/1097-0126(200009)49:9<993::Aid-Pi506>3.0.Co;2-6)

69. Semsarilar, M.; Perrier, S., 'Green' reversible addition-fragmentation chain-transfer (RAFT) polymerization. *Nature Chemistry* **2010,** *2* (10), 811-820. (doi: 10.1038/Nchem.853)

Chapter 2 Synthesis and Characterization of Linear Thermally Responsive Triblock Copolymers PEO-*b*-PDEAm-*b*-PDBAm

2.1 Introduction

Our group has a long-standing interest in linear three-component ABC triblock copolymers in which a thermally responsive block is located between a hydrophilic and a hydrophobic block. We first investigated poly(ethylene oxide)-*block*-poly(*N*-isopropylacrylamide)-*block*-poly(isoprene) ($PEO_{2.0}$-*b*-$PNIPAM_{4.5}$-*b*-$PI_{0.8}$, M_n=7.5kg/mol) triblock copolymers in water (Figure 2-1 and 2-2) and found them to form core-shell spherical micelles due to their large hydrophilic mass fraction (f ≈0.87 at 25 °C), which assembled into large vesicles after heating above the LCST of thermally responsive PNIAPAM block at 65 °C for 3 weeks (f ≈0.27 at 65 °C).[1]

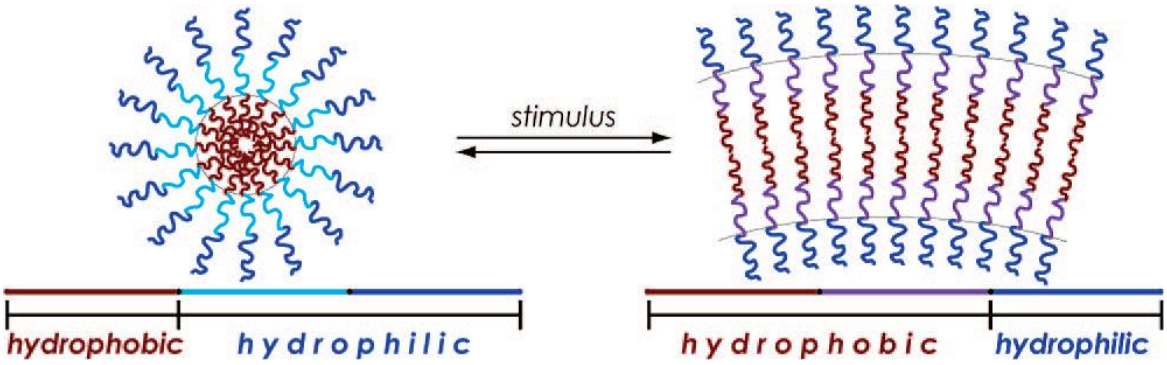

Figure 2-1. Schematic illustration of the expected change in amphiphilic balance for ABC triblock copolymer chains with a stimulus-responsive B block (bottom) and interfacial curvature for assemblies of these triblock copolymers (top) in water upon passage through the lower critical solution temperature of the B block. Reprinted with permission from reference[1]. Copyright (2008) American Chemical Society.

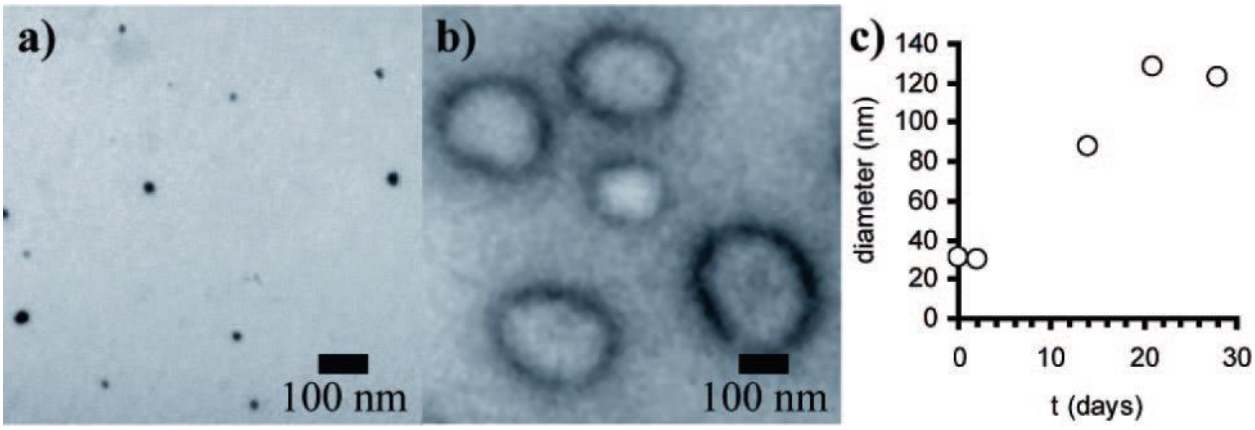

Figure 2-2. TEM images of copolymer $PEO_{2.0}$-*b*-$PNIPAM_{4.5}$-*b*-$PI_{0.8}$ (a) as drop-cast from aqueous solution at room temperature (OsO_4 stain) and (b) as drop-cast from aqueous solution heated at 65 °C for 4 weeks (OsO_4 stain). (c) DLS diameter with time of aqueous aggregates at 65 °C. Reprinted with permission from reference[1]. Copyright (2008) American Chemical Society.

A number of factors affecting the rate of transformation of these PNIPAM-based copolymers from micelles to vesicles have been identified. O'Reilly and co-workers demonstrated that poly(*tert*-butyl acrylate)-*block*-PNIPAM diblock copolymers ($PtBuA_{3.2}$-*b*-$PNIPAM_{2.8,}$ M_n=6.6 kg/mol) (Figure 2-3), with a much lower molecular weight quaternary amine end as the hydrophilic component, could undergo a similar but much more rapid micelle-to-vesicle transition when heated at 65 °C for 1 week.[2]

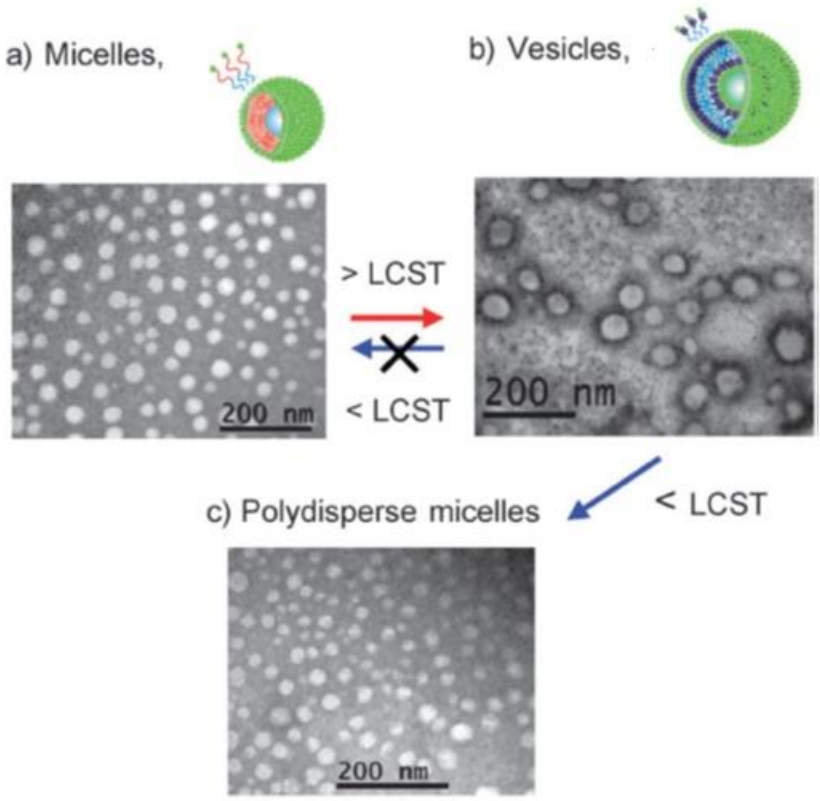

Figure 2-3. Representative $PtBuA_{3.2}$-*b*-$PNIPAM_{2.8}$ TEM micrographs: (a) micelles, at 25 °C stained with uranyl acetate; (b) vesicles, at 65 °C stained with ammonium molybdate; (c) polydisperse micelles after cooling back the vesicles, to 25 °C, stained with uranyl acetate. Adapted from reference[2], with permission from Royal Society of Chemistry.

Jiang and coworkers have claimed that reducing the restriction to the mobility of the PNIPAM chains imposed by a solid micellar core is one of the key factors in realizing a fast transition.[3] From another point of view, we hypothesized that the dehydration of PNIPAM-containing micelles could result in interchain hydrogen bonding between PNIPAM amide groups that would kinetically trap micelles and slow further rearrangement. Subsequently, we synthesized another thermally responsive triblock copolymers poly(ethylene oxide)-*block*-poly(ethylene

oxide-stat-butylene oxide)-block-poly(isoprene) ($PEO_{2.3}$-*b*-PEO/$BO_{5.3}$-*b*-$PI_{2.3}$, M_n=9.9kg/mol) in which a random copolymer of ethylene oxide and butyl oxide that cannot undergo interchain hydrogen bonding was used as the central responsive block. The rate of transformation from micelles to vesicles with PEO-*b*-PEO/BO-*b*-PI systems (Figure 2-4) is more rapid (on the order of several hours) than that observed for PEO-*b*-PNIPA-*b*-PI assemblies (several weeks).[4]

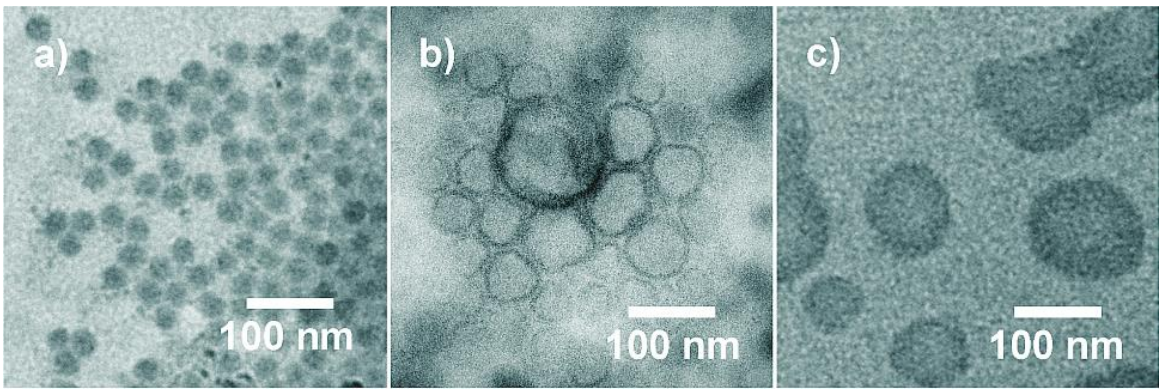

Figure 2-4. TEM images of $PEO_{2.3}$-*b*-PEO/$BO_{5.3}$-*b*-$PI_{2.3}$ assemblies. (a) Cross-linked aggregates at 25 °C, D_{ave} = 22 nm (0.3 mg/mL, stained by OsO_4 vapor); (b) Aggregates cross-linked after 2 days at 70 °C, D_{ave} = 58 nm (0.5 mg/mL, stained by OsO_4 vapor); and (c) Aggregates cross-linked after 2 weeks at 70 °C, D_{ave} = 106 nm (0.5 mg/mL, stained by OsO_4 vapor and then uranyl acetate solution). Reprinted with permission from reference[4]. Copyright (2010) American Chemical Society.

In this thesis, we describe the design and synthesis of another class of thermally responsive ABC triblock copolymers via RAFT polymerization, poly(ethylene oxide)-block-poly(*N*,*N*-diethylacrylamide)-block-poly(*N*,*N*-dibutylacrylamide) (PEO-*b*-PDEAm-*b*-PDBAm), in which the stimulus-responsive block is poly(*N*,*N*-diethylacrylamide), which cannot form strong

interchain hydrogen bonds and has an LCST in water similar to that of PNIPAM (LCST ≈ 32 °C)[5-6]. After the synthesis, transmission electron microscopy (TEM), dynamic light scattering (DLS), and rheology were used to characterize the thermally responsive behavior of these triblock polymers.

2.2 Experimental

Materials

2,2-Azobis(isobutyronitrile) (AIBN, 98%, Sigma-Aldrich) was recrystallized from methanol. Carbon disulfide (99.9+%, EMD), triethylamine (99.9+%, EMD), 1,4-dioxane (99.9+%, EMD), tetrahydrofuran (99.9%, EMD), and dichloromethane (99.8%, EMD) were used after storage over molecular sieves (4Å, 1-2 mm beads, Alfa Aesar) overnight. Poly(ethylene oxide) methyl ether (PEO) (Sigma-Aldrich, M_n = 2000 g/mol, $Đ$ =1.02) was freeze-dried from benzene before use. All other chemicals and solvents were purchased from Fisher or Sigma-Aldrich at the highest available purity and used as received.

Characterization

Nuclear Magnetic Resonance Spectroscopy (NMR). ^{1}H NMR spectroscopy was carried out on a 300 MHz Varian Gemini 2300 spectrometer using $CDCl_3$ as solvent. Chemical shifts were referenced to the residual proton peak of $CDCl_3$ (7.26 ppm).

Gel Permeation Chromatography (GPC). GPC was performed at 40 °C using tetrahydrofuran (THF, HPLC grade, J.T. Baker) eluent at a flow rate of 1.0 mL/minute at 40 °C. The apparatus consisted of a K-501 pump (Knauer), a K-3800 Basic Autosampler (Marathon), two PL-gel 5 μm Mixed-D columns (300 X 7.5 mm, rated for polymers between 200-400,000 g/mol, Polymer Laboratories), and a PL-ELS 1000 Evaporative Light Scattering Detector (Polymer Laboratories).

A PL Datastream unit (Polymer Laboratories) was used to acquire data, which was analyzed based on narrow polydispersity polystyrene standards in the molecular weight range of 580-400,000 g/mol (EasiCal PS-2, Polymer Laboratories).

Synthetic Procedures

Esterification of PEO_{45}-OH with α-bromophenylacetic acid Acid[7]

Poly(ethylene oxide) methyl ether ($MeOPEG_{45}$) (6.00 g, 3.00 mmol, M_n = 2.0 kg/mol) was dissolved in dichloromethane (40 mL). To this solution, α-bromophenylacetic acid (1.29 g, 6.00 mmol), DMAP (49 mg, 0.40 mmol), and dicyclohexylcarbodiimide (2.07 g, 10.0 mmol) were added at room temperature. The reaction mixture was then stirred at room temperature for 24 h under nitrogen. After filtration, the solution was precipitated into cold hexanes (400 mL). The crude precipitate was redissolved in THF (30 mL) and precipitated into cold hexanes (500 mL), filtered and dried under vacuum to afford α-bromophenylacetate terminated poly(ethylene oxide) (5.05 g, 80% after 2 precipitations).

^{1}H NMR ($CDCl_3$, 300 MHz): 3.36 (3H, s, O-CH_3), 3.55-3.92 (4H per repeating unit, s, CH_2-CH_2-O), 5.39 (1H, s, CHCl), 7.36-7.55 (5H, m, Ar-H).

Synthesis of PEO_{45} Macro-CTA[7]

Carbon disulfide (0.40 mL, 6.60 mmol) was added dropwise to a solution of phenylmagnesium chloride (1.20 mL of a 3.0 M solution in diethyl ether, 3.60 mmol) in dry tetrahydrofuran (10 mL) under nitrogen. The reaction mixture was stirred for 30 min under nitrogen at room temperature, resulting in a dark-red solution. This solution was added to a solution of functionalized PEO (4.00

g, 1.80 mmol) in dry tetrahydrofuran (40 mL), and the reaction mixture was heated at reflux under nitrogen for 24 h. The solution was then filtered and precipitated into hexanes (500 mL) to yield the PEO_{45} Macro-CTA, **2**, as a pink solid. The crude product was further purified by a second precipitation into hexanes (500 mL) from tetrahydrofuran (30 mL), filtered and dried under vacuum (3.07 g, 75% after 2 precipitations).

^{1}H NMR ($CDCl_3$, 300 MHz): 3.33 (s, O-CH_3), 3.53-3.94 (s, CH_2-CH_2-O), 5.65 (1H, s, -S(Ph)CH-CO_2Me), 7.20-7.50 (8H, m, Ar-H), 7.93-8.00 (2H, d, ArCSS).

Synthesis of *N*,*N*-diethylacrylamide (DEAm)[8]

Diethylamine (4.10 mL, 39.3 mmol) and triethylamine (5.50 mL, 39.5 mmol) were dissolved in dichloromethane (100 mL). The solution was cooled to 0 °C and a solution of acryloyl chloride (3.32 mL, 39.2 mmol) in dichloromethane (20 mL) was added dropwise over 1 h. The reaction mixture was stirred under nitrogen at 0 °C for 1 h and allowed to warm to room temperature over 1 h. The reaction mixture was then washed with saturated sodium bicarbonate solution (50 mL × 2) and saturated sodium chloride solution (50 mL × 2). The organic fraction was dried over anhydrous magnesium sulfate, filtered, and concentrated under reduced pressure. The product was dissolved in ethyl acetate (30 mL) and was washed with saturated sodium bicarbonate solution (50 mL × 2) and saturated sodium chloride solution (50 mL × 2). Drying over anhydrous magnesium sulfate, followed by filtration and concentration under reduced pressure, yielded an oil that was distilled to yield 2.25 g (45%) of *N*,*N*-diethylacrylamide (b.p. = 58-59 °C at 0.6 Torr).

^{1}H NMR (300 MHz, $CDCl_3$): δ 1.16 (m, 6H), 3.36 (m, 2H), 3.42 (m, 2H), 5.64 (dd, 1H, cis β -CH_2, J = 10.3 and 2.0 Hz), 6.32 (dd, 1H, trans β -CH_2, J = 16.7 and 2.0 Hz), 6.53 (dd, 1H, α-CH_2, J = 16.7 and 10.3 Hz).

Synthesis of *N*,*N*-dibutylacrylamide (DBAm)[8]

Dibutylamine (6.70 mL, 39.3 mmol) and triethylamine (5.50 mL, 39.5 mmol) were dissolved in dichloromethane (100 mL). The resulting solution was cooled to 0 °C, and a solution of acryloyl chloride (3.32 mL, 39.2 mmol) in dichloromethane (20 mL) was added dropwise over 1 h at 0 °C. The reaction mixture was stirred under nitrogen at 0 °C for 1 h and at room temperature for 1 h. The solution was then washed with saturated sodium bicarbonate solution (50 mL × 2) and saturated sodium chloride solution (50mL × 2). It was then dried over anhydrous magnesium sulfate, filtered, and concentrated under reduced pressure. The product was dissolved in ethyl acetate (30 mL) and was washed with saturated sodium bicarbonate solution (50 mL × 2) and saturated sodium chloride solution (50mL × 2). Drying over anhydrous magnesium sulfate, followed by filtration and concentration under reduced pressure, yielded an oil that was distilled to yield 4.30 g (40%) of *N*,*N*-dibutylacrylamide (bp = 95-96 °C at 0.6 Torr).

^{1}H NMR (300 MHz, $CDCl_3$): δ 1.16 (m, 6H), 1.36 (m, 2H), 1.54 (m, 2H), 3.36 (m, 2H), 3.42 (m, 2H), 5.64 (dd, 1H, cis β -CH_2, J= 10.3 and 2.0 Hz), 6.32 (dd, 1H, trans β -CH_2, J =16.7 and 2.0 Hz), 6.53 (dd, 1H, α-CH_2, J = 16.7 and 10.3 Hz)

Synthesis of 3-Azidopropylamine[9]

A solution of 3-chloropropylamine hydrochloride (5.00 g, 38.8 mmol), sodium azide (7.50 g, 115 mmol) and potassium iodide (0.02 g) in water (37.5 mL) was heated at 80 °C for 24 h. After most of the water was removed under vacuum by Rotavap, the reaction mixture was cooled in an ice bath. Diethyl ether (62.5 mL) and sodium hydroxide pellets (5.00 g) were added slowly while maintaining the temperature below 10 °C. After separation of the organic phase, the aqueous layer was further extracted with diethyl ether (50 mL × 4). The combined organic layers were dried over

anhydrous magnesium sulfate and concentrated to obtain 3-azidopropylamine, which was purified by vacuum distillation to obtain a colorless liquid. (2.50 g, 64% yield). (b.p. 32 °C /1.7 mbar).

^{1}H NMR (300 MHz, $CDCl_3$): δ 1.7 (m, 2H), 2.8 (t, 2H, $–CH_2NH_2$, J=6.9Hz), 3.3 (t, 2H, $–CH_2N_3$, J=6.9Hz).

Synthesis of 3-azidopropylacrylamide[9]

3-Azidopropylamine (2.50 g, 25 mmol), triethylamine (2.90 mL, 31.0 mmol), and hydroquinone (0.01 g) were dissolved in dichloromethane (40 mL). The mixture was cooled to 0 °C in an ice-water bath. Acryloyl chloride (1.70 mL, 21.0 mmol) in dichloromethane (10 mL) was then added dropwise within 1 h under nitrogen atmosphere. After stirring for 12 h at room temperature, the mixture was filtered to remove insoluble salts. The organic layer was washed with saturated sodium bicarbonate solution (20 mL × 2) and saturated sodium chloride solution (20 mL × 2). After drying over anhydrous magnesium sulfate and filtration, the solvent was removed under reduced pressure. The product was further purified by flash chromatography (SiO_2/CH_2Cl_2, R_f = 0.6) to afford a light yellow liquid (1.4 g, 43%).

^{1}H NMR (300 MHz, $CDCl_3$): δ 1.8 (2H, m), 3.5 (4H, m), 5.7 (dd, 1H, cis β -CH_2, J= 10.3 and 2.0 Hz), 6.3 (dd, 1H, trans β -CH_2, J =16.7 and 2.0 Hz), 6.5 (dd, 1H, α-CH_2, J = 16.7 and 10.3 Hz)

Synthesis of 4-azidotoluene[10]

p-Toluidine (5.00 mL, 5.25 g, 49.0 mmol) was dissolved in an HCl solution (6 M, 50 mL) at room temperature. Upon cooling to 0 °C and addition of a solution of $NaNO_2$ (3.50 g, 50.0 mmol) in water (18 mL), the reaction mixture was stirred for 10 min at 0-5 °C. A solution of sodium azide (3.30 g, 50.0 mmol) in water (40 mL) was added dropwise. After addition was complete, the ice

bath was removed and the reaction mixture was allowed to stir for three hours. The reaction mixture was diluted with ethyl acetate (150 mL), washed with brine (50 mL × 2), and dried over sodium sulfate. The solvent was evaporated to give a brown liquid (5.50 g, 82%).

^{1}H NMR (300 MHz, $CDCl_3$): δ 2.3 (3H, s), 6.9 (2H, d), 7.2 (2H, d) IR: 2100 cm-1 (N_3)

Synthesis of 4-azidobenzyl bromide[10]

A solution of 4-azidotoluene (5.40 g, 40.6 mmol), *N*-bromosuccinimide (6.50 g, 36.5 mmol) and AIBN (0.10 g, 0.60 mmol) in CCl_4 (40 mL) was refluxed under a nitrogen atmosphere for 24 h. The solvent was evaporated and the residue was purified by column chromatography on silica gel using hexane as the eluent to afford a light yellow liquid (5.50 g, 72%).

^{1}H NMR (300 MHz, $CDCl_3$): δ 4.5 (2H, s), 7.0 (2H, d), 7.4 (2H, d)

Synthesis of *N*-(4-azidophenyl)phthalimide[10]

A mixture of 4-azidobenzyl bromide (5.50 g, 26.0 mmol) and potassium phthalimide (5.45 g, 28.6 mmol) in dimethylformamide was heated at 80 °C under a nitrogen atmosphere for 24 h. After cooling to room temperature, the reaction mixture was poured into ice water (100mL). After filtration, the precipitate was washed with water and dried in vacuum to give a yellow solid (6.80 g, 95%).

^{1}H NMR (300 MHz, $CDCl_3$): δ 4.8 (2H, s), 7.0-7.4 (4H, m), 7.5-7.9 (4H, m)

Synthesis of 4-azidobenzylamine[10]

A solution of N-(4-azidophenyl)phthalimide (6.80 g, 24.7 mmol) and aqueous hydrazine (12 mL, 51%, 185 mmol) in methanol (100 mL) was refluxed under nitrogen for 3 h. The precipitate that

formed was dissolved by adding sodium hydroxide solution (100 mL, 10%). The solution was extracted with dichloromethane (50 mL × 3). The combined organic phases were washed with water (50 mL × 2), dried over sodium sulfate, and concentrated to obtain 4-azidobenzylamine, which was purified by vacuum distillation to give a light yellow oil. (2.10 g, 55%, b.p. 75 °C /0.4 mmHg).

^{1}H NMR (300 MHz, $CDCl_3$): δ 1.4 (s, 2H), 3.8 (t, 2H), 6.8-7.4 (m, 4H).

Synthesis of *N*-(4-azidobenzyl)acrylamide

4-Azidobenzylamine (2.00 g, 13.0 mmol), triethylamine (1.95 mL, 14.0 mmol), and hydroquinone (0.01 g) were dissolved in dichloromethane (40 mL). The mixture was cooled to 0 °C in an ice-water bath. Acryloyl chloride (1.18 mL, 14.0 mmol) in dichloromethane (10 mL) was then added dropwise within 1 h under a nitrogen atmosphere. After stirring for 12 h at room temperature, the organic layer was washed with saturated sodium bicarbonate solution (20 mL × 2) and saturated sodium chloride solution (20 mL × 2). After drying over anhydrous magnesium sulfate and filtration, the solvent was removed under reduced pressure. The product was further purified by column chromatography on silica gel using dichloromethane as the eluent giving white solid (1.50 g, 50%).

^{1}H NMR (300 MHz, $CDCl_3$): δ 4.5 (2H, d), 5.7 (dd, 1H, cis β-CH_2, J= 10.3 and 2.0 Hz), 6.3 (dd, 1H, trans β-CH_2, J =16.7 and 2.0 Hz), 6.5 (dd, 1H, α-CH_2, J = 16.7 and 10.3 Hz), 7.0-7.4 (4H, m)

Synthesis of PEO_{45}-*b*-$PDEAm_x$ diblock copolymers

In a typical protocol for the synthesis of PEO_{45}-*b*-$PDEAm_{41}$, DEAm (1.20 g, 6.30 mmol), PEO-CTA (0.46 g, 0.2 mmol), and AIBN (0.004 g, 0.024 mmol) were added along with 1,4-dioxane (1

mL) to a Schlenk flask. The Schlenk flask was degassed via three freeze–pump–thaw cycles, backfilled with nitrogen and then placed in a preheated oil bath at 80 °C. The polymerization was halted after 24 h by cooling under liquid nitrogen followed by exposure to air. The viscous reaction mixture was dissolved in dichloromethane (5 mL) and precipitated into cold hexanes (200 mL) to give the diblock copolymer as a pink solid. (Yield: 75%, 1.25 g, Conversion> 80% calculated by comparison of residual DEAm monomer vinyl peaks in the ^{1}H NMR spectrum of the crude reaction mixture, M_n = 7.5 kg/mol calculated from the ^{1}H NMR spectrum of the pure diblock, $Đ$ = 1.2)

Synthesis of PEO$_{45}$-*b*-PDEAm$_x$-*b*-PDBAm$_y$ triblock copolymers

A typical protocol for the synthesis of PEO$_{45}$-*b*-PDEAm$_{41}$-*b*-PDBAm$_{12}$ is as follows: DBAm (0.11 g, 0.60 mmol), PEO$_{45}$-*b*-PDEAm$_{41}$ (0.38 g, 0.05 mmol), and AIBN (0.001 g, 0.006 mmol) were added along with 1,4-dioxane (1 mL) to a Schlenk flask. The Schlenk flask was degassed via three freeze–pump–thaw cycles, backfilled with nitrogen and then placed in a preheated oil bath at 80 °C. The reaction solution was stirred 36 h to ensure complete DBAm monomer conversion (>99%) and the polymerization was halted by cooling the reaction vessel in liquid nitrogen followed by exposure of the polymerization solution to air. The viscous reaction mixture was dissolved in dichloromethane (5 mL) and precipitated into cold hexane (200 mL) to give the triblock copolymer as a pink solid. (Yield: 80%, 0.40 g, Conversion > 99% determined by disappearance of monomer *N*,*N*-dibutylacrylamide vinyl peaks in the ^{1}H NMR of crude reaction mixture, Mn = 9.8 kg/mol calculated by conversion, $Đ$ = 1.4)

Syntheisis of PEO-*b*-PDEAm$_x$-*b*-PDBAm$_y$* triblock copolymers

A typical protocol for the synthesis of PEO$_{45}$-*b*-PDEAm$_{41}$-*b*-PDBAm$_{12}$* is as follows: DBAm (0.11 g, 0.6 mmol), PEO$_{45}$-*b*-DEAm$_{41}$ (0.38 g, 0.05 mmol), *N*-(4-azidobenzyl)acrylamide (0.01g,

0.1 mmol) and AIBN (0.001 g, 0.006 mmol) were added along with 1,4-dioxane (1 mL) to a Schlenk flask. The Schlenk flask was degassed via three freeze–pump–thaw cycles, backfilled with nitrogen and then placed in a preheated oil bath at 80 °C. The reaction solution was stirred 36 h to ensure complete DBAm monomer conversion (>99%) and the polymerization was halted by cooling the reaction vessel in liquid nitrogen followed by exposure of the polymerization solution to air. The viscous reaction mixture was dissolved in dichloromethane (5 mL) and precipitated into cold hexane (200 mL) to give the triblock copolymer as a yellow solid. (Yield: 80%, 0.40g, Conversion > 99%, M_n = 10.0 kg/mol, $Đ$ =1.4)

2.3 Results and discussion

Synthesis of PEO Macro-CTA

We used PEO as the hydrophilic block of our thermally responsive ABC triblock copolymer based not only on its recognized biocompatibility and solubility in both aqueous and organic solution,[11-13] but also to allow comparison of the new thermally responsive polymers with previously investigated PEO-*b*-PNIPAM-*b*-PI[1] and PEO-*b*-PEO/BO-*b*-PI[4] copolymers. A method reported by Müller and coworkers[7] was adapted for the preparation of a PEO Macro-CTA (M_n = 2.3 kg/mol) from poly(ethylene glycol) monomethyl ether (M_n = 2 kg/mol) (Scheme 2-1).

Scheme 2-1. Synthesis of PEO_{45} Macro-CTA

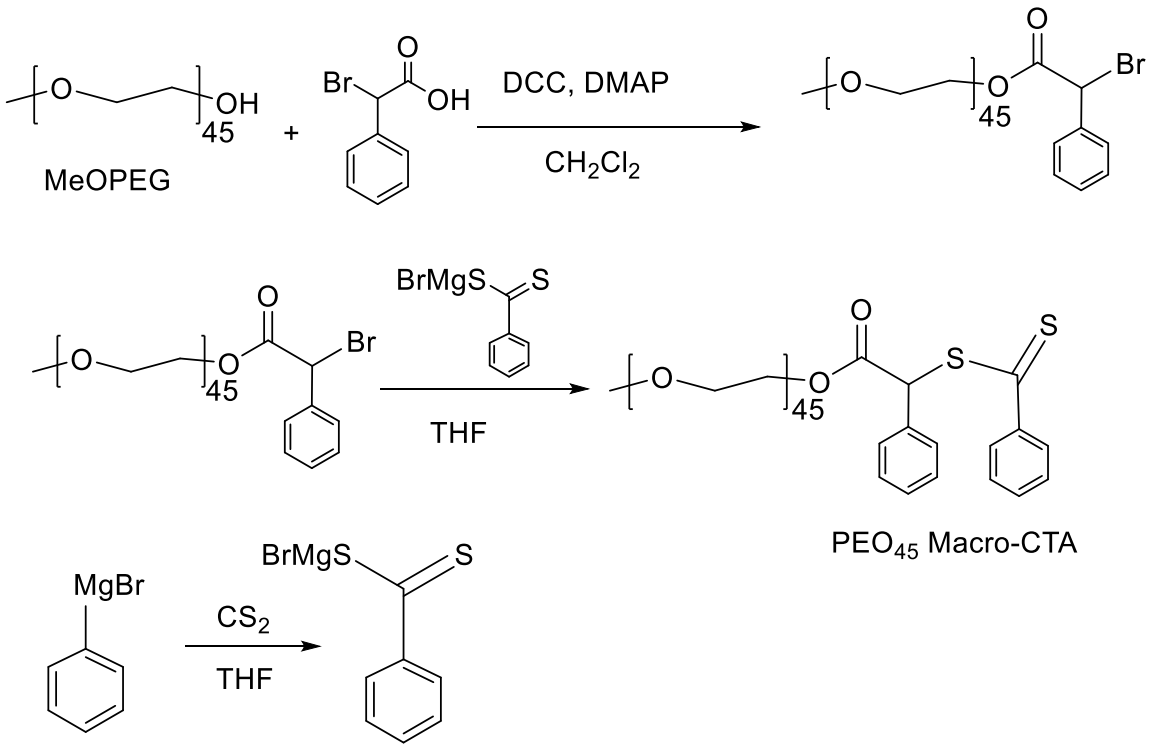

Synthesis of Monomer N, N-diethylacrylamide, N, N-dibutylacrylamide, 3-azidopropyl-acrylamide and N-(4-azidobenzyl) acrylamide

N,*N*-Diethylacrylamide and *N*,*N*-dibutylacrylamide were prepared by the reaction of diethylamine or dibutylamine with acryloyl chloride and purified by vacuum distillation.[8] The azide-functionalized monomer 3-azidopropylacrylamide was synthesized by a two-step reaction from 3-azidopropylamine.[14] *N*-(4-azidobenzyl)acrylamide was prepared in a five-step procedure starting from *p*-toluidine, following a reported procedure for the synthesis of 4-azidobenzylamine.[15] (Scheme 2-2).

Scheme 2-2. Synthesis of *N*,*N*-diethylacrylamide, *N*,*N*-dibutylacrylamide, 3-azidopropylacrylamide and *N*-(4-azidobenzyl)acrylamide

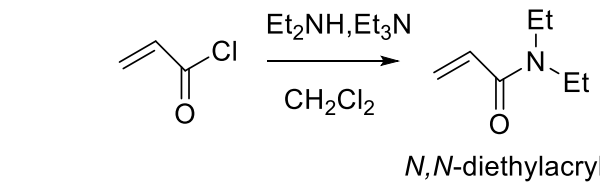

N,*N*-diethylacrylamide

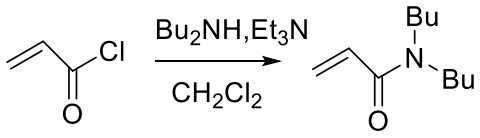

N,*N*-dibutylacrylamide

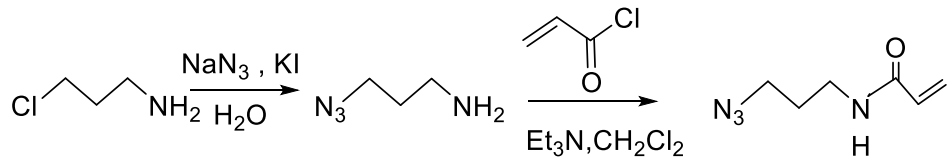

3-azidopropylacrylamide

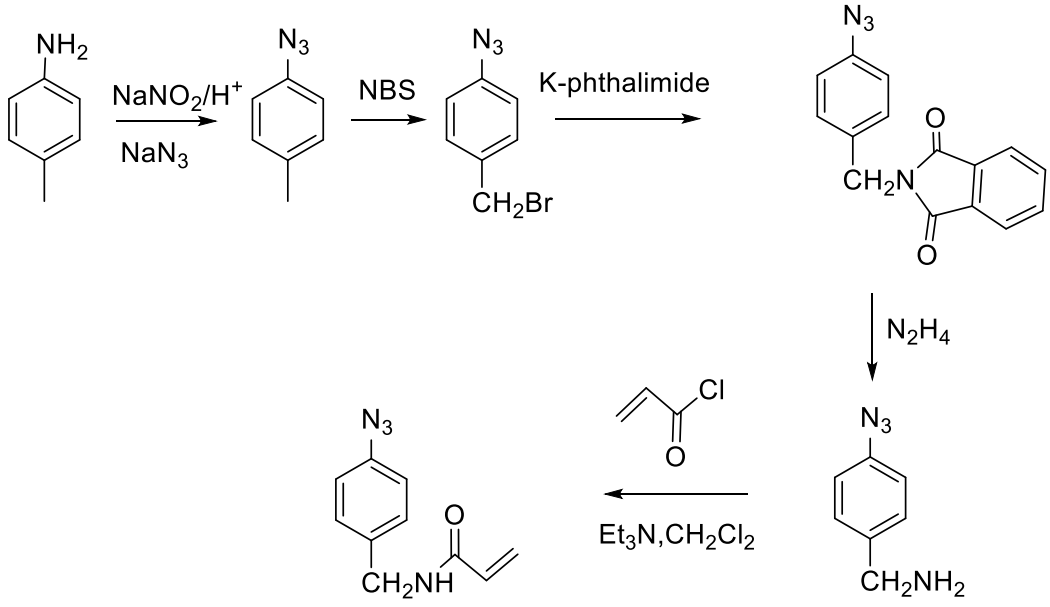

N-(4-azidobenzyl)acrylamide

Synthesis of PEO-b-PDEAm Diblock Copolymers and PEO-b-PDEAm-b-PDBAm Triblock Copolymers

N,*N*-Diethylacrylamide was chosen for the second block not only because PDEAm is a thermoresponsive polymer with a reported thermal transition temperature (LCST ≈32 °C)[5-6] close to human body temperature but also because PDEAm does not contain any hydrogen bond donor groups. Based on studies of PEO-*b*-PNIPAM-*b*-PI and PEO-*b*-PEO/PBO-*b*-PI thermally responsive polymers, we believed that the absence of strong interchain hydrogen bonding in the central thermally responsive block would accelerate the reaggregation of small assemblies into larger assemblies. *N*,*N*-Dibutylacrylamide, which is similar in structure to *N*,*N*-diethylacrylamide and ease of synthesis and polymerization by RAFT, was chosen as a monomer for the hydrophobic block. There is literature precedent for preparation of PEO-*b*-DMA diblock copolymers by RAFT polymerization with similar PEO-based macro-CTAs reported by McCormick and coworkers.[16] Using AIBN as the initiator, DEAm and DBAm were sequentially polymerized with the PEO macro-CTA in a controlled manner in 1,4-dioxane at 80 °C for 24h(Scheme 2-3). Our attempts to conduct the polymerization at 70 °C for 24 h, as previously reported for preparation of PEO-*b*-DMA diblock copolymers,[16] were not successful due to very slow conversion.

Scheme 2-3. Synthesis of PEO_{45}-*b*-$PDEAm_x$ Diblock Copolymers and PEO_{45}-*b*-$PDEAm_x$-*b*-$PDBAm_y$ Triblock Copolymers

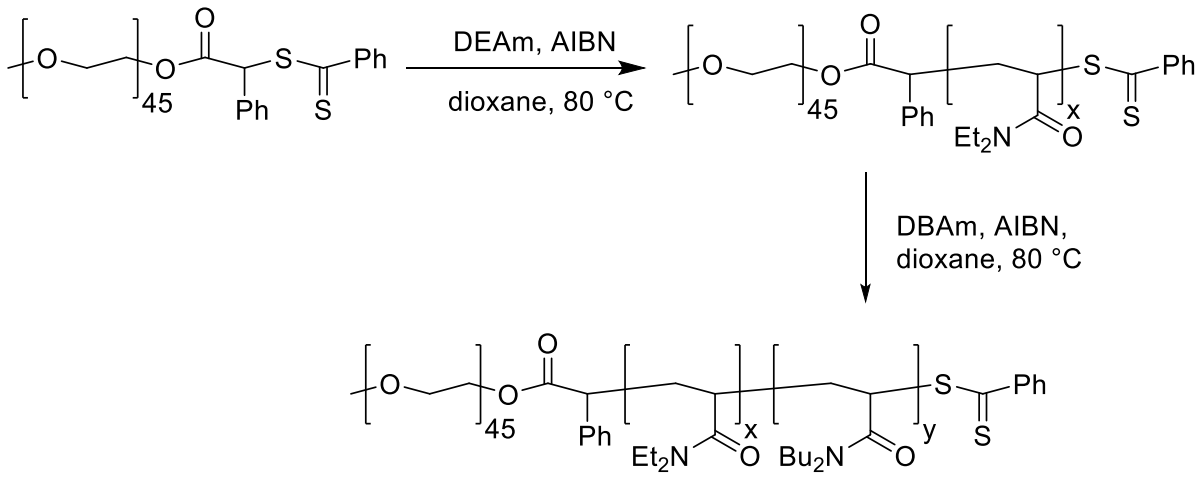

Monomer conversion was estimated based upon integrations of residual monomer vinyl proton peaks in ^{1}H NMR spectra of the crude reaction mixtures. PEO_{45}-*b*-$PDEAm_{41}$ is described as an example. In the ^{1}H NMR spectra of the PEO_{45}-*b*-$PDEAm_{41}$ crude reaction mixtures (Figure 3-5), the integration of the residual DEAm vinyl proton peak at 6.51 ppm was set to 1.00. The integrated area (42.75) under the two $-CH_3$ peaks (δ 0.8-1.2 ppm) from DEAm and PDEAm was then compared to the residual vinyl proton peak. Assuming that blocking efficiency of PEO-CTA is 100%, and all monomer that was lost from the reaction mixture was converted to polymer, the calculated conversion by ^{1}H NMR is: 1-[1/(42.75/6)] = 0.86. The calculated conversion value was then used to calculate $M_{n,HNMR}$ by equation 2-1 below:

$$M_{n,HNMR}=\frac{[\text{Monomer}]}{[\text{CTA}]}\times M.W.(\text{Monomer})\times conversion + M.W.(\text{PEO}-\text{CTA}) \qquad (2\text{-}1)$$

where *M.W.* (Monomer) is the molecular weight of monomer; *M.W.* (PEO-CTA) is the molecular weight of the PEO-CTA; [Monomer] and [CTA] are, respectively, concentrations of monomer and PEO-CTA in the initial reaction mixture.

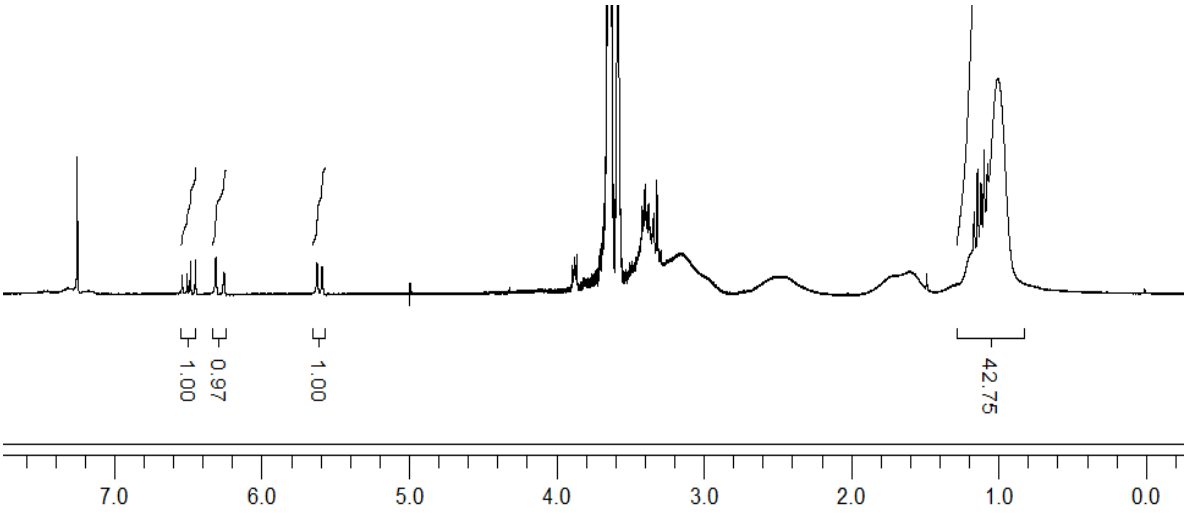

Figure 2-5. ^{1}H NMR spectrum of PEO_{45}-*b*-$PDEAm_{41}$ crude mixture after 24 h polymerization at 80 °C.

For PEO_{45}-*b*-$PDEAm_x$-*b*-$PDBAm_y$ triblock copolymers, after 40-48 h at 80 °C, a very small DBAm vinyl residue proton peak was observed in the ^{1}H NMR spectrum of crude mixture (see Figure 2-6). In this case, we assumed greater than 99% DBAm conversion was achieved.

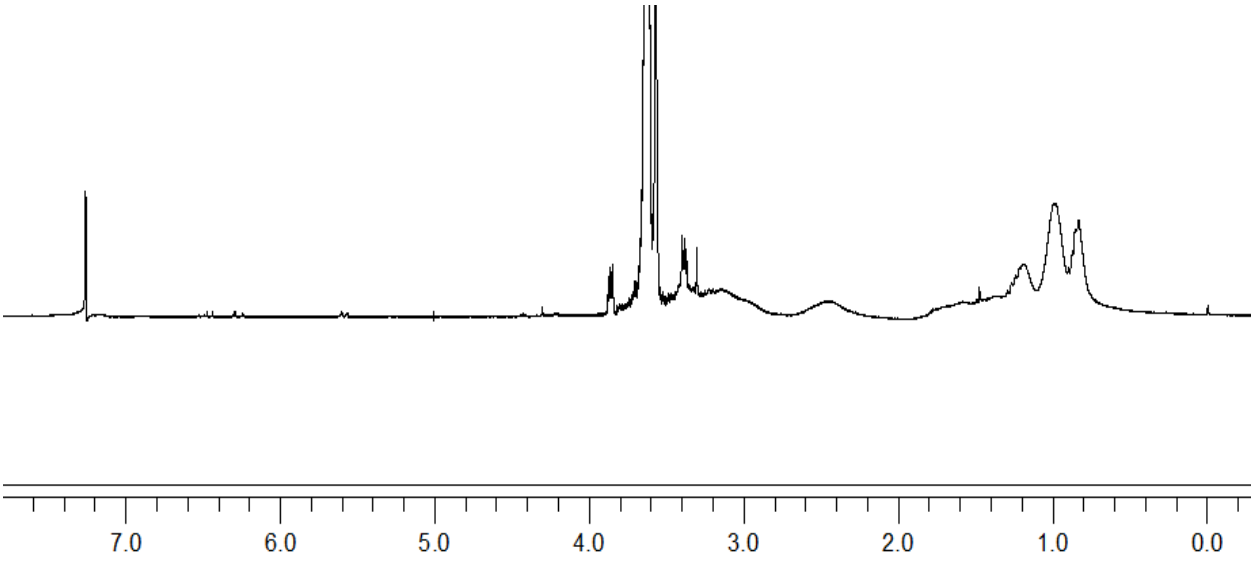

Figure 2-6. ^{1}H NMR spectrum of PEO_{45}-*b*-$PDEAm_{41}$-*b*-$PDBAm_{12}$ crude mixture after 40 h polymerization at 80 °C.

Figure 2-7 compares three different ^{1}H NMR spectra of purified PEO_{45} macro-CTA (top), PEO_{45}-$PDEAm_{41}$ diblock (mid), and PEO_{45}-$PDEAm_{41}$-$PDBAm_{12}$ triblock copolymers (bottom). The peak around 3.5-4 ppm results from the four protons per repeating unit (CH_2-CH_2-O-) in the PEO block, and the broad peak around 0.8-1.4 ppm arises from the –CH_3 protons in the PDEAm and PDBAm blocks. The two broad peaks around 1.5-3 ppm are three backbone protons per repeating unit (-CH_2-CHR-) in the PDEAm and PDBAm blocks.

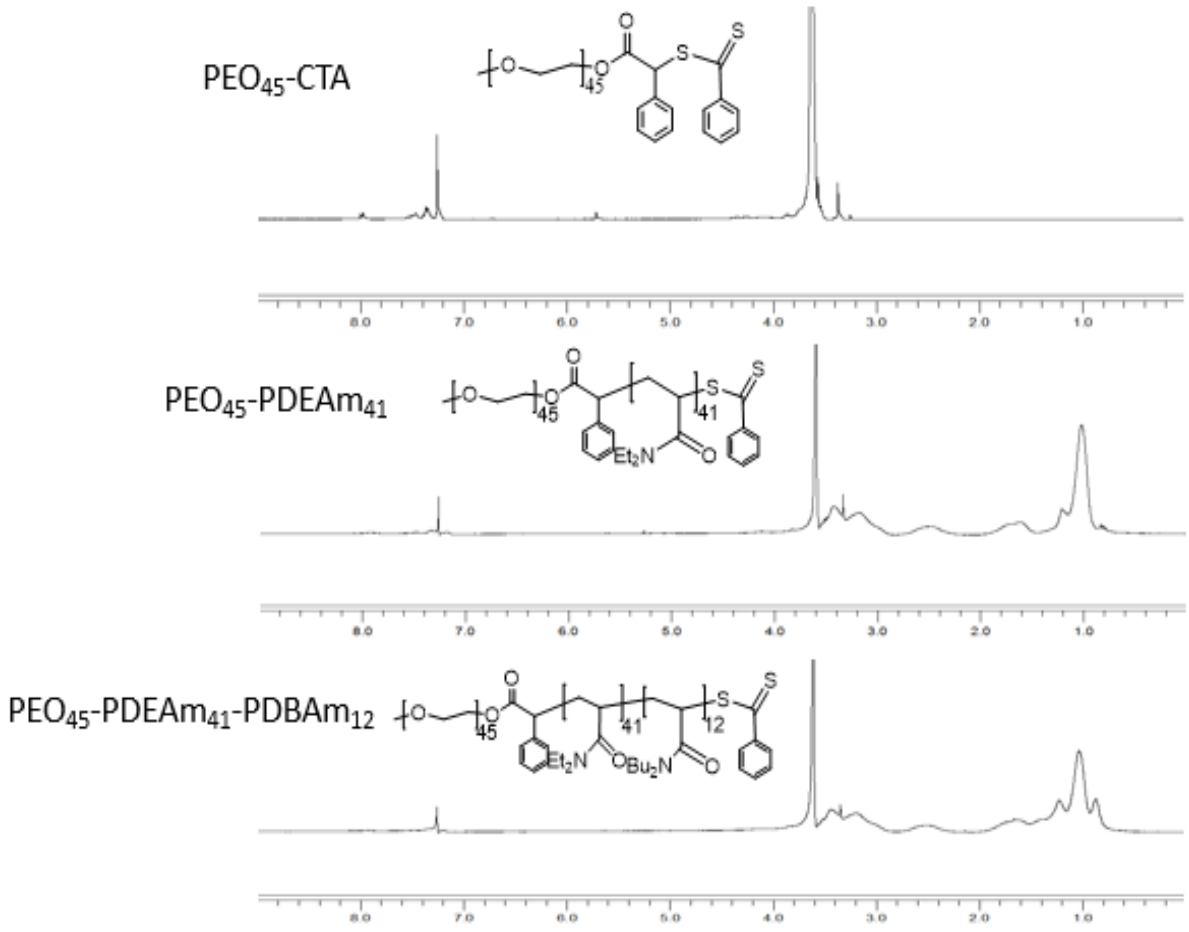

Figure 2-7. ^{1}H NMR spectra of PEO_{45} macro-CTA (top), PEO_{45}-$PDEAm_{41}$ diblock (middle) and PEO_{45}-$PDEAm_{41}$-$PDBAm_{12}$ triblock copolymers (bottom).

The clear shifts in retention time for the four SEC traces confirmed the different molecular weights of PEO-PDEAm diblock copolymers (Figure 2-8). Figure 2-9 compares GPC traces for PEO_{45} macro-CTA (blue), PEO_{45}-$PDEAm_{41}$ diblock (red) and PEO_{45}-PDEAm41-$PDBAm_{22}$ triblock copolymers (black) in tetrahydrofuran. The shifts in retention times from macro-CTA to diblock copolymer to triblock copolymer, the low polydispersities ($Đ$ slightly increase from 1.2 to 1.3), and the absence of significant low molecular weight shoulders observed in GPC traces, suggest that PDEAm and PDBAm blocks were efficiently grown from the PEO macro-CTA in a controlled manner.

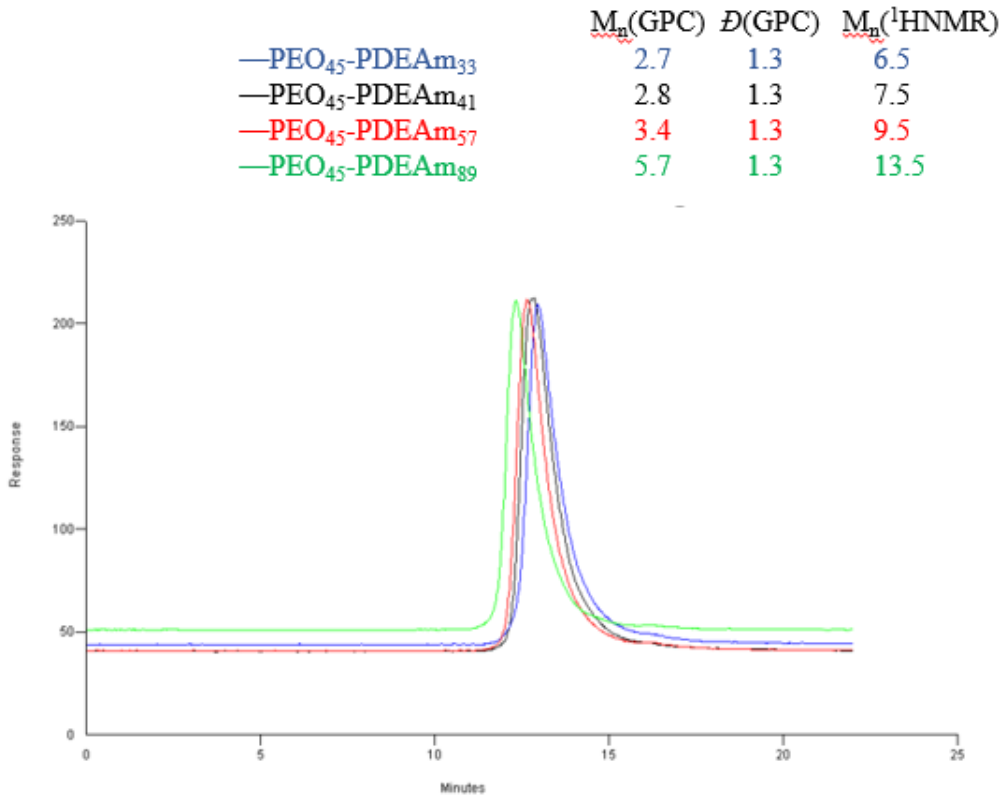

Figure 2-8. GPC traces of PEO_{45}-$PDEAm_{33}$ diblock (blue), PEO_{45}-$PDEAm_{41}$ diblock (black), PEO_{45}-$PDEAm_{57}$ diblock (red) and PEO_{45}-$PDEAm_{89}$ diblock (green) in tetrahydrofuran. All M_n values are reported in kg/mol.

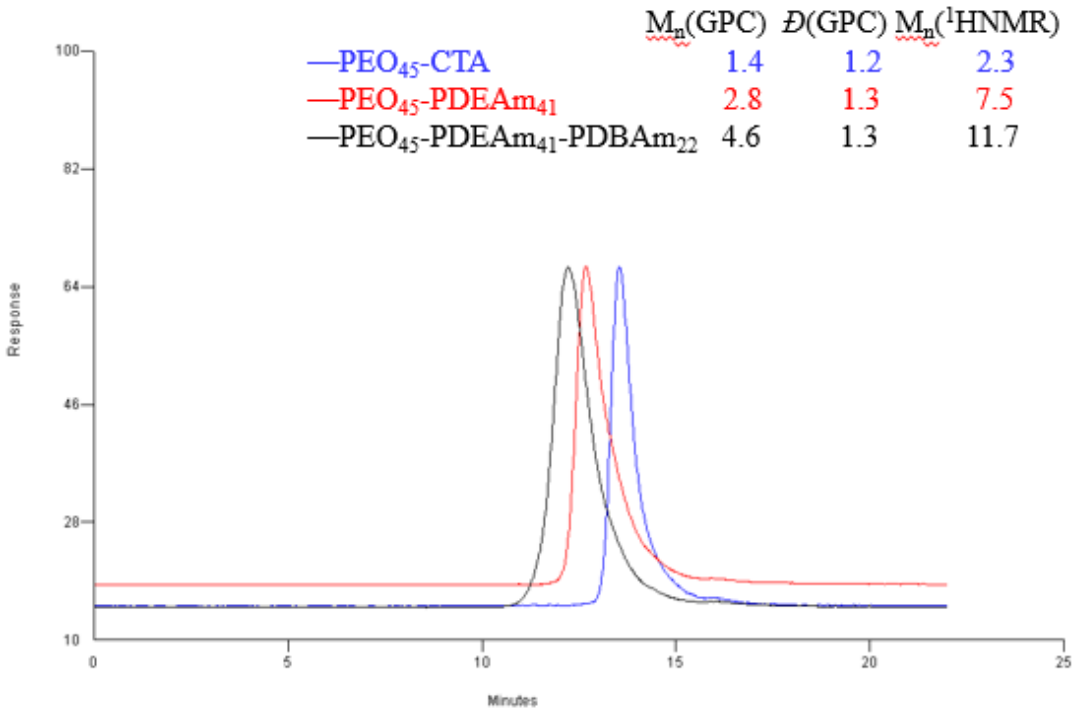

Figure 2-9. GPC traces of PEO_{45} macro-CTA (blue), PEO_{45}-$PDEAm_{41}$ diblock (red) and PEO_{45}-$PDEAm_{41}$-$PDBAm_{22}$ triblock copolymer (black) in tetrahydrofuran. All M_n values are reported in kg/mol.

Two PEO_{45}-*b*-$PDEAm_{41}$-*b*-$PDBAm_x$* triblock copolymers (x = 12, 22) containing photo-cross-linkable azide-functionalized monomers in the PDBAm block were also synthesized by copolymerization of *N*,*N*-dibutylacrylamide with *N*-(4-azidobenzyl)acrylamide in a 10/1 molar ratio at 80 °C. The yellow color of the purified PEO_{45}-*b*-$PDEAm_{41}$-*b*-$PDBAm_x$* samples, different

from the pink color in the PEO_{45}-*b*-$PDEAm_{41}$-*b*-$PDBAm_x$, suggested successful incorporation of azide photo cross-linker monomer into the hydrophobic block through copolymerization. The acryloyl and phenyl proton peaks were too small for integration in the ^1H NMR spectra (Figure A1.15) of PEO_{45}-*b*-$PDEAm_{41}$-*b*-$PDBAm_x$* triblock copolymers, since the degree of polymerization of *N*-(4-azidobenzyl)acrylamide is only 1 or 2 in the hydrophobic block.

Scheme 2-4. Synthesis of PEO_{45}-*b*-$PDEAm_{41}$-*b*-$PDBAm_x$* Triblock Copolymers

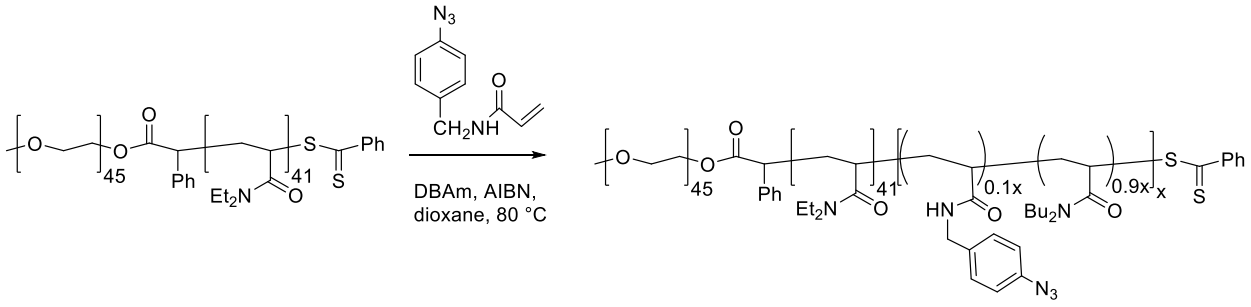

2.4 Conclusion

A library of PEO_{45}-*b*-$PDEAm_x$-*b*-$PDBAm_y$ triblock copolymers, each containing PEO blocks of identical molecular weight ($Mn,_{PEO}$ = 2000 g/mol), poly(*N*,*N*-diethylacrylamide) (PDEAm) blocks with 4 different compositions ($Mn,_{PDEAm} \approx$ 4200, 5200, 7200, 11200 g/mol), and poly(*N*,*N*-dibutylacrylamide) (PDBAm) hydrophobic blocks over a range of molecular weights (2 kg/mol < Mn < 33 kg/mol), was successfully synthesized by RAFT polymerization. The hydrophobic weight fractions of the PDBAm blocks (W_{PDBAm}), calculated by the mass of the PDBAm block to the total mass of polymer, vary from 0.1 to 0.8 in the PEO_{45}-*b*-$PDEAm_x$-*b*-$PDBAm_y$ series. ^{1}HNMR studies of crude mixtures indicated more than 80% PDEAm conversions were achieved within 24 h at 80 °C, while more than 99% PDBAm conversions were achieved at polymerization times of 40 h or longer at 80 °C. In addition, two PEO_{45}-*b*-$PDEAm_{41}$-*b*-$PDBAm_x$* (x=12, 22) triblock copolymers containing photo-cross-linkable azide groups in the hydrophobic

block were also synthesized by copolymerization of *N*,*N*-dibutylacrylamide with *N*-(4-azidobenzyl)acrylamide in a 10/1 molar ratio. The results are summarized in Table 2-1 and Table 2-2.

Table 2-1. RAFT polymerization conditions for PEO-PDEAm, PEO-PDEAm-PDBAm and PEO-PDEAm-PDBAm* block copolymers.[a]

	CTA/monomer/AIBN (mmol)	1,4-Dioxane (mL)	time (h)	Conversion (^{1}HNMR)
PEO_{45}-$PDEAm_{41}$	0.40/19/0.048	2.0	24	86%
PEO_{45}-$PDEAm_{41}$-$PDBAm_{6}$	0.08/0.48g/0.012	1.0	40	>99%
PEO_{45}-$PDEAm_{41}$-$PDBAm_{12}$	0.10/1.2/0.012	1.0	40	>99%
PEO_{45}-$PDEAm_{41}$-$PDBAm_{16}$	0.13/2.1/0.016	1.0	40	>99%
PEO_{45}-$PDEAm_{41}$-$PDBAm_{22}$	0.10/2.2/0.012	1.0	43	>99%
PEO_{45}-$PDEAm_{41}$-$PDBAm_{50}$	0.04/2.1/0.005	1.0	48	>99%
PEO_{45}-$PDEAm_{41}$-$PDBAm_{92}$	0.04/3.7/0.005	1.0	48	>99%
PEO_{45}-$PDEAm_{41}$-$PDBAm_{176}$	0.04/7.1/0.005	1.2	48	>99%
PEO_{45}-$PDEAm_{89}$	0.20/56/0.024	2.0	26	90%
PEO_{45}-$PDEAm_{89}$-$PDBAm_{12}$	0.025/0.31/0.003	1.0	48	>99%
PEO_{45}-$PDEAm_{89}$-$PDBAm_{24}$	0.025/0.62/0.003	1.0	48	>99%
PEO_{45}-$PDEAm_{89}$-$PDBAm_{32}$	0.025/0.81g/0.003	1.0	48	>99%
PEO_{45}-$PDEAm_{89}$-$PDBAm_{37}$	0.025/0.94/0.003	1.0	48	>99%
PEO_{45}-$PDEAm_{89}$-$PDBAm_{74}$	0.025/1.87/0.003	1.0	48	>99%
PEO_{45}-$PDEAm_{89}$-$PDBAm_{109}$	0.025/2.74/0.003	1.0	48	>99%
PEO_{45}-$PDEAm_{89}$-$PDBAm_{173}$	0.025/4.4/0.003	1.0	48	>99%
PEO_{45}-$PDEAm_{89}$-$PDBAm_{296}$	0.025/7.5/0.003	1.0	72	>99%
PEO_{45}-$PDEAm_{57}$	0.30/19.6/0.036	2.0	24	87%
PEO_{45}-$PDEAm_{57}$- $PDBAm_{12}$	0.10/12.3/0.012	1.5	48	>99%
PEO_{45}-$PDEAm_{57}$- $PDBAm_{26}$	0.025/0.65/0.003	1.0	48	>99%
PEO_{45}-$PDEAm_{57}$- $PDBAm_{52}$	0.025/1.3/0.003	1.0	48	>99%

PEO_{45}-$PDEAm_{33}$	0.22/7.3/0.03	1.5	24	84%
PEO_{45}-$PDEAm_{33}$- $PDBAm_{6}$	0.075/0.46/0.009	1.2	48	>99%
PEO_{45}-$PDEAm_{41}$-$PDBAm_{12}$*	0.05/0.6/0.006	1.0	40	>99%
PEO_{45}-$PDEAm_{41}$-$PDBAm_{22}$*	0.05/1.1/0.006	1.0	40	>99%

(a) All polymerizations run in 1,4-dioxane at 80 °C.

Table 2-2. Molecular characteristics of PEO-PDEAm, PEO-PDEAm-PDBAm and PEO-PDEAm-PDBAm* block copolymers.

	M_n (^{1}H NMR) by block (kg/mol)[a]	M_n (SEC) (kg/mol)[b]	M_w/M_n (SEC)[b]	Hydrophobic weight fraction (W_{PDBAm})[c] at 25 °C
PEO_{45}-CTA	O2.0	1.4	1.2	0
PEO_{45}-$PDEAm_{41}$	O2.0-E5.2	2.8	1.3	0
PEO_{45}-$PDEAm_{41}$-$PDBAm_{6}$	O2.0-E5.2-B1.1	3.6	1.3	0.13
PEO_{45}-$PDEAm_{41}$-$PDBAm_{12}$	O2.0-E5.2-B2.2	3.8	1.3	0.22
PEO_{45}-$PDEAm_{41}$-$PDBAm_{16}$	O2.0-E5.2-B2.9	4.1	1.3	0.28
PEO_{45}-$PDEAm_{41}$-$PDBAm_{22}$	O2.0-E5.2-B4.2	4.6	1.3	0.36
PEO_{45}-$PDEAm_{41}$-$PDBAm_{50}$	O2.0-E5.2-B9.2	6.4	1.4	0.55
PEO_{45}-$PDEAm_{41}$-$PDBAm_{92}$	O2.0-E5.2-B16.8	8.1	1.5	0.70
PEO_{45}-$PDEAm_{41}$-$PDBAm_{176}$	O2.0-E5.2-B32.2	11.4	1.7	0.80
PEO_{45}-$PDEAm_{89}$	O2.0-E11.3	5.1	1.3	0
PEO_{45}-$PDEAm_{89}$-$PDBAm_{12}$	O2.0-E11.3-B2.2	5.7	1.4	0.14
PEO_{45}-$PDEAm_{89}$-$PDBAm_{24}$	O2.0-E11.3-B4.4	5.9	1.5	0.24
PEO_{45}-$PDEAm_{89}$-$PDBAm_{32}$	O2.0-E11.3-B6.0	6.2	1.5	0.30
PEO_{45}-$PDEAm_{89}$-$PDBAm_{37}$	O2.0-E11.3-B6.8	6.4	1.6	0.33
PEO_{45}-$PDEAm_{89}$-$PDBAm_{74}$	O2.0-E11.3-B13.6	7.4	1.6	0.50
PEO_{45}-$PDEAm_{89}$-$PDBAm_{109}$	O2.0-E11.3-B20.0	7.8	1.7	0.60

PEO_{45}-$PDEAm_{89}$-$PDBAm_{173}$	O2.0-E11.3-B31.7	10.0	1.7	0.70
PEO_{45}-$PDEAm_{89}$-$PDBAm_{296}$	O2.0-E11.3-B54.2	12.2	1.9	0.80
PEO_{45}-$PDEAm_{57}$	O2.0-E7.2	3.4	1.3	0
PEO_{45}-$PDEAm_{57}$- $PDBAm_{12}$	O2.0-E7.2-B2.2	4.4	1.3	0.19
PEO_{45}-$PDEAm_{57}$- $PDBAm_{26}$	O2.0-E7.2-B4.8	4.6	1.5	0.33
PEO_{45}-$PDEAm_{57}$- $PDBAm_{52}$	O2.0-E7.2-B9.5	5.5	1.6	0.50
PEO_{45}-$PDEAm_{33}$	O2.0-E4.2	2.7	1.3	0
PEO_{45}-$PDEAm_{33}$- $PDBAm_{6}$	O2.0-E4.2-B1.1	3.1	1.3	0.14
PEO_{45}-$PDEAm_{41}$-$PDBAm_{12}$*	O2.0-E5.2-B2.4*	3.7	1.3	0.25
PEO_{45}-$PDEAm_{41}$-$PDBAm_{22}$*	O2.0-E5.2-B4.6*	4.6	1.3	0.38

[a] Block names are abbreviated as O (PEO), E (PDEAm), and B (PDBAm). The number appearing after each letter corresponds to the molecular weight of each blocks in kg/mol as determined by ^{1}H NMR. Calculation based on the polymerization conversions determined by ^{1}H NMR of crude reaction mixtures and the true molecular weight of the PEO-CTA. [b] SEC in THF calibrated with PS standards. [C] Hydrophobic weight fraction (W_{PDBAm}) calculated by the mass of the PDBAm block to the total mass of polymer.

References (Chapter 2)

1. Sundararaman, A.; Stephan, T.; Grubbs, R. B., Reversible restructuring of aqueous block copolymer assemblies through stimulus-induced changes in amphiphilicity. *J. Am. Chem. Soc.* **2008,** *130* (37), 12264-12265. (doi: 10.1021/ja8052688)

2. Moughton, A. O.; O'Reilly, R. K., Thermally induced micelle to vesicle morphology transition for a charged chain end diblock copolymer. *Chem Commun (Camb)* **2010,** *46* (7), 1091-1093. (doi: 10.1039/b922289h)

3. Wei, K.; Su, L.; Chen, G.; Jiang, M., Does PNIPAM block really retard the micelle-to-vesicle transition of its copolymer? *Polymer* **2011,** *52* (16), 3647-3654. (doi: 10.1016/j.polymer.2011.06.005)

4. Cai, Y.; Aubrecht, K. B.; Grubbs, R. B., Thermally induced changes in amphiphilicity drive reversible restructuring of assemblies of ABC triblock copolymers with statistical polyether blocks. *J. Am. Chem. Soc.* **2011,** *133* (4), 1058-1065. (doi: 10.1021/ja109262h)

5. Lessard, D. G.; Ousalem, M.; Zhu, X. X.; Eisenberg, A.; Carreau, P. J., Study of the phase transition of poly(N,N-diethylacrylamide) in water by rheology and dynamic light scattering. *J Polym Sci Pol Phys* **2003,** *41* (14), 1627-1637. (doi: 10.1002/polb.10517)

6. Watanabe, R.; Takaseki, K.; Katsumata, M.; Matsushita, D.; Ida, D.; Osa, M., Characterization of poly(N,N-diethylacrylamide) and cloud points in its aqueous solutions. *Polym. J.* **2016,** *48* (5), 621-628. (doi: 10.1038/pj.2015.120)

7. Walther, A.; Millard, P. E.; Goldmann, A. S.; Lovestead, T. M.; Schacher, F.; Barner-Kowollik, C.; Muller, A. H. E., Bis-Hydrophilic Block Terpolymers via RAFT Polymerization: Toward Dynamic Micelles with Tunable Corona Properties. *Macromolecules* **2008,** *41* (22), 8608-8619. (doi: 10.1021/ma801215q)

8. Bergbreiter, D. E.; Aviles-Ramos, N. A.; Ortiz-Acosta, D., A combinatorial approach to studying the effects of N-alkyl groups on poly(N-alkyl and N,N-dialkylacrylamide) solubility. *J. Comb. Chem.* **2007,** *9* (4), 609-617. (doi: 10.1021/cc070016m)

9. Jiang, X.; Zhang, J.; Zhou, Y.; Xu, J.; Liu, S., Facile preparation of core-crosslinked micelles from azide-containing thermoresponsive double hydrophilic diblock copolymer via click chemistry. *J. Polym. Sci., Part A: Polym. Chem.* **2008,** *46* (3), 860-871. (doi: 10.1002/pola.22430)

10. Klapötke, T. M.; Krumm, B.; Piotrowski, H.; Polborn, K.; Holl, G., Synthesis and Structures of Trifluoromethyl-, Fluoro-, and Azido-Substituted Hexabenzylhexaazaisowurtzitanes and Isolation of a Novel Hexaazaisowurtzitane-Based Polycycle. *Chemistry – A European Journal* **2003,** *9* (3), 687-694. (doi: 10.1002/chem.200390077)

11. Jones, M. W.; Mantovani, G.; Blindauer, C. A.; Ryan, S. M.; Wang, X.; Brayden, D. J.; Haddleton, D. M., Direct peptide bioconjugation/PEGylation at tyrosine with linear and branched polymeric diazonium salts. *J. Am. Chem. Soc.* **2012,** *134* (17), 7406-7413. (doi: 10.1021/ja211855q)

12. Duncan, R., The dawning era of polymer therapeutics. *Nat Rev Drug Discov* **2003,** *2* (5), 347-360. (doi: 10.1038/nrd1088)

13. Harris, J. M.; Chess, R. B., Effect of pegylation on pharmaceuticals. *Nat Rev Drug Discov* **2003,** *2* (3), 214-221. (doi: 10.1038/nrd1033)

14. Jiang, X. Z.; Zhang, J. Y.; Zhou, Y. M.; Xu, J.; Liu, S. Y., Facile preparation of core-crosslinked micelles from azide-containing thermoresponsive double hydrophilic diblock

copolymer via click chemistry. *J Polym Sci Pol Chem* **2008,** *46* (3), 860-871. (doi: 10.1002/pola.22430)

15. Klapotke, T. M.; Krumm, B.; Piotrowski, H.; Polborn, K.; Holl, G., Synthesis and structures of trifluoromethyl-, fluoro-, and azido-substituted hexabenzylhexaazaisowurtzitanes and isolation of a novel hexaazaisowurtzitane-based polycycle. *Chemistry* **2003,** *9* (3), 687-694. (doi: 10.1002/chem.200390077)

16. Li, Y. T.; Lokitz, B. S.; McCormick, C. L., RAFT synthesis of a thermally responsive ABC triblock copolymer incorporating N-acryloxysuccinimide for facile in situ formation of shell cross-linked micelles in aqueous media. *Macromolecules* **2006,** *39* (1), 81-89. (doi: 10.1021/ma052116r)

Chapter 3 Self-assembly and Thermoresponsive Behavior of PEO-*b*-PDEAm-*b*-PDBAm Triblock Copolymers

3.1 Introduction

As described in Chapter 1.3, morphologies of amphiphilic block copolymer assemblies can be predicted by the packing parameter p[1-2] or a simplified model hydrophilic mass fraction f.[3] If the water solubility of the hydrophilic or hydrophobic block can be altered as a response to an external temperature change, the hydrophilic fraction f would change in response to the stimulus, and the morphology of the final stimuli-responsive polymer aggregates would be expected to undergo significant changes in shape and size. Several examples of thermally responsive polymers that can undergo thermally induced morphological transitions between two or more well-defined structures in dilute solution have been reported. Laschewsky and coworkers reported that the co-called "schizophrenic" block copolymers of *N*-isopropylacrylamide (NIPAM) and *3*-[*N*-(3-methacrylamidopropyl)-*N*,*N*-dimethyl]ammoniopropane sulfonate (SPP) could form PSPP-core micelles below 20 °C and PNIPAM-core micelles above 34 °C.[4] O'Reilly and coworkers reported that poly(*tert*-butyl acrylate)-*block*-PNIPAM diblock copolymers ($PtBuA_{3.2}$-*b*-$PNIPAM_{2.8}$, M_n=6.6 kg/mol) with a quaternary amine end could undergo a micelle-to-vesicle transition when heated at 65 °C for 1 week.[5] Recently, Steven Armes and coworkers reported that poly(glycerol monomethacrylate)-*block*-poly(2-hydroxypropyl methacrylate) ($PGMA_{54}$− $PHPMA_{140}$) diblock

copolymers could undergo a sphere-to-worm transition upon heating at 21°C.[6-9] Compared with AB diblock copolymers, there are very few literature reports describing thermally induced morphological transition of ABC triblock copolymers.[10-13]

Herein, we demonstrate the self-assembly of PEO-*b*-PDEAm-*b*-PDBAm triblock copolymers at 25 °C and their thermally induced morphological transitions between different aggregated structures upon heating. PEO-*b*-PDEAm-*b*-PDBAm triblock copolymers with different compositions in dilute solutions (0.10 w/w%) were found out to undergo micelle-to-vesicle, micelle-to-worm and micelle-to-large compound micelle transitions upon heating above the LCST of thermally responsive PDEAm block. In addition, based on a study of the thermally induced micelle-to-worm transition in dilute solution (0.10 w/w%), we designed a novel rapidly reversible thermoresponsive PEO-*b*-PDEAm-*b*-PDBAm triblock copolymer worm gel at a higher copolymer concentration (5.0 w/w%). There is a significant structural difference between this worm gel and other reported ABC thermally responsive micellar gels[14-21] in which A and C are both hydrophobic blocks and B is a hydrophilic bridging block. Hillmyer and Lodge reported poly(ethylene-*alt*-propylene)-*b*-poly(ethylene oxide)-*b*-poly(*N*-isopropyl-acrylamide) (PEP-*b*-PEO-*b*-PNIPAm) triblock copolymers that form micelles in water at lower temperatures with hydrophobic PEP cores surrounded by hydrophilic PEO-PNIPAm coronae. After heating above the lower critical solution temperature (LCST) of the PNIPAm block, these micelles associate to form soft hydrogels.[18, 21] Similarly, Duvall and coworkers synthesized an ABC triblock polymer poly(propylenesulfide)-*block*-poly(*N*,*N*-dimethylacrylamide)-*block*-poly(*N*-isopropyl-acrylamide)] ($PPS_{4.4}$-*b*-$PDMA_{15.9}$-*b*-$PNIPAAM_{16.5}$, M_n=37.1 kg/mol) that forms physically cross-linked hydrogels through association of spherical micelles into a micellar network.[19] At 25 ˚C, PPS-*b*-PDMA-*b*-PNIPAAM forms spherical micelles (66 nm) comprising a hydrophobic PPS core

and PNIPAAM on the outer corona. Upon heating above 37 ˚C, which exceeds the lower critical solution temperature (LCST) of PNIPAAM, micelle solutions (≥2.5 wt %) sharply transitioned into stable, hydrated gels. TEM and STEM-EDS (Figure 3-1) showed an increase in the number and density of micelles and a more ordered structure for samples dried at 37 °C.

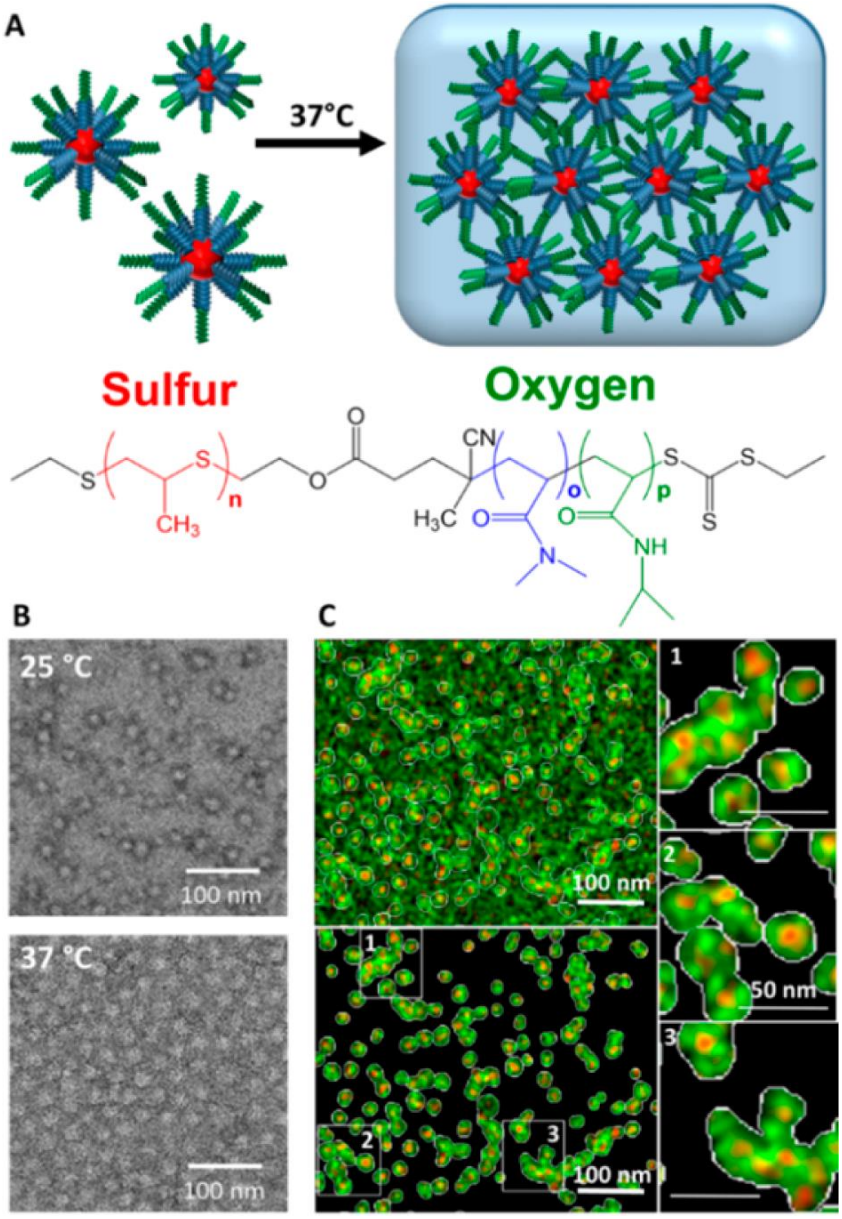

Figure 3-1. TEM/STEM-EDS confirmation of temperature dependent morphology switch for PPS_{60}-*b*-$PDMA_{150}$-*b*-$PNIPAAM_{150}$ triblock copolymers. (A) Schematic representation of micelle

gelation at 37 °C and polymer architecture coordinating with STEM-EDS element maps. (B) TEM images of PPS_{60}-*b*-$PDMA_{150}$-*b*-$PNIPAAM_{150}$ micelles at 25 and 37 °C. (C) STEM-EDS element maps for sulfur (red) and oxygen (green) of PPS_{60}-*b*-$PDMA_{150}$-*b*-$PNIPAAM_{150}$ core−shell compartments at 37 °C with image thresholding and background subtraction. Core-forming PPS produces the red signal for sulfur, while oxygen (appearing green) is present in the PDMA and PNIPAAM corona-forming blocks. Reprinted with permission from reference[19]. Copyright (2014) American Chemical Society.

As far as we are aware, there are few literature reports describing thermally responsive ABC triblock copolymer worm gels. Recently, Armes and coworkers reported that poly(glycerol monomethacrylate)-*block*-poly(2-hydroxypropyl methacrylate) ($PGMA_{54}$− $PHPMA_{140}$) diblock copolymers, synthesized via RAFT aqueous dispersion polymerization, can form relatively soft, free-standing worm hydrogels (Figure 3-2) in water (10 w/w%) at room temperature that undergo de-gelation due to a worm-to-sphere morphological transition on cooling to 5 °C.[6-9]

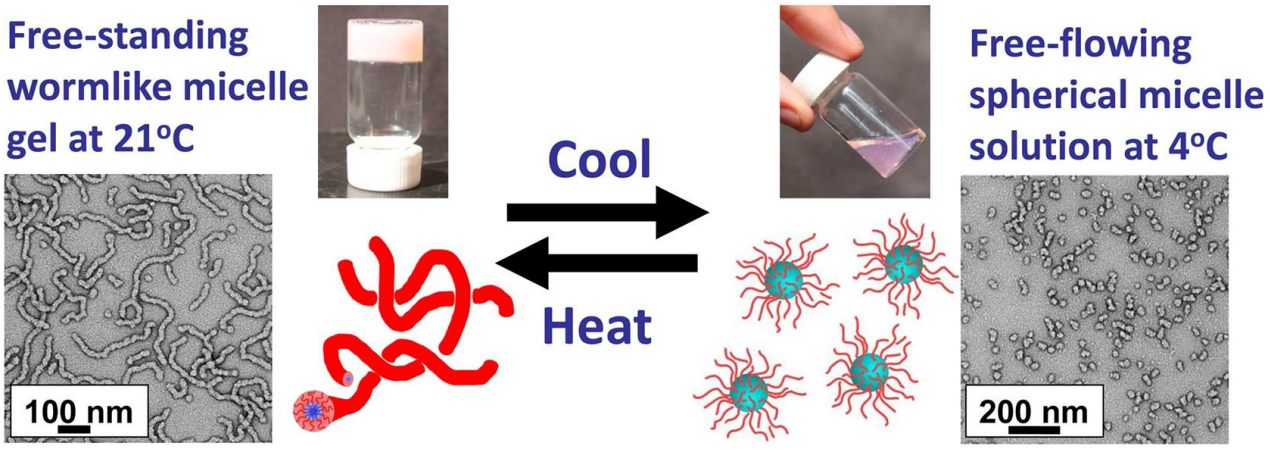

Figure 3-2. Thermally responsive aqueous solution behavior of a 10 w/w % aqueous dispersion of $PGMA_{54}$−$PHPMA_{140}$ diblock copolymer particles. Reprinted with permission from reference[9]. Copyright (2014) American Chemical Society

3.2 Characterization

Dynamic Light Scattering (DLS). Intensity-average hydrodynamic diameters of the dispersions (0.10 w/v %) in disposable cuvettes were obtained by DLS using a Malvern Zetasizer NanoZS instrument, which was equipped with a 633 nm laser source and a backscattering detector. All data were averaged over three consecutive runs. Temperature-dependent DLS studies were performed at 0.2 °C/min heating rate from 25 °C to 60 °C.

Transmission Electron Microscopy (TEM). PEO-*b*-PDEAm-*b*-PDBAm polymers, synthesized by RAFT polymerization in Chapter 2.2, were dissolved in water at 25 °C to generate 0.10 w/w % dispersions. Copper grids (400 mesh, Ted Pella product #01822) were plasma glow-discharged for 60 s to create a hydrophilic surface. Individual samples (0.10 w/v %, 5 μL) were adsorbed onto the freshly glow-discharged grids for 3 min and then blotted with filter paper to remove excess solution. To stain the aggregates, uranyl acetate (0.20 w/v %) solution (4 μL) was soaked on the sample-loaded grid for 15 s. After blotting excess stain solution, the grid was left to air-dry. For TEM sample preparation at higher temperature, the grid was immersed in the polymer solution heating at 55 °C or 60 °C on a hot plate for 2-3 min and then stained as described above, and excess uranyl acetate solution was removed immediately via blotting after 15s. The grids were observed by TEM with a JEOL-1400 electron microscope at 120 kV at the Center for Functional Nanomaterials, Brookhaven National Lab.

Rheology studies. All rheology studies were performed in oscillatory shear mode on either a TA Instruments AR-G2 rheometer or a TA Instruments DHR-II rheometer, using a 40-mm aluminum parallel plate geometry and a Peltier plate for temperature control. All oscillatory tests were performed within the linear viscoelastic region determined from strain sweeps at 55 °C and 10 Hz. Frequency sweeps at a fixed strain of 5% strain were performed at 25 °C (liquid), 45 °C (near

gelation point), and 55 °C (gel) to determine the G' and G". Temperature sweeps were performed at a fixed strain of 5% and an angular frequency of 1.0 Hz. A two-minute equilibration time was taken before measurement at each temperature.

3.3 Assembly of PEO_{45}-*b*-$PDEAm_x$-*b*-$PDBAm_y$ in water at 25 °C

A library of PEO_{45}-*b*-$PDEAm_x$-*b*-$PDBAm_y$ triblock copolymers, synthesized by RAFT polymerization in Chapter 2, was dissolved in distilled-deionized water (1 mg polymer/mL water; 0.1 w/w %) at 25 °C. The triblock copolymers with smaller hydrophobic blocks ($M_{n,PDBAm}$ < 3000g/mol) gave clear solutions after stirring for less than 1 h, while the triblock copolymers containing larger hydrophobic blocks ($M_{n,PDBAm}$ > 3000 g/mol) gave cloudy dispersions, even after stirring for over 24 h.

Transmission electron microscopy (TEM) studies on samples of PEO_{45}-*b*-$PDEAm_x$-*b*-$PDBAm_y$ triblock copolymers cast from dilute aqueous solution (0.1 w/w%) at 25 °C were conducted to access their morphologies. PEO_{45}-*b*-$PDEAm_{41}$-*b*-$PDBAm_{12}$ exclusively formed spherical micelles due to its large hydrophilic mass fraction (f = 0.78) at 25 °C (Figure 3-3a). Slightly increasing the hydrophobic PDBAm length leads to formation of a mixture of short worms and spherical micelles for PEO_{45}-*b*-$PDEAm_{41}$-*b*-$PDBAm_{16}$ (Figure 3-3b). PEO_{45}-*b*-$PDEAm_{41}$-*b*-$PDBAm_{22}$ with a still larger PDEAm chain formed long wormlike micelles (Figure 3-3c), while PEO_{45}-*b*-$PDEAm_{41}$-*b*-$PDBAm_{50}$ formed an interesting intermediate structure comprising highly branched wormlike micelles networks with Y-junctions and branching loops (Figure 3-3d), which is similar in structure to those reported by Bates and co-workers in poly(butadiene-*b*-ethylene oxide) (PB-PEO)[22] and Rolf Schubert and co-workers in poly(2-vinylpyridine-b-ethylene oxide) (P2VP-PEO) diblock copolymers.[23] Increasing the length of the hydrophobic block even further with PEO_{45}-*b*-$PDEAm_{41}$-*b*-$PDBAm_{92}$ resulted in the formation of a mixture of worms and vesicles

(Figure 3-3e). Finally, large compound micelles without any bilayer contrast, structurally similar to those observed by Eisenberg in polystyrene-*b*-poly(acrylic acid) (PS_{200}-*b*-PAA_4) diblock copolymers[24-25] and Armes in poly(glycerol monomethacrylate)-poly(2-hydroxypropyl methacrylate) (G_{55}-H_{2000}) diblock copolymers[26] were formed by PEO_{45}-*b*-$PDEAm_{41}$-*b*-$PDBAm_{176}$ due to a small hydrophilic mass fraction (f =0.2) (Figure 3-3f). It is consistent with the prediction that polymers with $f < 0.25$ leads to the formation of large inverted structures.[3]

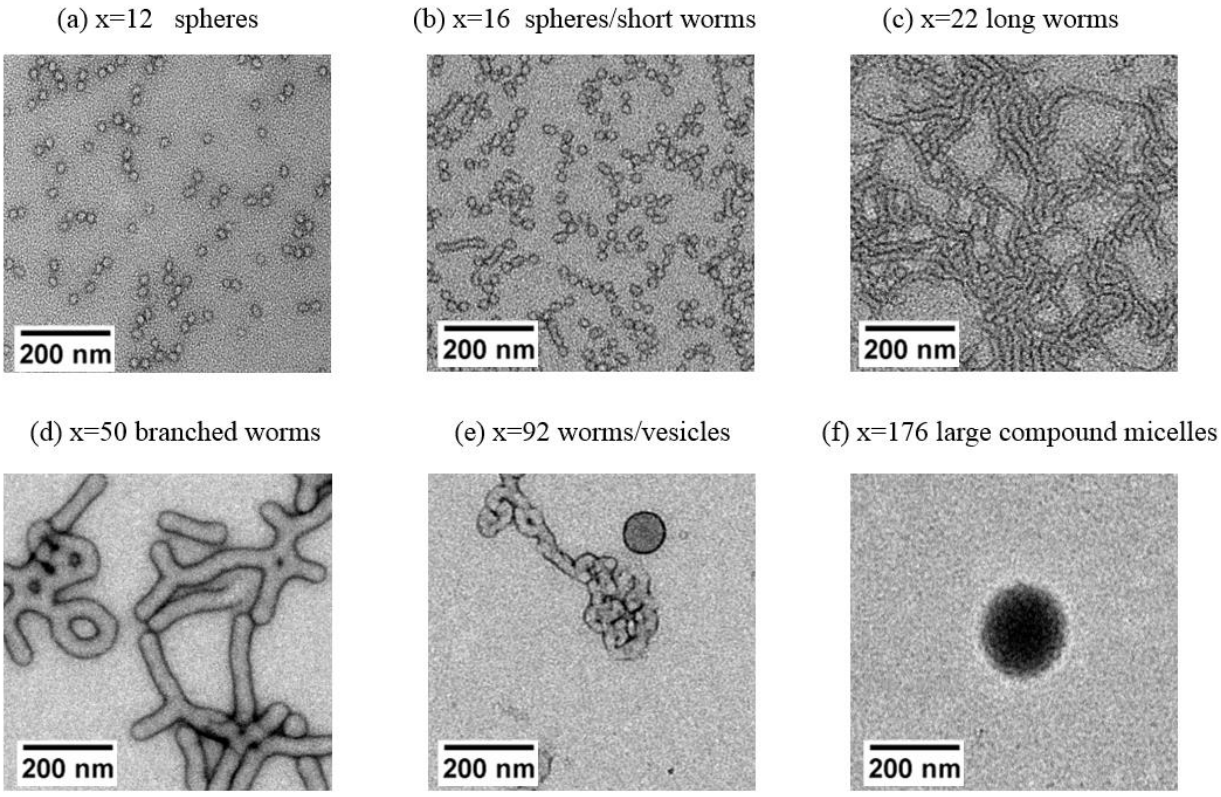

Figure 3-3. Representative TEM images of PEO_{45}-*b*-$PDEAm_{41}$-*b*-$PDBAm_x$ triblock copolymers in water (0.1 w/w %) at 25 °C , where x corresponds to (a) 12, (b) 16, (c) 22, (d) 50, (e) 92, (f) 176. Spherical, worm-like, vesicular and large compound spherical nanostructures are observed as

the length of hydrophobic PDBAm block increases. (See unprocessed micrographs in Appendix C)

From the series of PEO_{45}-*b*-$PDEAm_{89}$-*b*-$PDBAm_x$ triblock copolymers with a longer middle PDEAm block, a spherical micelle morphology was observed when the average degree of polymerization of the hydrophobic PDBAm block is 12. (Figure 3-4a). Increasing the average PDBAm degree of polymerization to 24 leads to formation of a mixture of worms and spherical micelles for PEO_{45}-*b*-$PDEAm_{89}$-*b*-$PDBAm_{24}$ (Figure 3-4b). In contrast, PEO_{45}-*b*-$PDEAm_{89}$-*b*-$PDBAm_x$ samples with higher degrees of PDBAm polymerization (x = 37, 74, and 173) formed vesicles (Figure 3-4c, 4d, 4e), with an apparent increase in the diameter of vesicles as the PDBAm hydrophobic length is increased. PEO_{45}-*b*-$PDEAm_{89}$-*b*-$PDBAm_{296}$, with the same hydrophilic mass fraction (f = 0.2) as PEO_{45}-*b*-$PDEAm_{41}$-*b*-$PDBAm_{176}$, formed large compound micelles (Figure 3-4f).

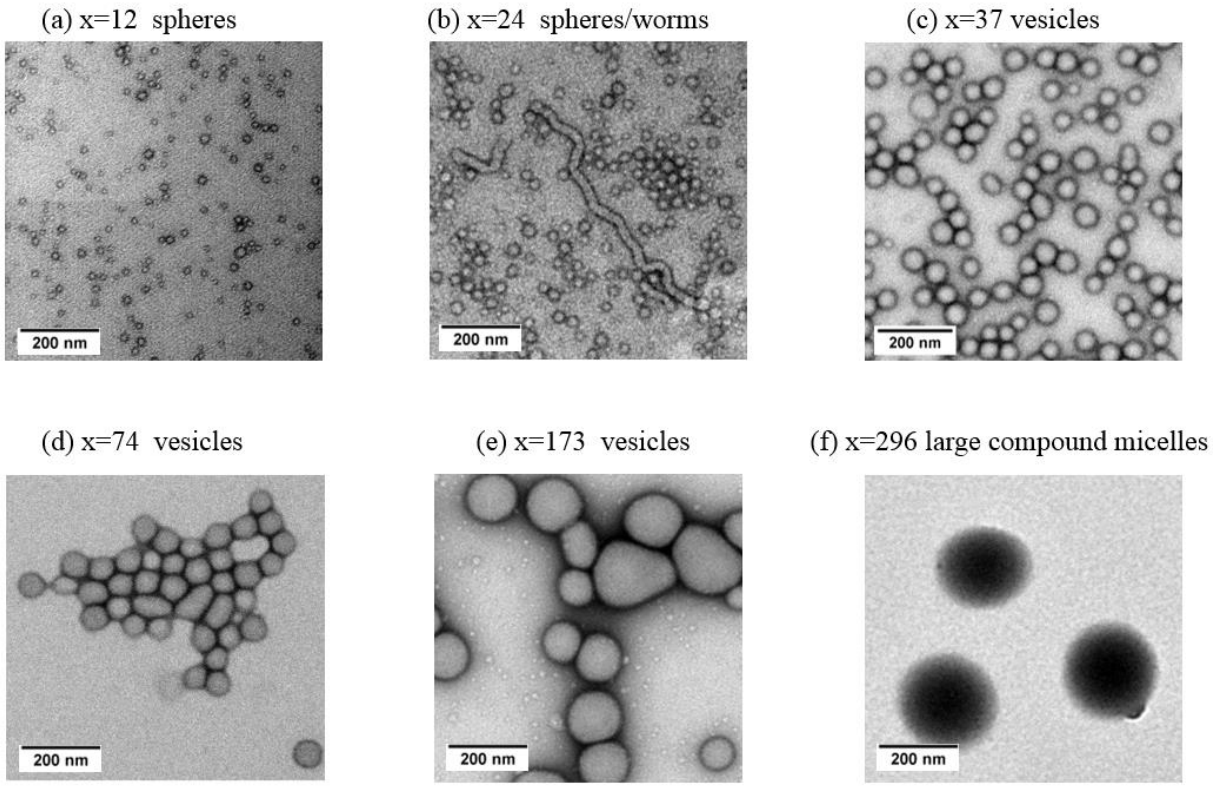

Figure 3-4. Representative TEM images of assembly morphologies in water (0.1 w/w %) observed for a series of six PEO_{45}-*b*-$PDEAm_{89}$-*b*-$PDBAm_x$ triblock copolymers at 25 °C, where x corresponds to (a) 12, (b) 24, (c) 37, (d) 74, (e) 173, (f) 296. Spherical, worm-like. vesicular and large compound spherical nanostructures are observed as the length of hydrophobic PDBAm block increases. (See unprocessed micrographs in Appendix C).

The hydrodynamic diameters (D_h) of polymer assemblies at 25 °C were measured by dynamic light scattering (DLS). The cloudy polymer dispersions resulting from polymers with larger PDBAm blocks (M_n > 3000 g/mol) were filtered (1 μm syringe filter) before DLS measurements. The DLS data (Figure 3-5 and 3-6) show that longer hydrophobic PDBAm blocks

lead to larger polymer aggregates within each polymer series, with the one exception that the hydrodynamic diameter of PEO_{45}-*b*-$PDEAm_{41}$-*b*-$PDBAm_{22}$ assemblies (D_h = 100 nm) is larger than that of PEO_{45}-*b*-$PDEAm_{41}$-*b*-$PDBAm_{50}$ assemblies(D_h = 92 nm). In DLS measurements, the reported hydrodynamic diameter of a nonspherical particle is the diameter of a sphere that has the same translational diffusion speed as the particle. As a result, assemblies such as PEO_{45}-*b*-$PDEAm_{41}$-*b*-$PDBAm_{50}$, with a branched worm-like morphology (Figure 3-3d) would be expected to show a smaller apparent diameter than assemblies with linear worm-like morphologies such as PEO_{45}-*b*-$PDEAm_{41}$-*b*-$PDBAm_{22}$ (Figure 3-3c).

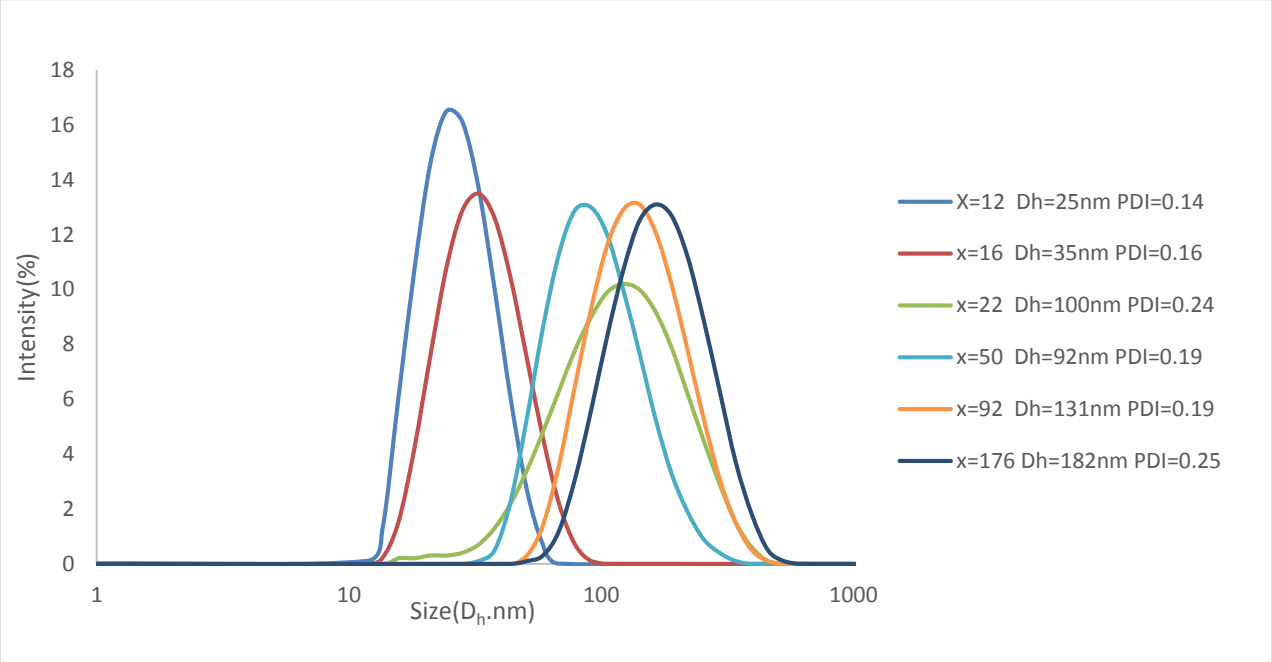

Figure 3-5. DLS particle size distributions (intensity vs mean hydrodynamic diameter, D_h) at 25 °C obtained for six PEO_{45}-*b*-$PDEAm_{41}$-*b*-$PDBAm_x$ triblock copolymers, where x corresponds to (a) 12, (b) 16, (c) 22, (d) 50, (e) 92, (f) 176.

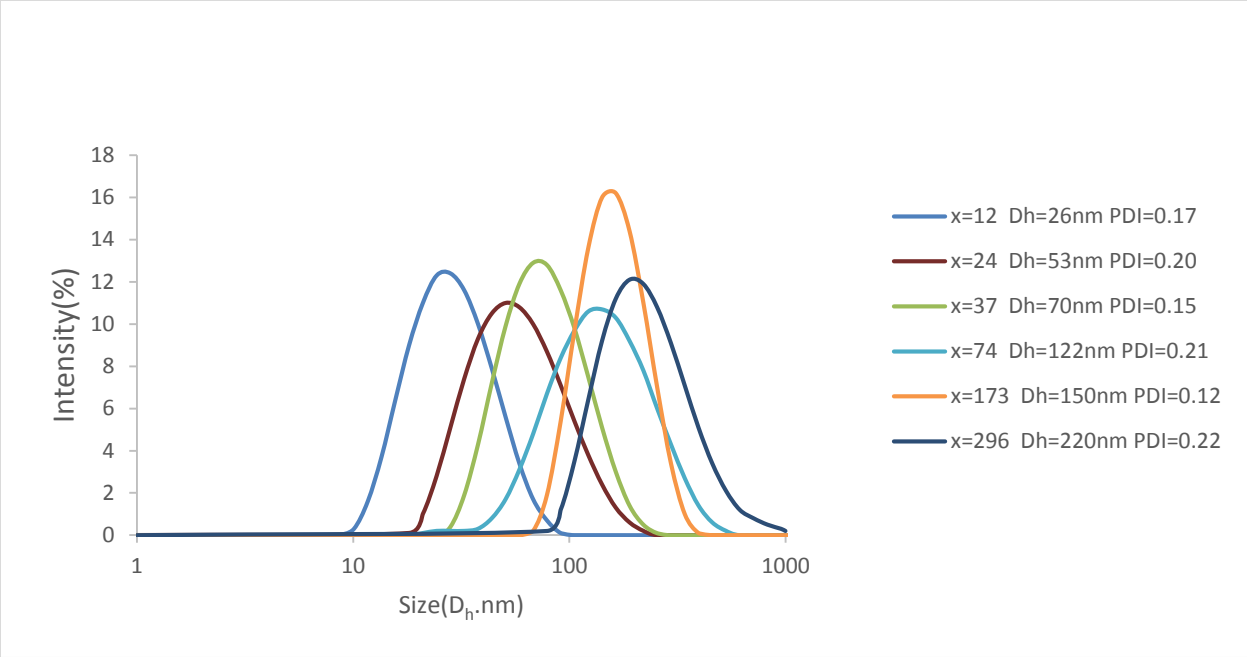

Figure 3-6. DLS particle size distributions (intensity vs mean hydrodynamic diameter, D_h) at 25 °C obtained for six PEO_{45}-*b*-$PDEAm_{89}$-*b*-$PDBAm_x$ triblock copolymers, where x corresponds to (a) 12, (b) 24, (c) 37, (d) 74, (e) 173, (f) 296.

Structural characteristics of PEO_{45}-*b*-$PDEAm_x$-*b*-$PDBAm_y$ assemblies in water (0.1 w/w %) at 25 °C as determined by TEM and DLS are summarized in Table 3-1. Generally when increasing the hydrophobic PDBAm block length while fixing the hydrophilic PEO_{45}-*b*-$PDEAm_x$ block at 25 °C, the hydrophilic mass fraction decreases, which is expected to lead to the formation of larger morphologies including worm-like micelles, vesicles and large compound spheres.[3] In addition, different molecular weights of middle thermally responsive PDEAm block could also influence the final morphology of polymer assembles. For example, worm-like morphologies were formed over a wider range of compositions in the PEO_{45}-$PDEAm_{41}$-$PDBAm_x$ triblock copolymers,

than was found in the library of PEO_{45}-$PDEAm_{89}$-$PDBAm_x$ polymers with much longer PDEAm middle blocks.

Table 3-1. Structural characteristics of PEO_{45}-*b*-$PDEAm_x$-*b*-$PDBAm_y$ assemblies in water (0.1 w/w %) at 25 °C.

	W_{PDBAm}[a] at 25 °C	D_h, nm (DLS)	TEM morphology at 25 °C
PEO_{45}-$PDEAm_{41}$-$PDBAm_{12}$	0.22	25	Spheres
PEO_{45}-$PDEAm_{41}$-$PDBAm_{16}$	0.28	35	Spheres/short worms
PEO_{45}-$PDEAm_{41}$-$PDBAm_{22}$	0.36	100	Long worms
PEO_{45}-$PDEAm_{41}$-$PDBAm_{50}$	0.55	92	Branched worms
PEO_{45}-$PDEAm_{41}$-$PDBAm_{92}$	0.70	131	Worms/vesicles
PEO_{45}-$PDEAm_{41}$-$PDBAm_{176}$	0.80	182	Large compound spheres
PEO_{45}-$PDEAm_{89}$-$PDBAm_{12}$	0.14	26	Spheres
PEO_{45}-$PDEAm_{89}$-$PDBAm_{24}$	0.24	53	Spheres/worms
PEO_{45}-$PDEAm_{89}$-$PDBAm_{32}$	0.30	61	Vesicles
PEO_{45}-$PDEAm_{89}$-$PDBAm_{37}$	0.33	70	Vesicles
PEO_{45}-$PDEAm_{89}$-$PDBAm_{74}$	0.50	120	Vesicles
PEO_{45}-$PDEAm_{89}$-$PDBAm_{109}$	0.60	123	Vesicles
PEO_{45}-$PDEAm_{89}$-$PDBAm_{173}$	0.70	150	Vesicles
PEO_{45}-$PDEAm_{89}$-$PDBAm_{296}$	0.80	220	Large compound spheres
PEO_{45}-$PDEAm_{57}$- $PDBAm_{12}$	0.18	26	Spheres
PEO_{45}-$PDEAm_{57}$- $PDBAm_{26}$	0.33	75	Vesicles
PEO_{45}-$PDEAm_{57}$- $PDBAm_{52}$	0.50	130	Vesicles
PEO_{45}-$PDEAm_{33}$- $PDBAm_{6}$	0.14	19	Spheres

[a] Hydrophobic weight fraction (W_{PDBAm}) calculated by the mass of the PDBAm block to the total mass of polymer.

3.4 Thermally induced size changes of polymer assemblies

Temperature dependent dynamic light scattering was conducted to characterize three aqueous solutions (0.10 w/w %) of PEO_{45}-*b*-$PDEAm_x$-*b*-$PDBAm_y$ triblock copolymers that form spherical micelles at 25 °C (PEO_{45}-$PDEAm_{33}$-$PDBAm_6$, PEO_{45}-$PDEAm_{41}$-$PDBAm_{12}$, PEO_{45}-$PDEAm_{89}$-$PDBAm_{12}$). At temperatures less than the lower critical solution temperature, the hydrodynamic diameters (D_h) of all three triblock polymers in water were less than 26 nm, which are close to the sizes of spherical micelles observed in TEM images (d_{TEM}≈16-21nm, Figure 3-3a and 3-4a). However, heating these dilute polymer solutions above the LCST of the PDEAm block results in a significant increase in apparent hydrodynamic diameter (D_h > 100nm) (Figure 3-7). When the PEO_{45}-$PDEAm_{33}$-$PDBAm_6$ solution was heated from 25 °C to 60 °C at 0.2 °C/min, D_h started to increase at around 50 °C (Figure 3-7a). The PEO_{45}-$PDEAm_{41}$-$PDBAm_{12}$ solution, showed an increase in D_h at around 46 °C (Figure 3-7b). For PEO_{45}-$PDEAm_{89}$-$PDBAm_{12}$, D_h began to increase at a slightly lower temperature (35 °C) (Figure 3-7c). These critical solution transition temperatures are close to those found for PDEAm homopolymers by Freitag[27] (LCST≈41 °C for M_n≈4.7 kg/mol) and Lessard[28] (LCST≈33 °C for M_n≈9.6 kg/mol) through cloud point measurements and differential scanning calorimetry (DSC).

(a)

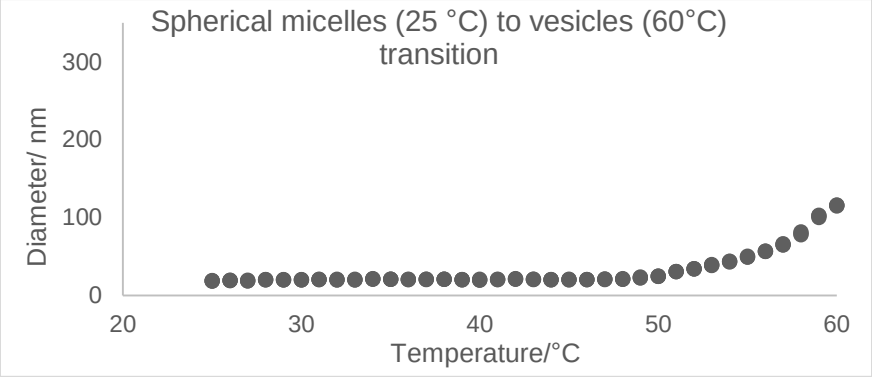
Spherical micelles (25 °C) to vesicles (60°C) transition
Diameter/ nm
300
200
100
0
20
30
40
50
60
Temperature/°C

(b)

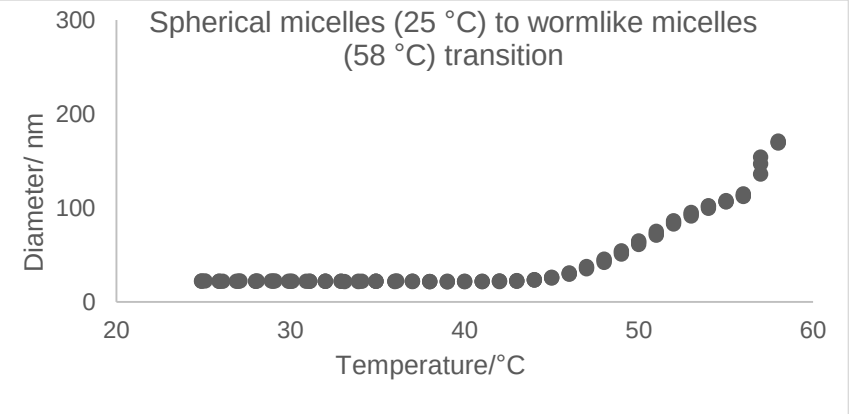
Spherical micelles (25 °C) to wormlike micelles (58 °C) transition
Diameter/ nm
300
200
100
0
20
30
40
50
60
Temperature/°C

(c)

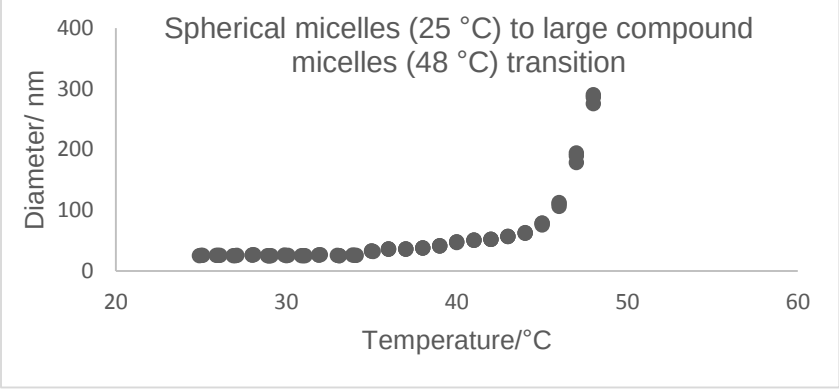
Spherical micelles (25 °C) to large compound micelles (48 °C) transition
Diameter/ nm
400
300
200
100
0
20
30
40
50
60
Temperature/°C

Figure 3-7. Temperature dependent DLS for 0.1 w/w% aqueous solutions of (a) PEO_{45}-$PDEAm_{33}$-$PDBAm_6$ (b) PEO_{45}-$PDEAm_{41}$-$PDBAm_{12}$ (c) PEO_{45}-$PDEAm_{89}$-$PDBAm_{12}$. Heat rate (0.2 min/°C). Three measurements were taken at each temperature.

In order to examine and observe the morphological transitions of these three thermally responsive triblock copolymers, the same aqueous dilute solutions (0.10 w/w %) were analyzed by TEM, following the procedure described in Chapter 3.2. TEM images of PEO_{45}-$PDEAm_{33}$-$PDBAm_6$ after heating at 60 °C for 10 min (Figure 3-8a), indicate a significant change in the shape and size of morphologies from spherical micelles at 25 °C to vesicles at 60 °C. TEM images of PEO_{45}-$PDEAm_{41}$-$PDBAm_{12}$ after heating at 55 °C for 10 min (Figure 3-8b), indicated a change in the shape and size of the assemblies from spherical micelles to worm-like micelles. TEM images of PEO_{45}-$PDEAm_{89}$-$PDBAm_{12}$ after heating at 55 °C for 10 min (Figure 3-8c), indicated a change in the shape and size of the assemblies from spherical micelles to large compound micelles. Because the central thermally responsive PDEAm block in the triblock copolymers changes from hydrophilic to hydrophobic after heating at temperatures above the LCST of the PDEAm block, the hydrophilic weight fraction (f) of triblock copolymers decreases from 0.85 to 0.27 for PEO_{45}-$PDEAm_{33}$-$PDBAm_6$, from 0.75 to 0.20 for PEO_{45}-$PDEAm_{41}$-$PDBAm_{12}$ and from 0.84 to 0.13 for PEO_{45}-$PDEAm_{89}$-$PDBAm_{12}$, resulting in significant changes in assembly shape and size. The fast transformation rate (within 10 minutes) from spheres to large aggregates (worms, vesicles and large compound micelles) further supports our hypothesis that the absence of strong interchain hydrogen bonding in the middle thermally responsive block accelerates rearrangement of polymer assemblies, as compared to the behavior observed for PEO-*b*-PNIPA-*b*-PI assemblies.

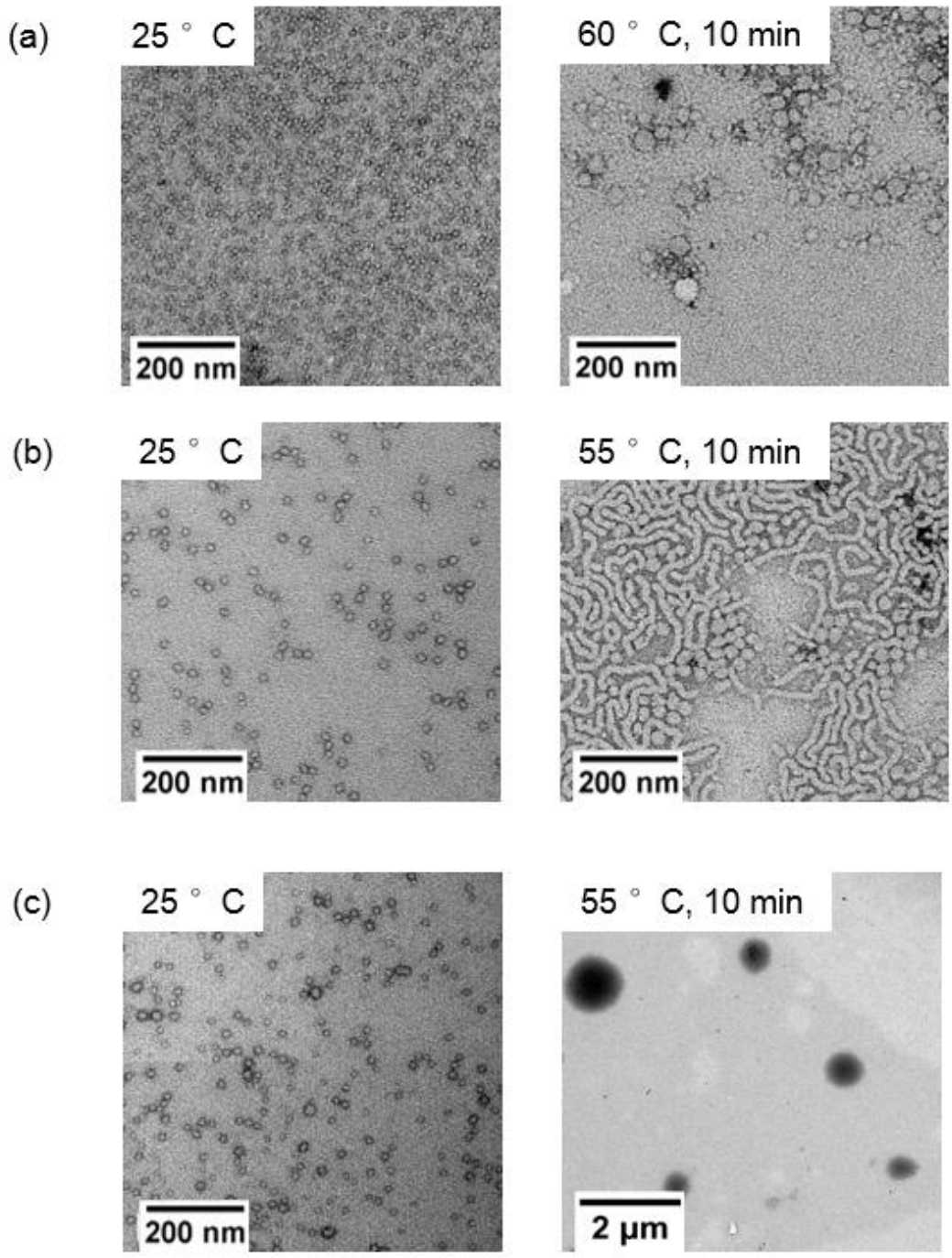

Figure 3-8. Representative TEM images of thermally induced transitions after heating for 10 min of: (a) PEO_{45}-$PDEAm_{33}$-$PDBAm_{6}$ from spherical micelles to vesicles at 60 °C; (b) PEO_{45}-$PDEAm_{41}$-$PDBAm_{12}$ from spherical micelles to wormlike micelles at 55 °C; and (c) PEO_{45}-

$PDEAm_{89}$-$PDBAm_{12}$ from spherical micelles to large compound micelles at 55 °C. All three samples were stained with uranyl acetate.

The thermally responsive behaviors of these three triblock copolymers were also confirmed by DLS experiments, indicating that the thermally induced size transitions are fully reversible (Figure 3-9). The apparent D_h of PEO_{45}-$PDEAm_{33}$-$PDBAm_6$ assemblies increased from 20 nm to 60 nm after heating at 60 °C for 10 min, values consistent with the average diameters of vesicles observed in the TEM images (Figure 3-8a). The apparent D_h of PEO_{45}-$PDEAm_{41}$-$PDBAm_{12}$ increased from 24 nm to 84 nm after heating at 55 °C for 10 min. It is known that the hydrodynamic diameter of a nonspherical particle reported in the DLS analysis is the diameter of a sphere that has the same translational diffusion speed as the particle. As a result, the D_h value of PEO_{45}-$PDEAm_{41}$-$PDBAm_{12}$ in the DLS does not directly correspond to the observed size of worm-like micelles in the TEM images (Figure 3-8b).. The apparent D_h of PEO_{45}-$PDEAm_{89}$-$PDBAm_{12}$ increased from 24 nm to 60 nm after heating at 55 °C for 10 min, which is not consistent with the sizes of aggregates (d > 300 nm) observed in the TEM images (Figure 3-8c). However, the temperature dependent DLS experiment (Figure 3-7c) showed D_h > 300 nm around 50 °C. We believe that the large compound micelles settle to the bottom of cuvette, which make the results of DLS measurement for this specific sample unreliable.

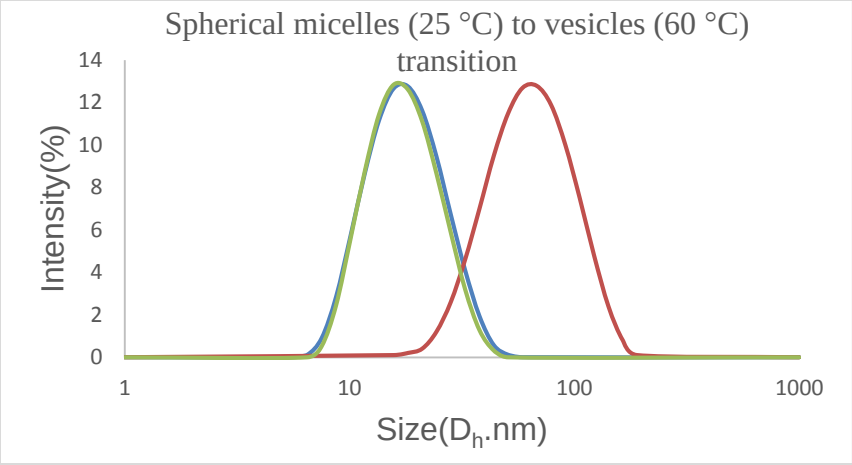

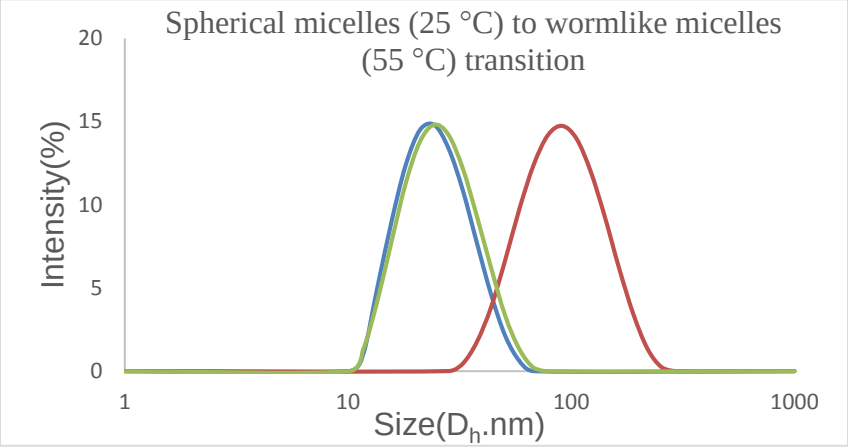

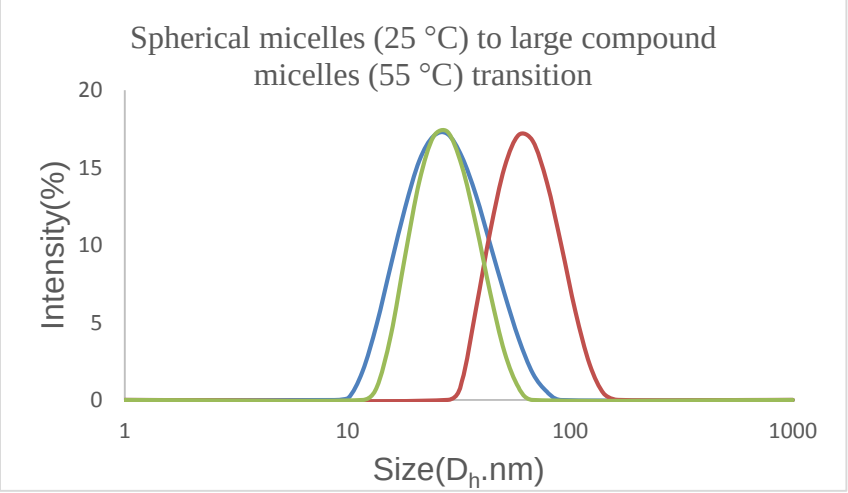

Figure 3-9. DLS studies of thermally induced transitions of (top) PEO_{45}-$PDEAm_{33}$-$PDBAm_{6}$, (middle) PEO_{45}-$PDEAm_{41}$-$PDBAm_{12}$, and (bottom) PEO_{45}-$PDEAm_{89}$-$PDBAm_{12}$. 25 °C before

heating (blue), after heating at 55 °C or 60 °C for 10 min (red) and cooling down to 25 °C after 5 min (green).

It is noteworthy that surfactants and block copolymers with worm-like micelle morphologies can form gels. Although gel formation is often attributed to multiple inter-worm interactions,[9, 29] there are several examples of worm-like micelles and fibrous networks that form gels with no inter-worm crosslinks.[30-31] Gelation in these cases has been attributed to topological interactions and requires that worms be sufficiently long and stiff to persist over the time scales probed by mechanical rheology.[31] To explore whether the conditions for gelation are met in our systems, the behavior of solutions of PEO_{45}-*b*-$PDEAm_{41}$-*b*-$PDBAm_{12}$, which undergo a thermally induced sphere-to-worm transition, was investigated at higher concentrations (≥5.0 w/w %). PEO_{45}-$PDEAm_{41}$-$PDBAm_{12}$ was dissolved in water at 5.0 w/w % and stirred at 25 °C to produce a clear and fluid solution (D_h = 21 nm). After heating at 55 °C for 10 min, the polymer solution formed a soft free-standing physical gel ($D_h > 10^3$ nm) (see Figure 3-10a). Repeated heating and cooling experiments indicate that the gelation is completely thermoreversible. In contrast, phase separation was observed in the PEO_{45}-*b*-$PDEAm_{89}$-*b*-$PDBAm_{12}$ aqueous solution (5.0 w/w %), as the large compound micelles ($D_h > 10^5$ nm) settled to the bottom of solution (see Figure 3-10b). For PEO_{45}-*b*-$PDEAm_{33}$-*b*-$PDBAm_6$ aqueous solutions (5.0 w/w %) which undergo a spherical micelle-to-vesicle transition, the solutions became cloudy after heating (D_h = 93 nm) but did not undergo gelation or phase separation (Figure 3-10c).

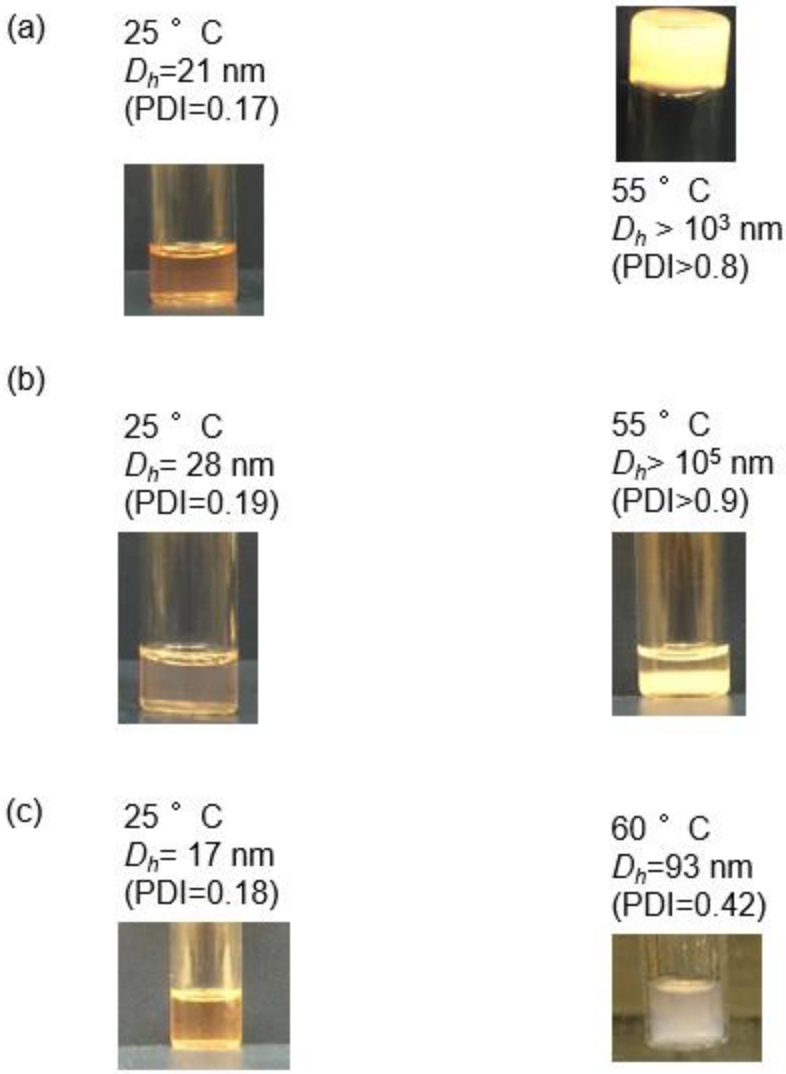

Figure 3-10. Thermally responsive behavior of 5.0 w/w % aqueous triblock copolymer solutions and the hydrodynamic diameters (D_h) and polydispersities (PDI) measured by DLS at 25 °C and after heating at the specified temperature for 10 min. (a) PEO_{45}-$PDEAm_{41}$-$PDBAm_{12}$ formed a free-standing gel; (b) PEO_{45}-$PDEAm_{89}$-$PDBAm_{12}$ underwent phase separation; (c) PEO_{45}-$PDEAm_{33}$-$PDBAm_{6}$ became cloudy but did not undergo gelation or phase separation.

Thermoresponsive behaviors of three PEO_{45}-*b*-$PDEAm_x$-*b*-$PDBAm_y$ assemblies in water are summarized in Table 3-2. All three PEO_{45}-*b*-$PDEAm_x$-*b*-$PDBAm_y$ triblock copolymers form clear spherical micelle solutions at 25 °C due to their large hydrophilic mass fractions ($f > 0.75$). After heating above the LCST of PDEAm block, three different thermally induced morphological transitions and solution behaviors were observed. Spherical micelle to worm-like micelle, vesicle, or large compound micelle transitions are anticipated due to the new thermodynamically favorable structures dictated by their small hydrophilic mass fractions ($f < 0.3$) at 55 °C. It is possible that worm morphology acts as the intermediate structure through spherical micelles to vesicles or large compound micelles. However, even after heating for three weeks, the worm morphologies were maintained (see Figure A3.19). Recently, Armes[32] reported poly(glycerol monomethacrylate)−poly(2-hydroxypropyl methacrylate ($HOOC\text{-}PGMA_{43}$−$PHPMA_{175–250}$) diblock polymers which undergo an irreversible vesicle-to-worm transition upon cooling. They hypothesized that worm phase is a kinetically trapped morphology, that prevents the formation of vesicles upon heating.

Table 3-2. Summary of thermoresponsive behavior from PEO-PDEAm-PDBAm triblock copolymers.

Triblock copolymer	*f*(25 °C)	Morphology at 25 °C	Solution behavior at 25 °C (5 w/w %)	*f*(55 °C)	Morphology at 55 °C	Solution behavior after heating 10 min at 55 °C (5 w/w %)
PEO_{45}-$PDEAm_{33}$-$PDBAm_6$	0.82	Spherical micelles	Clear solution	0.29	Vesicles	Cloudy solution
PEO_{45}-$PDEAm_{33}$-$PDBAm_6$	0.75	Spherical micelles	Clear solution	0.20	Wormlike micelles	Gel
PEO_{45}-$PDEAm_{33}$-$PDBAm_6$	0.84	Spherical micelles	Clear solution	0.13	Large compound micelles	Phase separation

3.5 Rheology of PEO_{45}-$PDEAm_{41}$-$PDBAm_{12}$ worm-like gels

Rheological measurements were performed on aqueous solutions and gels of triblock copolymer PEO_{45}-$PDEAm_{41}$-$PDBAm_{12}$ (≥5.0 w/w %). To measure the viscoelastic properties of gels, it is necessary to determine the linear viscoelastic region by measuring the elastic modulus G' and the loss modulus G" of the hydrogel (T = 55 °C) as a function of the strain amplitude from 0.02 to 5 % strain at 10 Hz. G' and G" were found to be independent of strain amplitude from 0.01-10% strain (Figure 3-11). Therefore to remain in the linear viscoelastic region. a strain of 5 % was used for all rheological measurements of polymer gels.

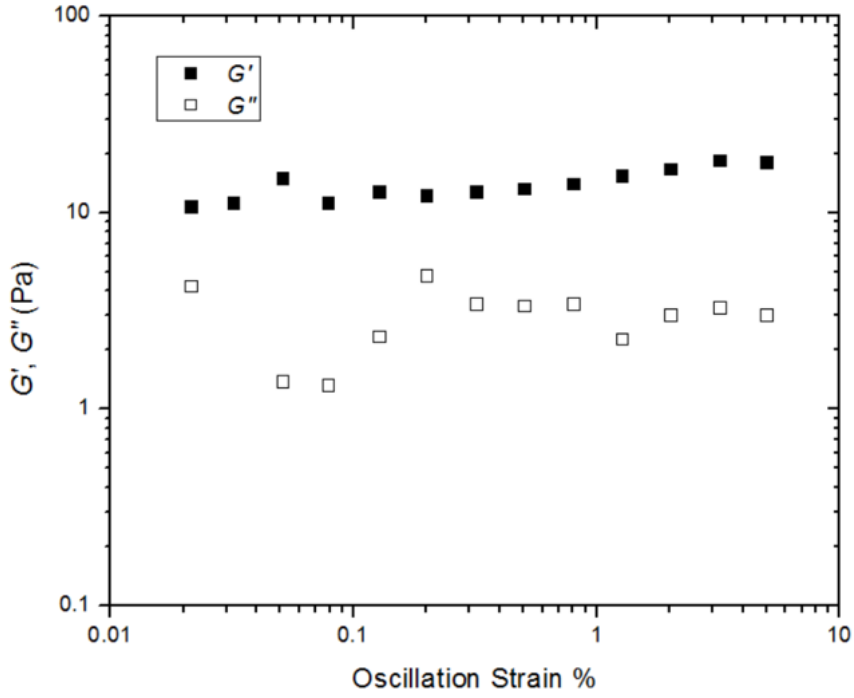

Figure 3-11. Strain sweep at 10 Hz for a 5.0 w/w % PEO_{45}-$PDEAm_{41}$-$PDBAm_{12}$ polymer gel at 55 °C.

Frequency sweeps of the rheological properties of a 5.0 w/w % PEO_{45}-$PDEAm_{41}$-$PDBAm_{12}$ polymer solution from 0.1 to 1000 Hz at strain of 5 % were conducted at 25 °C (liquid), 45 °C (LCST measured by DLS, see Figure 3-7b), and 55 °C (gel). (Figure 3-12) At 25 °C and 45 °C, G' and G" are very low (< 0.01 Pa) and show strong dependence on frequency, which is consistent with dilute polymer solution rheology characteristics. However, at 55 °C, G' is always higher than G", both of which are independent of frequency from 0.1 to 100 rad/s. This behavior is characteristic of an elastic gel.[29, 33-34] Frequency sweeps at three different polymer concentrations (5.0 w/w %, 7.5 w/w %, and 10.0 w/w %) at 55 °C were also carried out, and as expected, the elastic modulus increased with increasing concentration of polymer solution (Figure 3-13). At all three concentrations, G' values are always higher than G" values, and both moduli show little dependence on frequency from 0.1 to 100 rad/s.

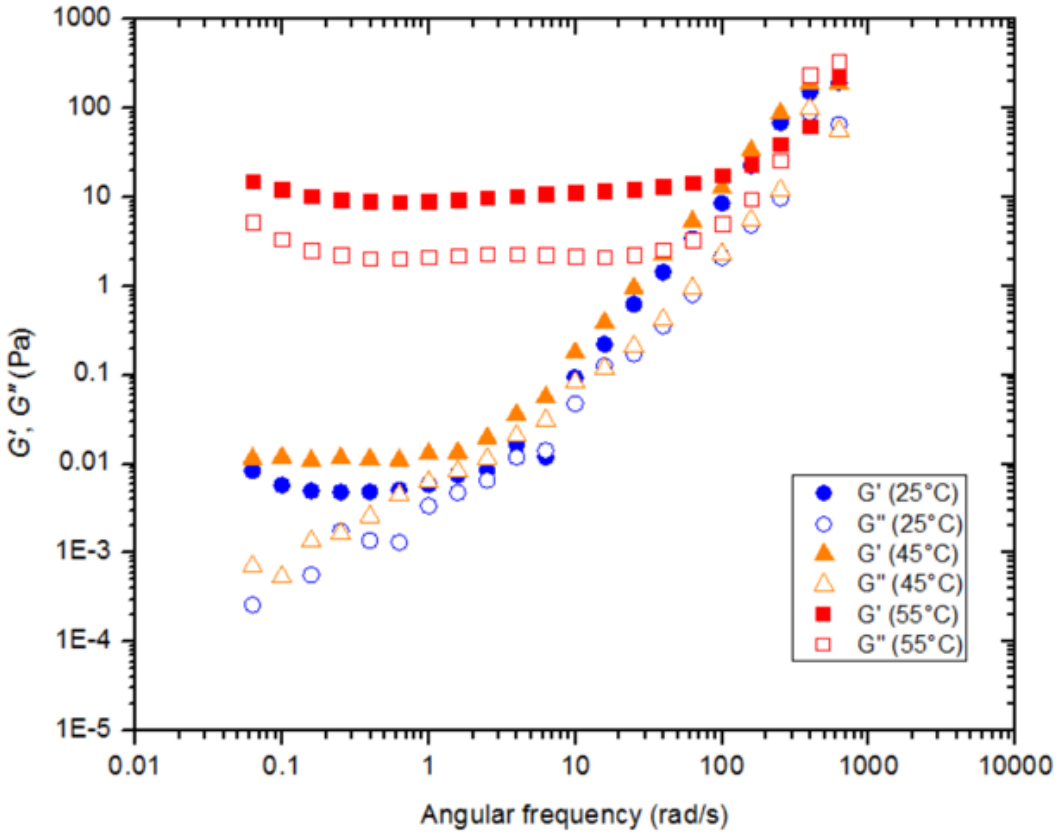

Figure 3-12. Frequency sweeps for 5.0 w/w % PEO_{45}-$PDEAm_{41}$-$PDBAm_{12}$ polymer solutions/gels at 25°C, 45 °C, and 55 °C at a strain of 5 %.

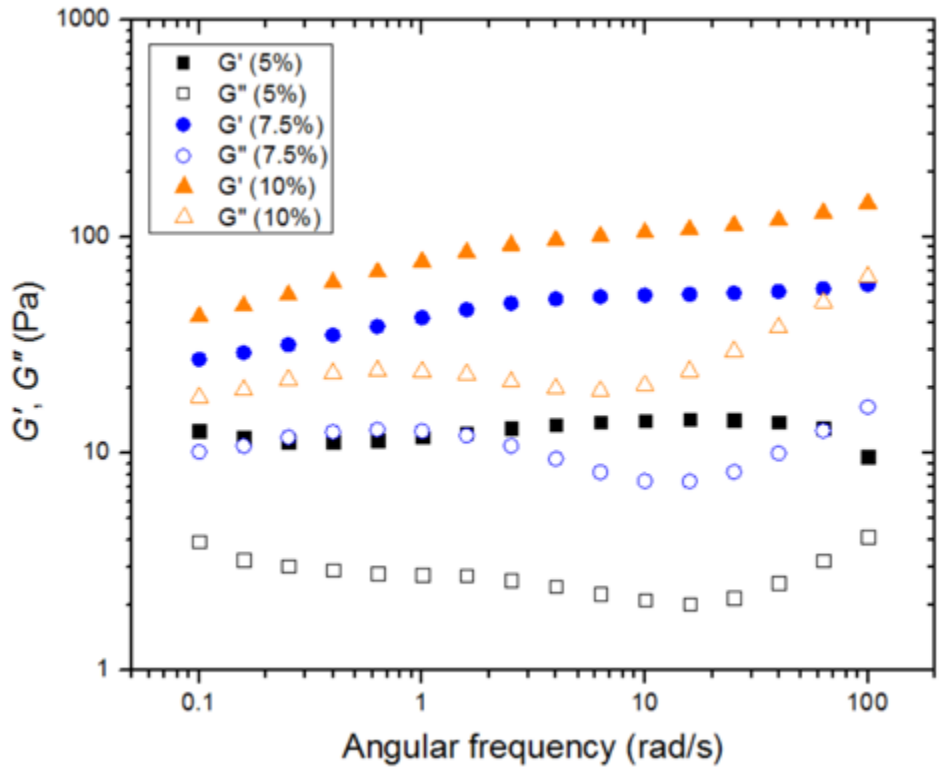

Figure 3-13. Frequency sweeps for PEO_{45}-$PDEAm_{41}$-$PDBAm_{12}$ polymer gels at 55 °C with 3 different concentrations (5.0 w/w%, 7.5 w/w%, 10.0 w/w%) at a strain of 5 %.

The temperature dependence of rheological properties of the gels at the three different polymer concentrations (5.0, 7.5, and 10.0 w/w%) were also studied from 25 to 55 °C (Figure 3-14). G' and G" are very low (< 0.1 Pa) at temperatures below the transition temperature. However, both G' and G" increase dramatically with increasing temperature due to gelation. At the three concentrations examined, the gelation temperature as defined as the crossing point of G' and G" [9, 29] is almost identical (around 49 °C), which is slightly higher than the critical solution temperature

(45 °C) observed in temperature dependent DLS experiments (Figure 3-7). It is possible that gelation requires more time for formation of longer worm and interworm entanglements.

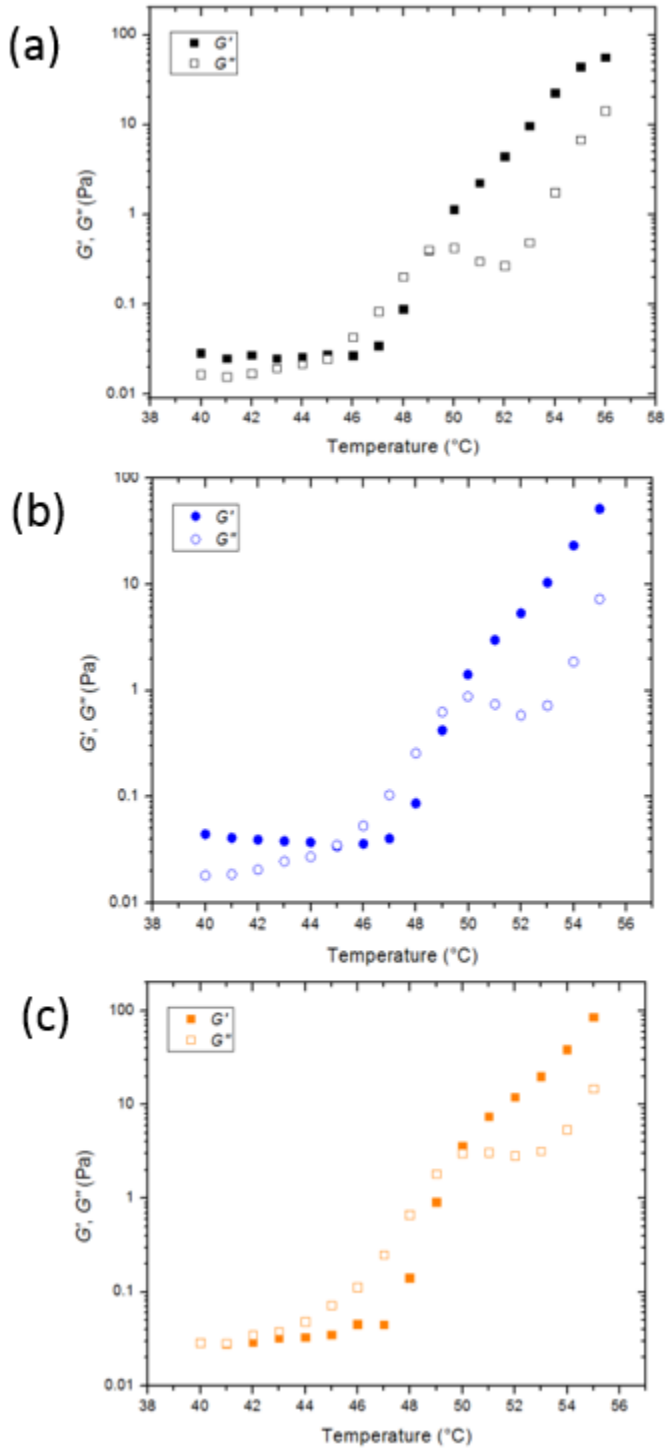

Figure 3-14. Temperature sweeps (1 Hz, 5% strain) for PEO_{45}-$PDEAm_{41}$-$PDBAm_{12}$ polymer gels at different concentrations (a) 5.0 w/w %, (b) 7.5 w/w %, (c) 10.0 w/w %.

The small plateau in G'' that can be observed in the temperature sweeps at all three different concentrations after the gel transition (49–52 °C) (Figure 3-14), is interesting. As discussed by Raghavan and Douglas[31], increasing temperature usually leads to the decrease of the micelles length and the relaxation time in surfactant wormlike micelles. Both of these effects contribute to increasing the viscous nature of the system, leading to a transition from gel-like behavior at low temperatures to viscoelastic behavior at high temperatures. However, our polymer samples that undergo a thermally induced morphological transition show the opposite behavior, with viscoelastic behavior at low temperatures and gel-like behavior at higher temperatures. In our case, increasing temperature would increase the micelles length from sphere-to-worm transition but decrease the relaxation time, which lead to a complex dependence of the moduli on temperature near the gel transition. In the end, the effect of increasing length micelles length dominates, and gel formation is favored.

3.6 Encapsulation of rhodamine B inside large compound micelles of PEO_{45}-$PDEAm_{89}$-$PDBAm_{12}$

Rhodamine B, a hydrophilic dye, was used to investigate the encapsulating ability of the large compound micelles formed by PEO_{45}-$PDEAm_{89}$-$PDBAm_{12}$ at temperatures above the PDEAm LCST (Figure 3-15). An aqueous solution of PEO_{45}-$PDEAm_{89}$-$PDBAm_{12}$ (5.0 w/w %) with rhodamine B (0.01 w/w %) (Figure 3-15a) was heated at 55 °C to induce phase separation resulting from the large compound micelles settling to the bottom of the vial (Figure 3-15b). The top aqueous layer (Figure 3-15c) and the bottom polymer-rich layer (Figure 3-15d) were separated

by pipet, and a small amount of 55 °C water was added to the bottom layer. After 10 min at 55 °C, the added water layer remained clear (Figure 3-15e) without any rhodamine B, as confirmed by UV-vis spectroscopy (Figure 3-16), indicating that the rhodamine B dye was successfully encapsulated inside the large compound micelles. Cooling the bottom layer down to 25 °C resulted in release of the dye and formation of a transparent solution (Figure 3-15f).

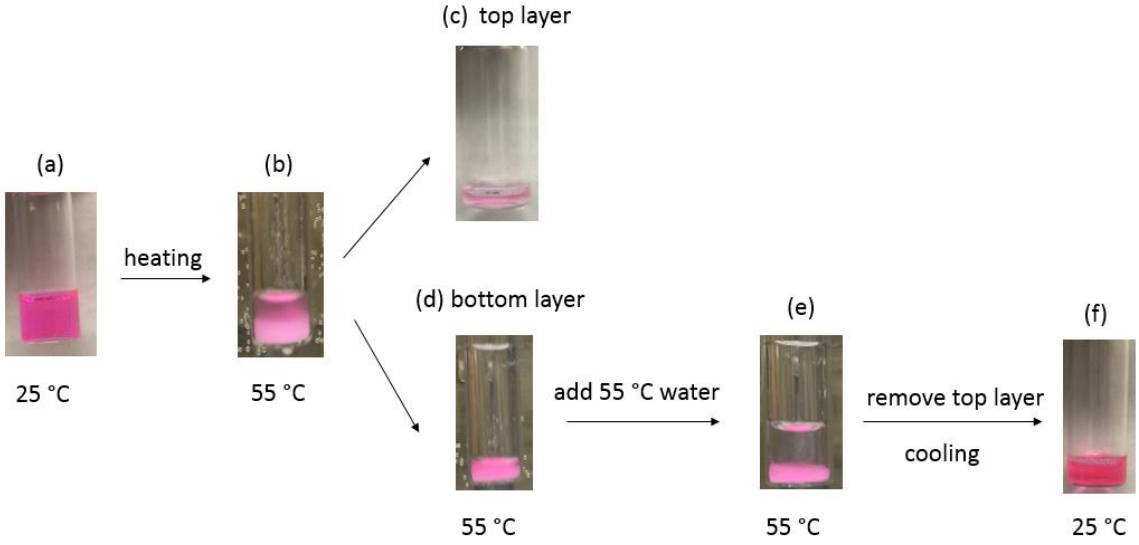

Figure 3-15. Encapsulation of rhodamine B in the PEO_{45}-$PDEAm_{89}$-$PDBAm_{12}$ solution. An aqueous solution of PEO_{45}-$PDEAm_{89}$-$PDBAm_{12}$ (5.0 w/w %) with rhodamine B (0.01 w/w %) (a) was heated at 55 °C to induce phase separation (b). The top aqueous layer (c) and the bottom polymer-rich layer (d) were separated by pipette, and a small amount of 55 °C water was added to the bottom layer. After 10 min at 55 °C, the added water layer remained clear (e) without any rhodamine B, as confirmed by UV-vis spectroscopy (Figure 3-16), indicating that the rhodamine

B dye was successfully encapsulated inside the large compound micelles. Cooling the bottom layer down to 25 °C resulted in release of the dye and formation of a transparent solution (f).

(a)

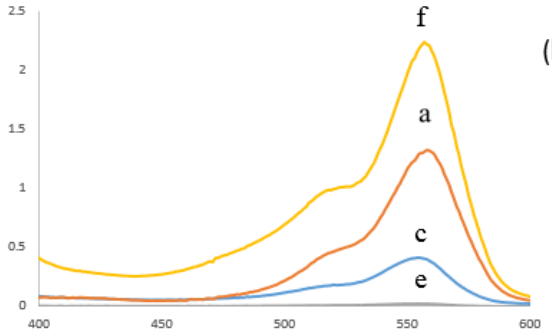

(b)

	Absorbance at 557nm	Concentration
a	1.328	0.01 w/w %
c	0.415	0.003 w/w %
e	0.026	0.0002 w/w %
f	2.234	0.017 w/w %

Figure 3-16. (a)UV-vis spectra and (b) absorbance and concentration for rhodamine B in the PEO_{45}-$PDEAm_{89}$-$PDBAm_{12}$ solutions: (a) initial solution at 25 °C, (c) top layer after phase separation at 55 °C, (e) top layer after 10 min adding 55 °C water to large compound micelle layer, (f) larger compound micelle layer cooled to 25 °C.

Based on this preliminary experiment, it was found that rhodamine B dye could be successfully encapsulated inside the large compound micelles. The mass ratio of rhodamine B dye to PEO_{45}-$PDEAm_{89}$-$PDBAm_{12}$ was 1/500 (molar ratio≈1/15), and the encapsulation efficiency was about 85%, estimated by the amount of rhodamine B dye incorporated in the large compound micelle layer (f) and dividing that value by the total amount of rhodamine B dye in the initial solution (a). The successful encapsulation of hydrophilic rhodamine B dyes by large compound micelles provides a promising strategy for the design of new delivery and separation devices. Further studies in this direction may include encapsulation of different types of particles/molecules

using different methods and modification of the triblock polymers to make encapsulation efficiency higher and transition temperature lower.

3.7 Conclusion

Dynamic light scattering (DLS) and transmission electron microscopy (TEM) were used to characterize the size and morphologies of nanostructures from the self-assembly of PEO-*b*-PDEAm-*b*-PDBAm triblock copolymers with different hydrophilic/hydrophobic block ratios in water at 25 °C. The thermally responsive behavior of these triblock copolymers was also investigated. The fast transformation rate (within 10 minutes) upon heating from small spherical micelles to large aggregates, including worm-like micelles, vesicles and large compound micelles, supports our hypothesis that the absence of strong interchain hydrogen bonding in the middle thermally responsive block of hydrophilic-responsive-hydrophobic ABC triblock copolymers could accelerate aggregate rearrangement. In addition, at a higher polymer concentration of 5.0 w/w%, the PEO_{45}-*b*-$PDEAm_{41}$-*b*-$PDBAm_{12}$ polymer solution forms a free-standing physical gel after heating at 55 °C for 10 min due to a thermally induced sphere-to-worm transition and interworm entanglements, as confirmed and characterized by rheology. In contrast, the PEO_{45}-*b*-$PDEAm_{89}$-*b*-$PDBAm_{12}$ copolymer solution was found to undergo phase separation after heating at 55 °C for 10 min as a result of sedimentation of large compound micelles. A preliminary experiment was also conducted, confirming the successful encapsulation of a hydrophilic dye Rhodamine B into the large compound micelle formed by PEO_{45}-*b*-$PDEAm_{89}$-*b*-$PDBAm_{12}$ upon heating.

Reference (Chapter 3)

1. Blanazs, A.; Armes, S. P.; Ryan, A. J., Self-Assembled Block Copolymer Aggregates: From Micelles to Vesicles and their Biological Applications. *Macromol. Rapid Commun.* **2009,** *30* (4-5), 267-277. (doi: 10.1002/marc.200800713)

2. Israelachvili, J. N., *Intermolecular and Surface Forces Preface to the Third Edition*. 2011; p Xvii-+.

3. Discher, D. E.; Ahmed, F., Polymersomes. *Annual Review of Biomedical Engineering* **2006,** *8*, 323-341. (doi: 10.1146/annurev.bioeng.8.061505.095838)

4. Arotcarena, M.; Heise, B.; Ishaya, S.; Laschewsky, A., Switching the inside and the outside of aggregates of water-soluble block copolymers with double thermoresponsivity. *J. Am. Chem. Soc.* **2002,** *124* (14), 3787-3793. (doi: 10.1021/ja012167d)

5. Moughton, A. O.; O'Reilly, R. K., Thermally induced micelle to vesicle morphology transition for a charged chain end diblock copolymer. *Chem Commun (Camb)* **2010,** *46* (7), 1091-1093. (doi: 10.1039/b922289h)

6. Warren, N. J.; Rosselgong, J.; Madsen, J.; Armes, S. P., Disulfide-Functionalized Diblock Copolymer Worm Gels. *Biomacromolecules* **2015,** *16* (8), 2514-2521. (doi: 10.1021/acs.biomac.5b00767)

7. Simon, K. A.; Warren, N. J.; Mosadegh, B.; Mohammady, M. R.; Whitesides, G. M.; Armes, S. P., Disulfide-Based Diblock Copolymer Worm Gels: A Wholly-Synthetic Thermoreversible 3D Matrix for Sheet-Based Cultures. *Biomacromolecules* **2015,** *16* (12), 3952-3958. (doi: 10.1021/acs.biomac.5b01266)

8. Kocik, M. K.; Mykhaylyk, O. O.; Armes, S. P., Aqueous worm gels can be reconstituted from freeze-dried diblock copolymer powder. *Soft Matter* **2014,** *10* (22), 3984-3992. (doi: 10.1039/c4sm00415a)

9. Blanazs, A.; Verber, R.; Mykhaylyk, O. O.; Ryan, A. J.; Heath, J. Z.; Douglas, C. W.; Armes, S. P., Sterilizable gels from thermoresponsive block copolymer worms. *J. Am. Chem. Soc.* **2012,** *134* (23), 9741-9748. (doi: 10.1021/ja3024059)

10. Sundararaman, A.; Stephan, T.; Grubbs, R. B., Reversible restructuring of aqueous block copolymer assemblies through stimulus-induced changes in amphiphilicity. *J. Am. Chem. Soc.* **2008,** *130* (37), 12264-12265. (doi: 10.1021/ja8052688)

11. Cai, Y.; Aubrecht, K. B.; Grubbs, R. B., Thermally induced changes in amphiphilicity drive reversible restructuring of assemblies of ABC triblock copolymers with statistical polyether blocks. *J. Am. Chem. Soc.* **2011,** *133* (4), 1058-1065. (doi: 10.1021/ja109262h)

12. Banerjee, R.; Dhara, D., Functional group-dependent self-assembled nanostructures from thermo-responsive triblock copolymers. *Langmuir* **2014,** *30* (14), 4137-4146. (doi: 10.1021/la500213h)

13. Dan, M. H.; Huo, F.; Xiao, X.; Su, Y.; Zhang, W. Q., Temperature-Sensitive Nanoparticle-to-Vesicle Transition of ABC Triblock Copolymer Corona-Shell-Core Nanoparticles Synthesized by Seeded Dispersion RAFT Polymerization. *Macromolecules* **2014,** *47* (4), 1360-1370. (doi: 10.1021/ma402370j)

14. Li, C.; Buurma, N. J.; Haq, I.; Turner, C.; Armes, S. P.; Castelletto, V.; Hamley, I. W.; Lewis, A. L., Synthesis and characterization of biocompatible, thermoresponsive ABC and ABA triblock copolymer gelators. *Langmuir* **2005,** *21* (24), 11026-11033. (doi: 10.1021/la0515672)

15. Reinicke, S.; Schmelz, J.; Lapp, A.; Karg, M.; Hellweg, T.; Schmalz, H., Smart hydrogels based on double responsive triblock terpolymers. *Soft Matter* **2009,** *5* (13), 2648-2657. (doi: 10.1039/b900539k)

16. Taribagil, R. R.; Hillmyer, M. A.; Lodge, T. P., Hydrogels from ABA and ABC Triblock Polymers. *Macromolecules* **2010,** *43* (12), 5396-5404. (doi: 10.1021/ma100464z)

17. Koonar, I.; Zhou, C.; Hillmyer, M. A.; Lodge, T. P.; Siegel, R. A., ABC triblock terpolymers exhibiting both temperature- and pH-sensitive micellar aggregation and gelation in aqueous solution. *Langmuir* **2012,** *28* (51), 17785-17794. (doi: 10.1021/la303712b)

18. Zhou, C.; Hillmyer, M. A.; Lodge, T. P., Efficient formation of multicompartment hydrogels by stepwise self-assembly of thermoresponsive ABC triblock terpolymers. *J. Am. Chem. Soc.* **2012,** *134* (25), 10365-10368. (doi: 10.1021/ja303841f)

19. Gupta, M. K.; Martin, J. R.; Werfel, T. A.; Shen, T.; Page, J. M.; Duvall, C. L., Cell protective, ABC triblock polymer-based thermoresponsive hydrogels with ROS-triggered degradation and drug release. *J. Am. Chem. Soc.* **2014,** *136* (42), 14896-14902. (doi: 10.1021/ja507626y)

20. Klouda, L., Thermoresponsive hydrogels in biomedical applications: A seven-year update. *Eur J Pharm Biopharm* **2015,** *97* (Pt B), 338-349. (doi: 10.1016/j.ejpb.2015.05.017)

21. Zhou, C.; Toombes, G. E. S.; Wasbrough, M. J.; Hillmyer, M. A.; Lodge, T. P., Structure of Two-Compartment Hydrogels from Thermoresponsive ABC Triblock Terpolymers. *Macromolecules* **2015,** *48* (16), 5934-5943. (doi: 10.1021/acs.macromol.5b00584)

22. Jain, S.; Bates, F. S., On the origins of morphological complexity in block copolymer surfactants. *Science* **2003,** *300* (5618), 460-464. (doi: 10.1126/science.1082193)

23. Rank, A.; Hauschild, S.; Forster, S.; Schubert, R., Preparation of monodisperse block copolymer vesicles via a thermotropic cylinder-vesicle transition. *Langmuir* **2009,** *25* (3), 1337-1344. (doi: 10.1021/la802709v)

24. Zhang, L.; Eisenberg, A., Multiple Morphologies of "Crew-Cut" Aggregates of Polystyrene-b-poly(acrylic acid) Block Copolymers. *Science* **1995,** *268* (5218), 1728-1731. (doi: 10.1126/science.268.5218.1728)

25. Zhang, L. F.; Eisenberg, A., Multiple morphologies and characteristics of "crew-cut" micelle-like aggregates of polystyrene-b-poly(acrylic acid) diblock copolymers in aqueous solutions. *J. Am. Chem. Soc.* **1996,** *118* (13), 3168-3181. (doi: DOI 10.1021/ja953709s)

26. Warren, N. J.; Mykhaylyk, O. O.; Ryan, A. J.; Williams, M.; Doussineau, T.; Dugourd, P.; Antoine, R.; Portale, G.; Armes, S. P., Testing the vesicular morphology to destruction: birth and death of diblock copolymer vesicles prepared via polymerization-induced self-assembly. *J. Am. Chem. Soc.* **2015,** *137* (5), 1929-1937. (doi: 10.1021/ja511423m)

27. Freitag, R.; Baltes, T.; Eggert, M., A Comparison of Thermoreactive Water-Soluble Poly-N,N-Diethylacrylamide Prepared by Anionic and by Group-Transfer Polymerization. *J Polym Sci Pol Chem* **1994,** *32* (16), 3019-3030. (doi: DOI 10.1002/pola.1994.080321603)

28. Lessard, D. G.; Ousalem, M.; Zhu, X. X.; Eisenberg, A.; Carreau, P. J., Study of the phase transition of poly(N,N-diethylacrylamide) in water by rheology and dynamic light scattering. *J Polym Sci Pol Phys* **2003,** *41* (14), 1627-1637. (doi: 10.1002/polb.10517)

29. Chu, Z.; Dreiss, C. A.; Feng, Y., Smart wormlike micelles. *Chem. Soc. Rev.* **2013,** *42* (17), 7174-7203. (doi: 10.1039/c3cs35490c)

30. Kumar, R.; Kalur, G. C.; Ziserman, L.; Danino, D.; Raghavan, S. R., Wormlike Micelles of a C22-Tailed Zwitterionic Betaine Surfactant: From Viscoelastic Solutions to Elastic Gels. *Langmuir* **2007,** *23* (26), 12849-12856. (doi: 10.1021/la7028559)

31. Raghavan, S. R.; Douglas, J. F., The conundrum of gel formation by molecular nanofibers, wormlike micelles, and filamentous proteins: gelation without cross-links? *Soft Matter* **2012,** *8* (33), 8539-8546. (doi: 10.1039/C2SM25107H)

32. Lovett, J. R.; Warren, N. J.; Armes, S. P.; Smallridge, M. J.; Cracknell, R. B., Order-Order Morphological Transitions for Dual Stimulus Responsive Diblock Copolymer Vesicles. *Macromolecules* **2016,** *49* (3), 1016-1025. (doi: 10.1021/acs.macromol.5b02470)

33. Jeong, B.; Kim, S. W.; Bae, Y. H., Thermosensitive sol-gel reversible hydrogels. *Adv Drug Deliv Rev* **2002,** *54* (1), 37-51. (doi: 10.1016/j.addr.2012.09.012)

34. Ahn, S. K.; Kasi, R. M.; Kim, S. C.; Sharma, N.; Zhou, Y. X., Stimuli-responsive polymer gels. *Soft Matter* **2008,** *4* (6), 1151-1157. (doi: 10.1039/b714376a)

Chapter 4 Synthesis of Thermally Responsive PEO-*b*-PDEAm-*b*-PLA Tri-Arm Star Copolymers

4.1 Introduction

After our investigation of thermally responsive PEO-*b*-PDEAm-*b*-PDBAm ABC triblock copolymers, a number of important questions remain unknown or partially answered about the thermally induced morphological transitions between different morphologies. Since most studies of thermally responsive polymer systems focus on a linear architecture, synthesis of a hydrophilic-responsive-hydrophobic three-arm star copolymer could be helpful in understanding how the nonlinear architecture affect the structure and response in the thermally responsive behavior of polymers (Figure 4-1). In the three-arm star copolymer architecture, the responsive block is only connected by one chain end compared to linear polymers in which the responsive block is linked to the rest of the polymer at both ends.

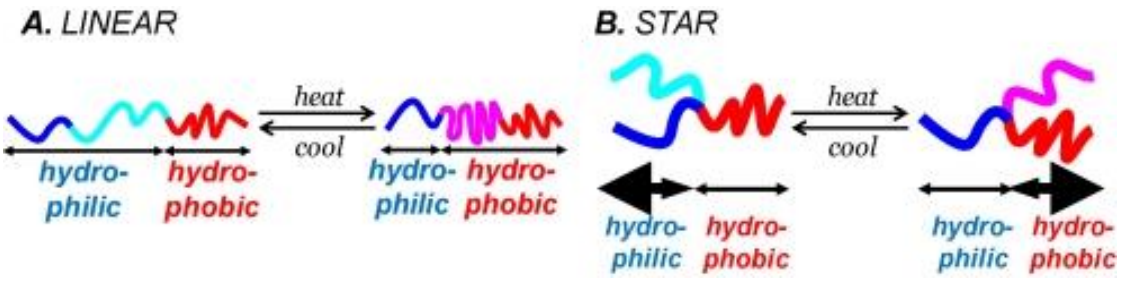

Figure 4-1. Comparison of thermally induced changes in amphiphilic balance for (A) linear hydrophilic-responsive-hydrophobic block copolymer and (B) hydrophilic-responsive-hydrophobic three-arm star copolymer. Reprinted from Ref.[1], with the permission from The Royal Society of Chemistry.

In this chapter, we describe the attempted synthesis of poly(ethylene oxide)-poly(*N*,*N*-diethylacrylamide)-poly(lactic acid) (PEO-S(PDEAm)-PLA), a new thermally responsive tri-arm block copolymer in order to provide better understanding of the effects of both polymer composition and architecture on thermally induced polymer assemblies. The general synthetic strategy is the use of a macromolecular thiol-ene reaction to couple thermally responsive PDEAm homopolymer prepared by RAFT polymerization to the block junction of the PEO-PLA amphiphilic diblock polymer prepared by ring opening polymerization of lactide from a PEO macroinitiator.

4.2 Experimental

Materials

Methoxy PEO amine, HCl salt (M_n = 2000 g/mol) was purchased from JenKem Technology (Beijing, China) and freeze-dried from benzene before use. 3,6-Dimethyl-1,4-dioxane-2,5-dione (D,L-lactide) was purchased from Sigma-Aldrich, recrystallized from THF, and stored in a N_2-filled dry box. 1,8-Diazabicyclo[5,4,0]undec-7-ene (DBU) from Sigma-Aldrich was distilled from CaH_2, dissolved in THF (20mg/mL), and stored above molecular sieves (4 Å 1-2 mm beads, Alfa Aesar) under N_2. Triethylamine (TEA) was purchased from J. T. Baker and passed through a basic alumina column prior to use. Trifluoroacetic acid (TFA) was purchased from Alfa Aesar. 1-(3-

Dimethylaminopropyl)-3-ethylcarbodiimide hydrochloride (EDC·HCl) was purchased from TCI. Hydroxybenzotriazole monohydrate (HOBt·H_2O) was purchased from Advanced ChemTech (Louisville, KY). BOC-Ser-OH (99%) was purchased from AAPPTec (Louisville, KY). All other chemicals and solvents were purchased from Fisher or Sigma-Aldrich and used as received.

Characterization

Nuclear Magnetic Resonance Spectroscopy (NMR). ^{1}H NMR spectroscopy was carried out on a 300 MHz Varian Gemini 2300 spectrometer using $CDCl_3$ as solvent. Chemical shifts were referenced to the residual proton peak of $CDCl_3$ (7.26 ppm).

Gel Permeation Chromatography (GPC). GPC was performed at 40 °C using THF (HPLC grade, J.T. Baker) eluent at a flow rate of 1.0 mL/minute at 40 °C. The apparatus consisted of a K-501 pump (Knauer), a K-3800 Basic Autosampler (Marathon), two PLgel 5 μm Mixed-D columns (300 X 7.5 mm, rated for polymers between 200-400,000 g/mol, Polymer Laboratories), and a PL-ELS 1000 Evaporative Light Scattering Detector (Polymer Laboratories). A PL Datastream unit (Polymer Laboratories) was used to acquire data, which was analyzed based on narrow polydispersity polystyrene standards in the molecular weight range of 580-400,000 g/mol (EasiCal PS-2, Polymer Laboratories).

Synthetic Procedures

Synthesis of macroinitiator mPEO-S(BOC)-OH[2]

Methoxy PEO amine, HCl salt (1.0 g, M_n = 2000 g/mol, 0.465 mmol), BOC-Ser-OH (135 mg, 0.66 mmol), HOBt (84 mg, 0.55 mmol), and TEA (110 mg, 1.1 mmol) were dissolved in CH_2Cl_2 (40 mL) and the resulting solution was stirred below 4 °C in an ice bath. EDC·HCl (105 mg, 0.55

mmol) was then added dropwise by syringe to the reaction solution in an ice bath. After addition of EDC, the reaction solution was stirred for 24 hours at room temperature. The mixture was washed with distilled water (10 mL) and brine solution (10 mL). The organic layer was dried with anhydrous $MgSO_4$, then filtered and concentrated by rotary evaporation. The resulting viscous yellow oil was dissolved in CH_2Cl_2 (1 mL) and precipitated into hexanes (20 mL) to afford a white solid (920 mg, ~85%).

^{1}H NMR ($CDCl_3$, 300 MHz): δ 3.4 (3H, s, -OCH_3), 3.5-4.0 (4H per repeating unit in PEO, br, -CH_2CH_2-O-), 1.4 (9H, s, Boc protecting group).

Synthesis of diblock copolymer PEO-S(Boc)-PLA through ring-opening polymerization of lactide with DBU[3-4]

Inside a N_2-filled glovebox, PEO2k-S(Boc)-OH macroinitiator (128 mg, 0.054 mmol) and D,L-lactide (117 mg, 0.81 mmol) were dissolved in THF (5 mL). A solution of DBU in THF (0.06 mL, 0.13 M in THF) was then added to the polymerization solution by syringe. After stirring at 25 °C for 2 h, benzoic acid (66.0 mg, 0.54 mmol) was added to terminate the polymerization. The reaction mixture was then concentrated and precipitated into diethyl ether (20 mL). The white precipitate was redissolved in THF (1 mL) and precipitated into hexanes/EtOAc (20 mL, 19:1 v/v) to afford a white solid (170 mg, ~70%).

^{1}H NMR ($CDCl_3$, 300 MHz): δ 3.4 (3H, s, OCH_3), 3.5-4.0 (4H per repeating unit in PEO, br, -CH_2CH_2O-), 1.4 (9H, s, Boc protecting group), 5.0-5.2 (1H per repeating unit in PLA, br, -CH-CH_3), 1.6-1.8 (3H per repeating unit in PLA, br, -CHCH_3).

Deprotection of diblock PEO-S(BOC)-PLA

Diblock copolymer PEO-S(BOC)-PLA (160.0 mg, 0.03 mmol) was dissolved in CH_2Cl_2 (2 mL), then TFA (1 mL, 12 mmol) was added and the resulting solution was stirred for 3 h at 25 °C. After rotary evaporation, the resulting solid was redissolved in THF (1 mL) and precipitated into isopropyl alcohol/Et_3N (20 mL, 19:1 v/v). The resulting suspension was centrifuged to afford a white solid (108 mg, ~72%) after drying in a vacuum oven.

^{1}H NMR ($CDCl_3$, 300 MHz): δ 3.4 (3H, s, OCH_3), 3.5-4.0 (4H per repeating unit in PEO, br, -CH_2CH_2O-), 5.0-5.2 (1H per repeating unit in PLA, br, -CH-CH_3), 1.6-1.8 (3H per repeating unit in PLA, br, -CHCH_3).

Synthesis of *N*-acryloxysuccinimide (NASI)[5]

N-Hydroxysuccinimide (5.0 g, 44 mmol) and triethylamine (6 mL, 45 mmol) were dissolved in dichloromethane (60 mL) in a flask cooled in an ice bath. Acryloyl chloride (3.8 mL, 46 mmol) was then added dropwise by syringe, and the resulting suspension was stirred in an ice bath for 20 min and then stirred for an additional 60 min at room temperature. The reaction mixture was filtered to remove triethylammonium chloride and the filtrate was washed with distilled water (50 mL) and brine (50 mL). The dichloromethane solution was dried over Na_2SO_4 and concentrated. The crude solid was purified by recrystallization from 6:1 hexanes/ethyl acetate solution to afford a white powder (5.9 g, 81%).

^{1}H NMR ($CDCl_3$, 300 MHz): δ 6.70 (dd, J = 17.3, 1.1 Hz, 1H, trans β-CH_2), 6.34(dd, J = 17.1, 10.8 Hz, 1H, α-CH=CH_2), 6.19(dd, J = 10.8, 1.1 Hz, 1H, cis β-CH_2), 2.87(s, 4H, CO-(CH_2)$_2$-CO).

Synthesis of chain-transfer agent S-Methoxycarbonylphenylmethyl Dithiobenzoate (MCPDB)[6]

Phenylmagnesium bromide (3 M in ether, 2.2 mL, 6.6 mmol) was dissolved in dry THF (5 mL). Carbon disulfide (0.4 mL, 6.8 mmol) was added dropwise at 40 °C to afford a dark brown solution. After stirring 30 min at 40 °C, methyl α-bromophenylacetate (1.37 g, 6 mmol) in THF (20 mL) was added into the solution and the reaction mixture was refluxed for 24 h under nitrogen. Ice water (10 mL) was then added to the reaction mixture and the resulting mixture was washed with ether (3 x 20 mL). The combined organic extracts were dried with anhydrous MgSO4. The crude product was purified by column chromatography (diethyl ether/hexanes (1:9)) to afford an orange-red oil (0.9 g, 50%)

^{1}H NMR ($CDCl_3$, 300 MHz): δ 3.6 (3H, s, O-C*H*$_3$), 5.6 (1H, s, -S(Ph)C*H*-CO_2Me), 7.2-7.5 (8H, m, Ar-*H*), 7.9 (2H, dd, -SC(Ar-*H*)S-).

Synthesis of poly(*N,N*-diethylacrylamide) (PDEAm)

In a typical protocol for the synthesis of PDEAm, DEAm (0.46 g, 3.6 mmol), MCPDB (0.063 g, 0.2mmol), and AIBN (0.003 g, 0.02 mmol) were added along with 1,4-dioxane (1 mL) to a Schlenk flask. The Schlenk flask was degassed via three freeze–pump–thaw cycles, backfilled with nitrogen and then placed in a preheated oil bath at 80 °C. The polymerization was halted after 24 h by cooling under liquid nitrogen followed by exposure to air. The viscous reaction mixture was dissolved in dichloromethane (5 mL) and precipitated into cold hexanes (200 mL) to give the diblock copolymer as a pink solid. (Yield: 70%, 0.37 g, Conversion=80% calculated by comparison of residual DEAm monomer vinyl peaks in the ^{1}H NMR spectrum of the crude reaction mixture, M_n(^{1}HNMR) = 2.5 kg/mol, $Đ$ = 1.3)

Coupling PEO-S(NH_2)-PLA with NASI

PEO-S(NH_2)-PLA (42 mg, 0.01 mmol), NASI (5.3 mg, 0.03 mmol) and TEA (1 mg, 0.01 mmol) were dissolved in dry THF (2 mL). The solution was stirred in an ice bath for 2 h and then allowed to warm to room temperature with stirring over 24 h. The reaction mixture solution was dialyzed against distilled water for 24 h in a dialysis bag (MWCO 3500 Da) to afford a white powder (16 mg, 40%) after freeze-drying.

Synthesis of thermally responsive tri-arm star copolymers PEO-S(PDEAm)-PLA[7]

Diblock copolymers PEO-PLA (49 mg, 0.01 mmol, M_n = 4.9 kg/mol), PDEAm (20 mg, 0.01 mmol, M_n = 2 kg/mol), DMPP (4 mg, 0.03 mmol) were dissolved in dry THF (2 mL). The solution was stirred under nitrogen for 5 minutes to ensure complete homogeneity. Diethylamine (50 μL) was then added to this solution and the mixture was allowed to stir 24 h under nitrogen. The reaction mixture solution was dialyzed against distilled water for 24 h in a dialysis bag (MWCO 3500) to afford a white powder (31 mg, 45%) after freeze-drying.

4.3 Results and Discussion

Synthesis of thermally responsive homopolymer poly(N,N-diethylacrylamide) (PDEAm)

N,N-Diethylacrylamide was chosen to allow comparison of the new thermally responsive star polymers with previously prepared linear PEO-PDEAm-PDBAm polymers (Chapter 2). Using AIBN and 1,4-dioxane as the initiator and solvent, *N,N*-diethylacrylamide was polymerized in a controlled manner at 80 °C with the RAFT chain-transfer agent MCPDB (Scheme 4-1). DEAm conversion was estimated by the method described in Chapter 2.3, based on integration of residual DEAm vinyl proton peaks in ^{1}H NMR spectra of the crude reaction mixtures (Figure 4-2). The

molecular weight of PDEAm was calculated from ^{1}H NMR spectra of purified PDEAm (Figure 4-3) and a low polydispersity ($Đ$ < 1.5) was measured by GPC.

Scheme 4-1. Synthesis of RAFT-CTA MCPDB and PDEAm Homopolymer at 80 °C

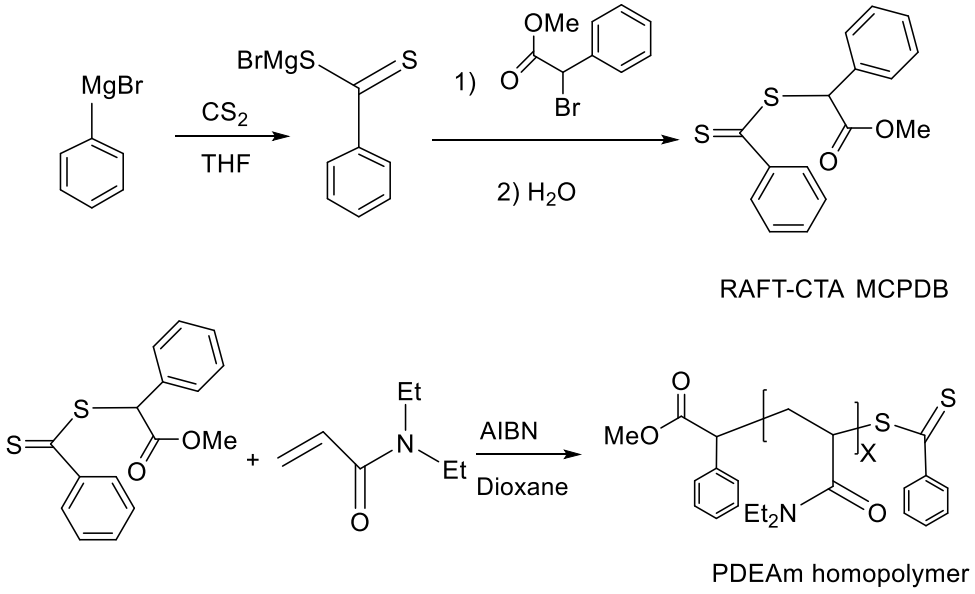

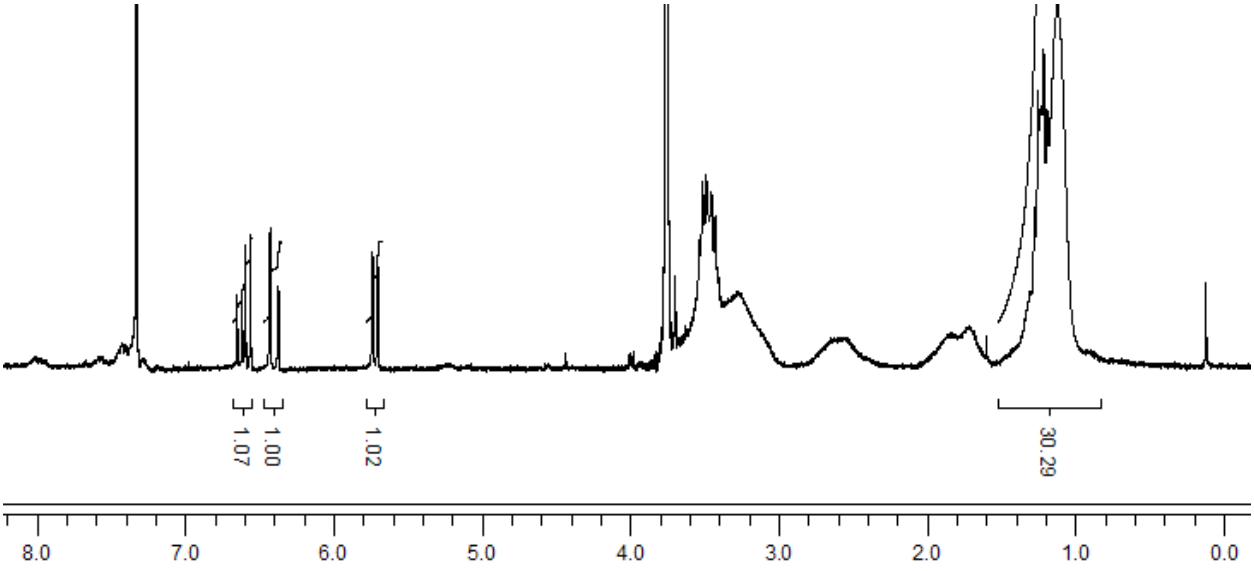

Figure 4-2. ^{1}H NMR spectrum of PDEAm$_{20}$ crude mixture after polymerization for 24 h at 80 °C.

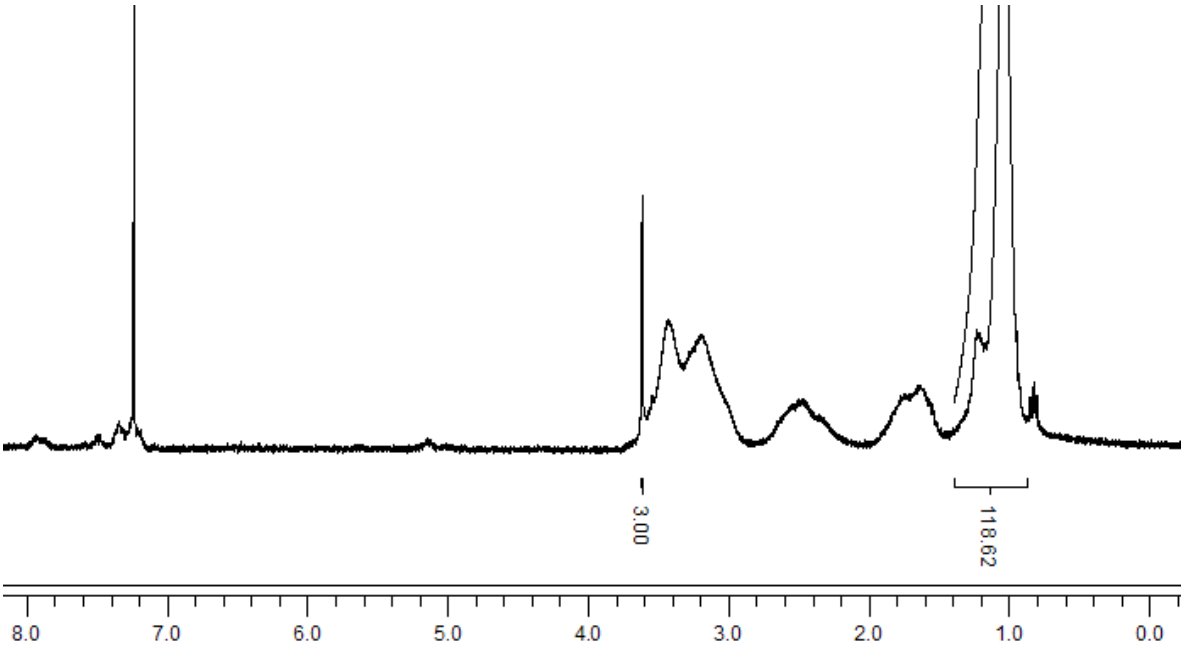

Figure 4-3. ^{1}H NMR spectrum of purified PDEAm$_{20}$ polymer.

Synthesis of diblock copolymer PEO-S(Boc)-PLA

The macroinitiator PEO-S(Boc)-OH was prepared by the coupling of Boc–protected serine with methoxy PEO amine, as reported by Sureshbabu[2]. Based on the ^{1}H NMR spectrum of macroinitiator PEO-S(Boc)-OH, the disappearance of the triplet peak (δ = 3.2 ppm, 2H) corresponding to the protons of the methylene group adjacent to the terminal amine group of PEO-NH_2 and appearance of a new singlet peak (δ = 1.4 ppm, 9H) corresponding to the three methyl groups in the Boc protecting group, confirmed complete conversion to PEO-S(Boc)-OH from PEO-NH_2. The hydroxyl group in the PEO-S(Boc)-OH was subsequently used to initiate the ring opening polymerization (ROP) of lactide with DBU as a catalyst at 25 °C to afford the diblock copolymer PEO-S(Boc)-PLA.[3-4]

Scheme 4-2. Synthesis of diblock copolymer PEO-S(Boc)-PLA

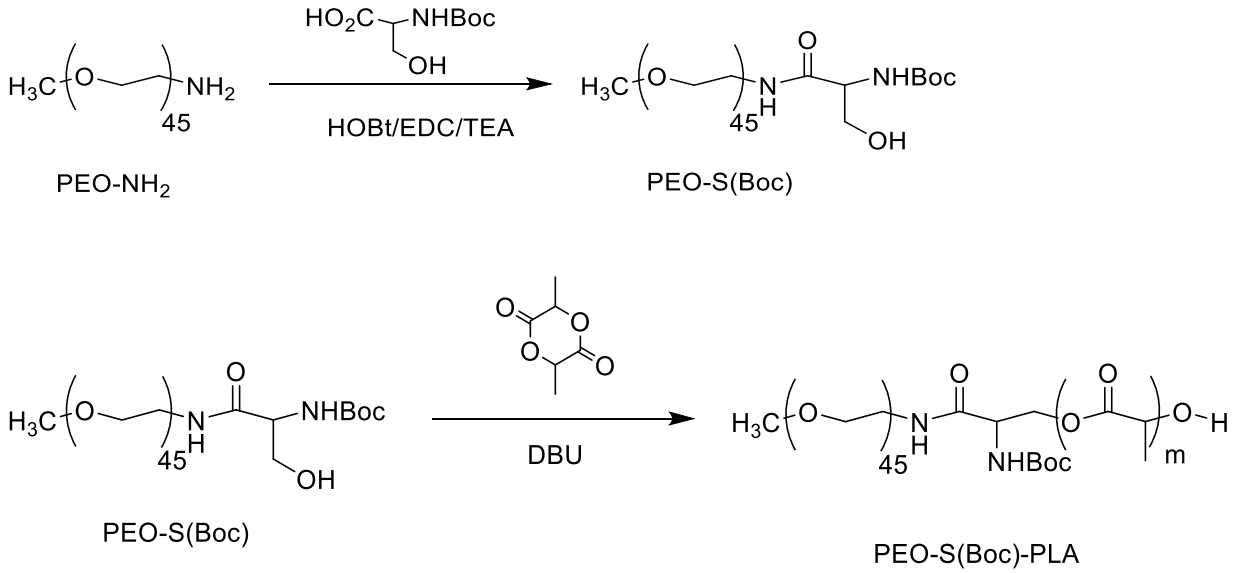

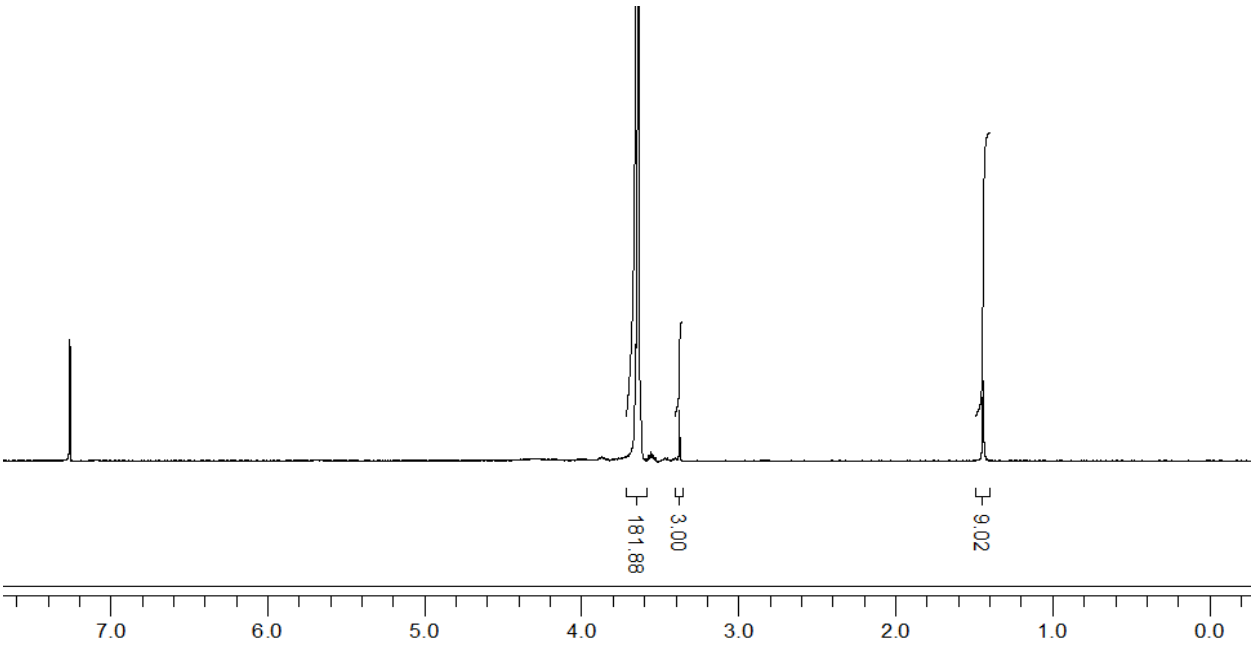

Figure 4-4. ^{1}H NMR spectrum of macroinitiator PEO-S(Boc)-OH.

Monomer conversion was calculated by comparing the integrated areas of the methine proton peaks of residual lactide (5.02 ppm) and in the PEO-S(Boc)-PLA diblock copolymer (5.18 ppm). For example, in Figure 4-5, conversion = 1 / (1 + 0.14) = 0.88. The small aromatic peaks (8.20 - 7.40 ppm) are protons of benzoic acid, which was used to terminate the polymerization. Assuming that blocking efficiency of PEO-S(Boc)-OH is 100%, and all monomer that was lost from the reaction mixture is converted to polymer, the molecular weight of diblock PEO-S(Boc)-PLA can be calculated based on conversion or the ^{1}H NMR spectrum of purified PEO-S(Boc)-PLA. For example, for the polymerization shown in Figure 4-6, the number of repeating units in the PLA block was calculated to be 19 by comparing the integration of the PLA methine proton to that of the terminal PEO methyl group. So M_n = 19×72+2188=3556 g/mol.

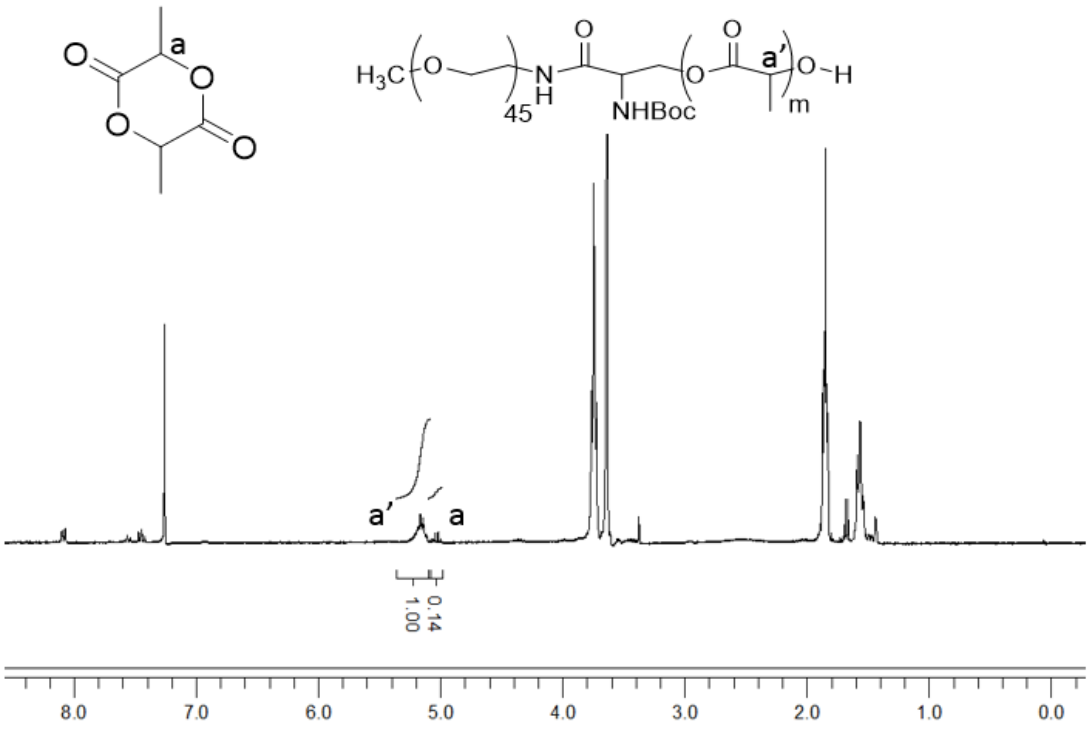

Figure 4-5. [1]H NMR spectrum of crude PEO-S(Boc)-PLA. The small aromatic peaks from 7.40 - 8.20 ppm are aromatic protons from benzoic acid, which was used to terminate the polymerization.

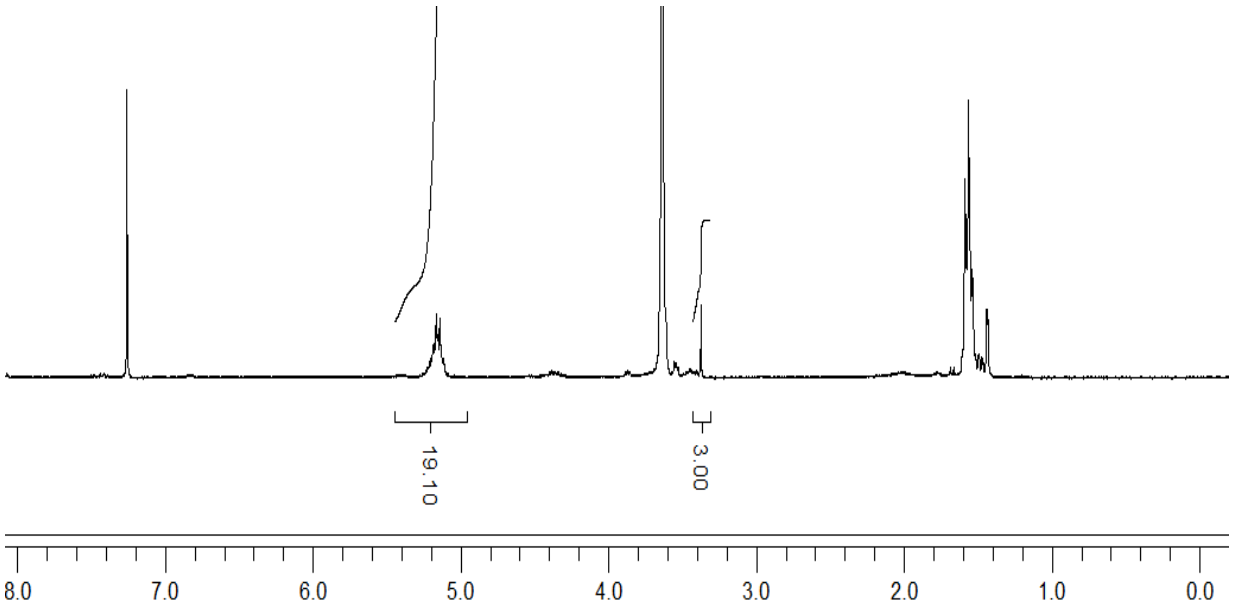

Figure 4-6. ^{1}H NMR spectrum of pure PEO-S(Boc)-PLA.

Synthesis of thermally responsive tri-arm star copolymers PEO-S(PDEAm)-PLA

Lowe and coworkers have reported the use of a macromolecular thiol-ene click reaction to couple PDEAm homopolymers prepared by RAFT polymerization (M_n = 4.4 kg/mol) with trimethyolpropane triacrylate to afford 3-arm star polymers [7]. It should be possible to use the same strategy to couple the PDEAm with a dithiobenzoate end-group with PEO-PLA diblock copolymers with an acryloyl group at the block junction. We first converted the dithiobenzoate group in homopolymer PDEAm to a thiol group through aminolysis.[8] A reducing agent, Zn/acetic acid, was used after the aminolysis to cleave any disulfide bonds formed during aminolysis. After aminolysis, reduction, and precipitation into hexanes, the pink PDEAm homopolymer became white, indicating successful removal of dithiobenzoate end-group. The GPC traces in Figure 4-7 suggested no significant change in the molecular weight of the polymers after aminolysis.

Scheme 4-3. Aminolysis and Reduction of PDEAm Polymer

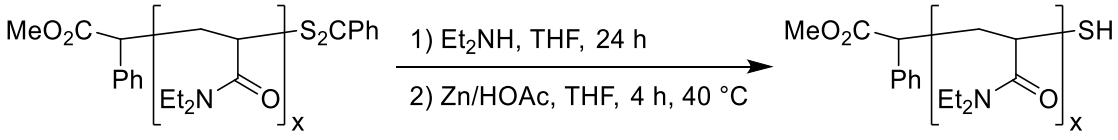

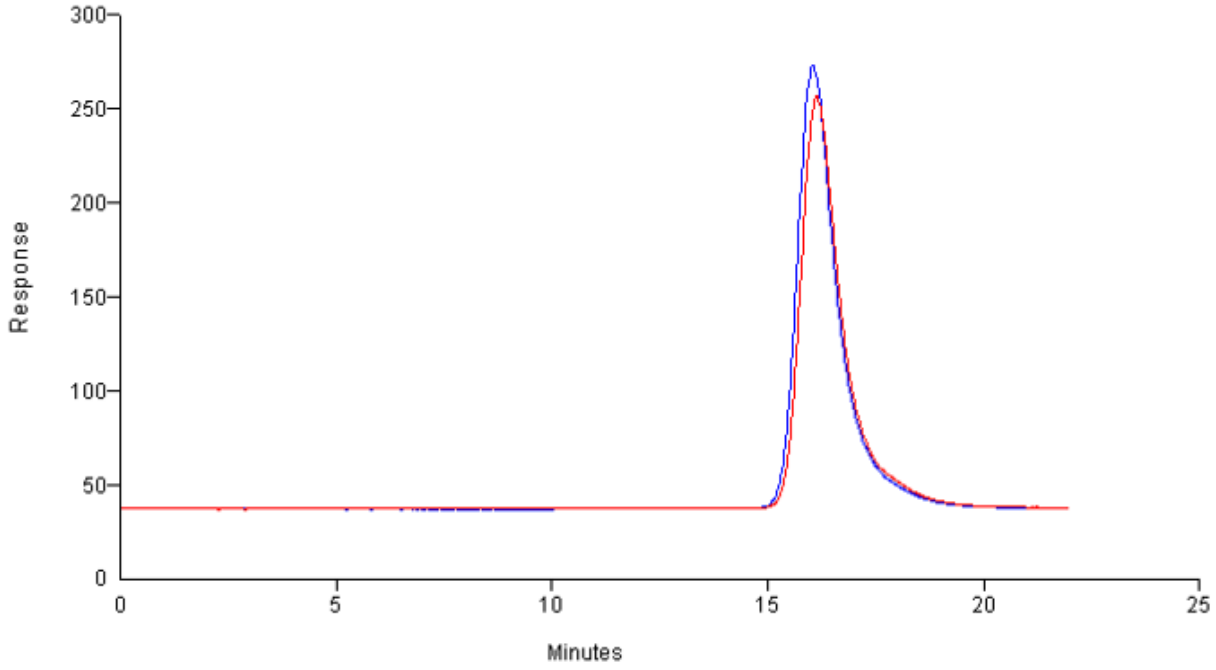

Figure 4-7. GPC traces of PDEAm polymer before (blue) and after (red) aminolysis.

We tried to introduce an alkene functional group at the block junction of PEO-PLA diblock polymers to allow coupling of PDEAm-SH by a thiol-ene reaction. After the synthesis of the PEG-S(BOC)-PLA diblock copolymer, the BOC protecting group was removed by reaction with trifluoroacetic acid (TFA) in dichloromethane (Scheme 4-4). The deprotection reaction can be confirmed by the disappearance of the BOC methyl protons at 1.43 ppm in the ^{1}H NMR spectrum. Then the free amine group was treated with *N*-acryloxysuccinimide (NASI), which was prepared by the reaction of *N*-hydroxysuccinimide and acryloyl chloride,[5] to afford the acrylamide functional group. In the ^{1}H NMR spectrum of diblock PEO-S(COCH=CH$_2$)-PLA copolymers after dialysis (Figure 4-8), the peaks at δ 5.8, 6.4, and 6.9 ppm attributed to the acryloyl protons were distinct from the peaks observed in the ^{1}H NMR spectrum of *N*-acryloxysuccinimide at δ 6.2, 6.3 and 6.7 ppm. These acryloyl proton peaks (Figure 4-8) were too small to accurately estimate the conversion for the acryloylation reaction.

Scheme 4-4. Synthesis of PEO-S(COCH=CH_2)-PLA

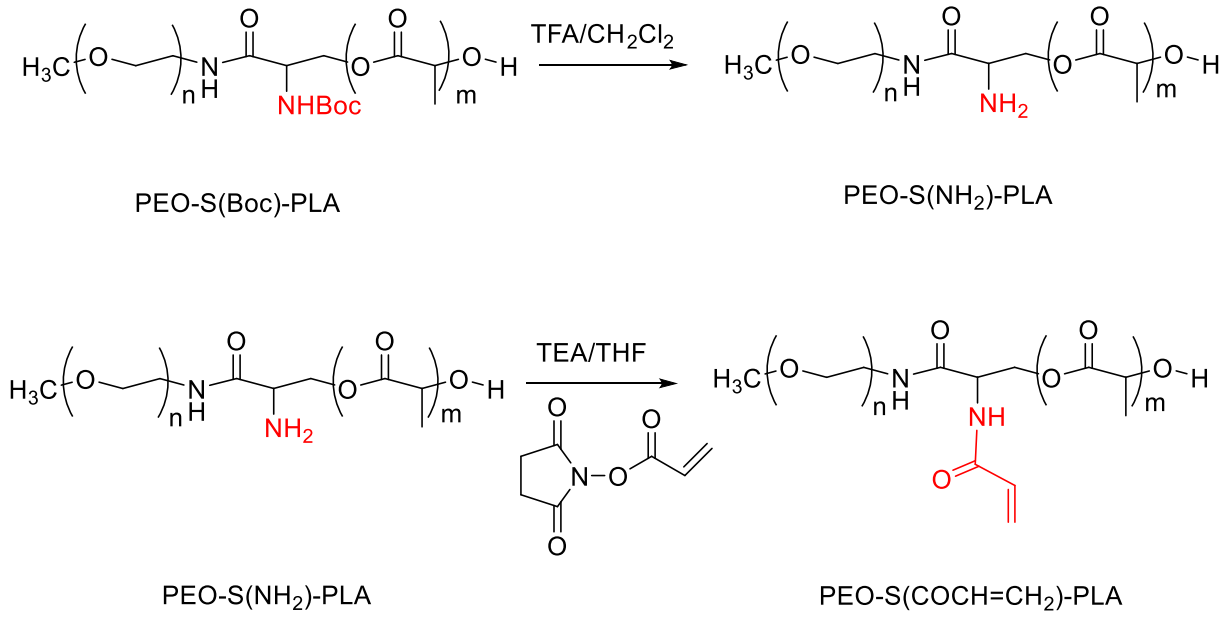

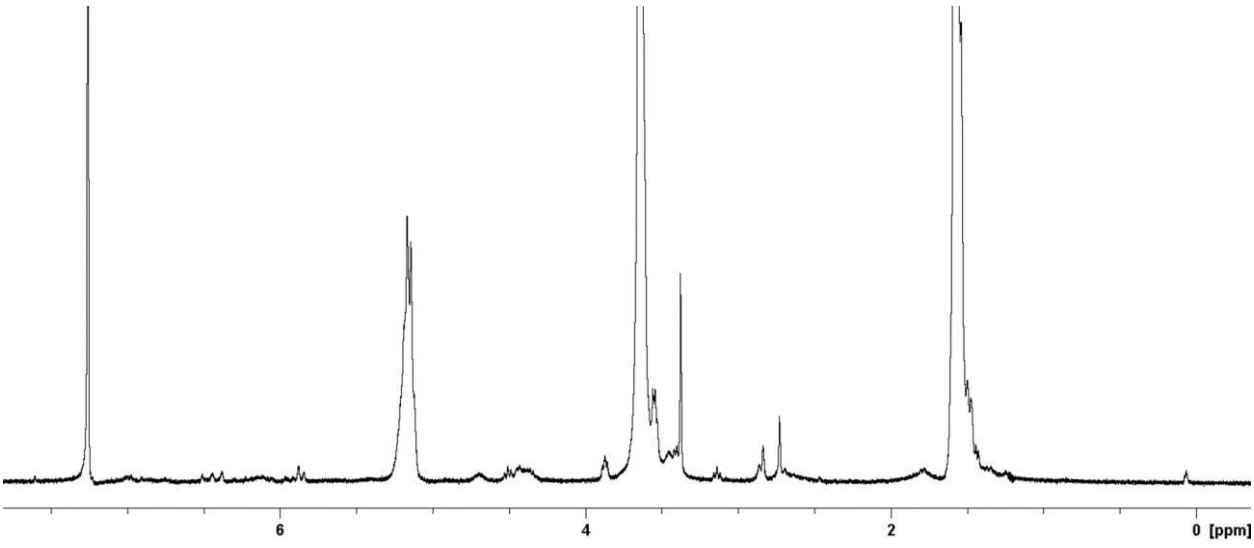

Figure 4-8. ^{1}H NMR spectrum of PEO-S(COCH=CH_2)-PLA after dialysis.

The method reported by Lowe[7] was adapted to couple PDEAm-SH with PEO-S(COCH=CH_2)-PLA with dimethylphenylphosphine (DMPP) as a thiol-ene catalyst in tetrahydrofuran ([PDEAm-SH]/[PEO-S(COCH=CH_2)-PLA] = 1) (Scheme 4-5). In the ^{1}H NMR

spectrum of PEO-S(PDEAm)-PLA after dialysis (Figure 4-9), disappearance of acrylamide alkene protons in the range of 5.8 ppm and 7 ppm, indicated that the thiol-ene coupling reaction occurred. However, a large polydispersity ($Đ$ =1.8) in the GPC traces of tri-arm star polymers in THF (Figure 4-10) showed that full coupling of PDEAm and PEO-S($COCH=CH_2$)-PLA was not successful.

Scheme 4-5. Synthesis of PEO-S(PDEAm)-PLA

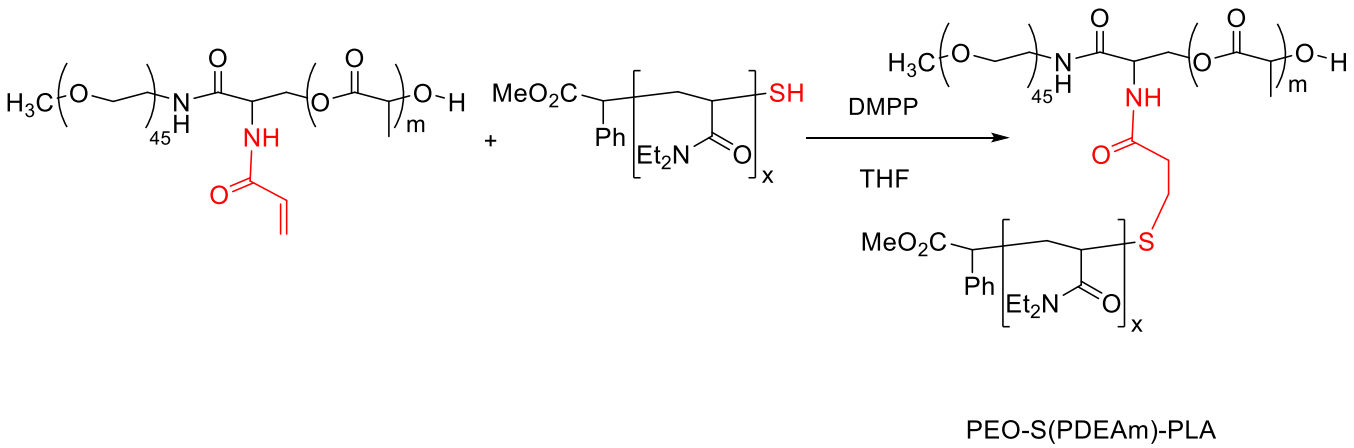

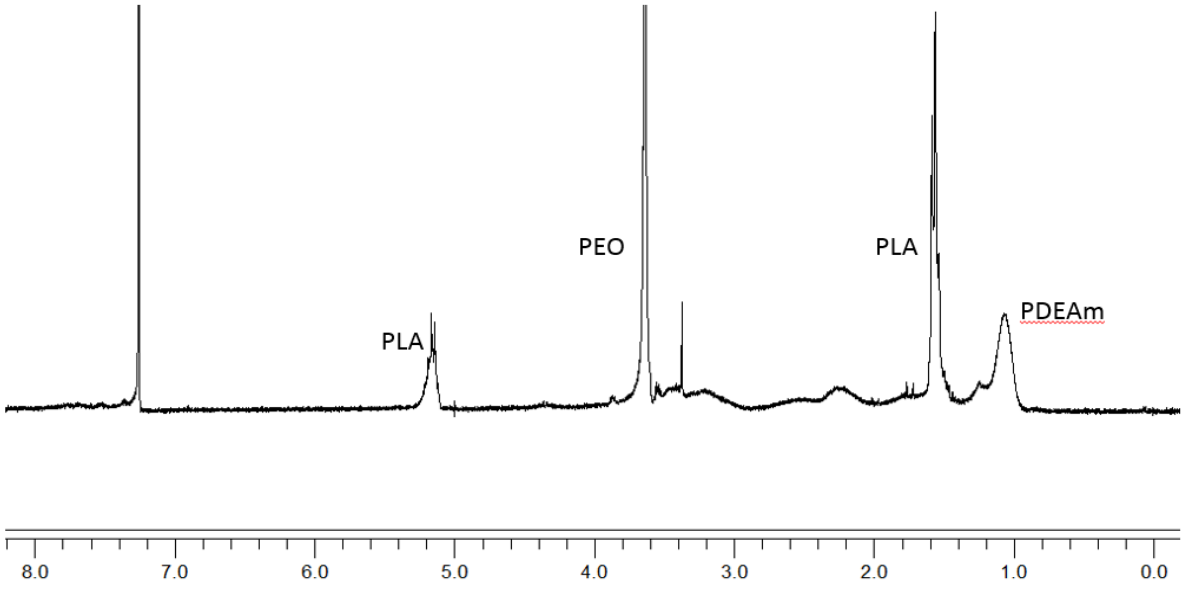

Figure 4-9. ^{1}H NMR spectrum of PEO-S(PDEAm)-PLA after dialysis.

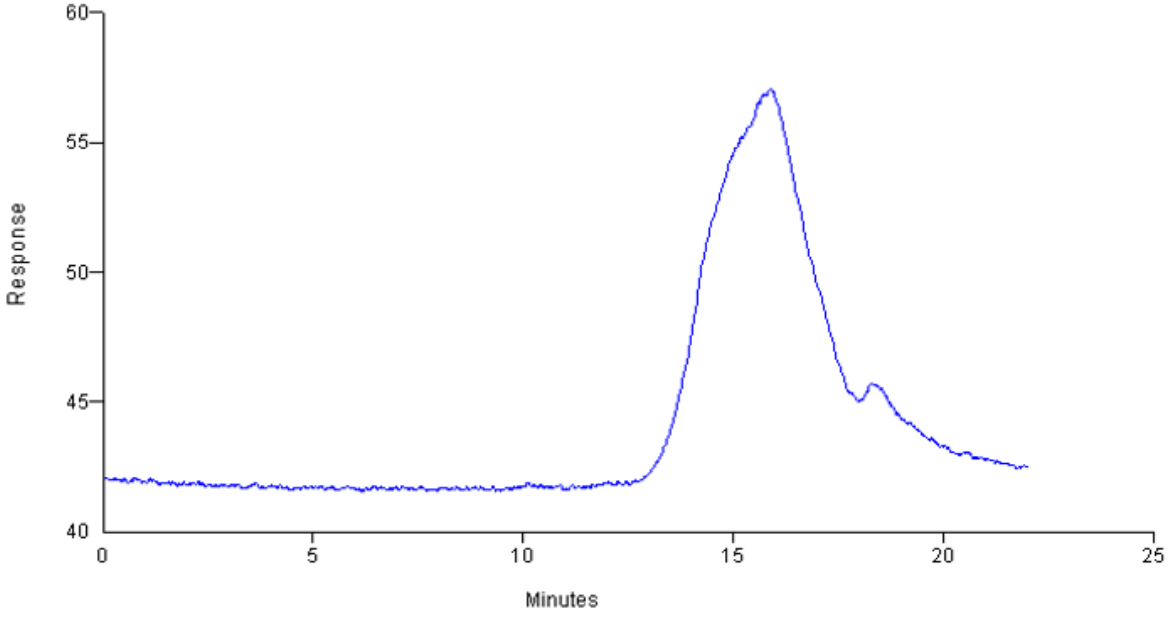

Figure 4-10. GPC traces of PEO-S(PDEAm)-PLA tri-arm star copolymer after dialysis.

4.4 Conclusion

In this chapter, we demonstrated the attempted synthesis of a new thermally responsive tri-arm block copolymer, poly(ethylene oxide)-poly(*N*,*N*-diethylacrylamide)-poly(lactic acid) (PEO-S(PDEAm)-PLA). However, difficulties were encountered in charactering the coupling efficiency of final macromolecular thiol-ene reaction between PDEAm-SH and PEO-S(COCH=CH_2)-PLA. In the future endeavors, cycloaddition reactions including azide-alkene cycloaddition [9] or Diels–Alder reaction[10] might be exploited to synthesize the target PEO-S(PDEAm)-PLA) star tri-arm block copolymer, since these click reactions are efficient, versatile and selective. In addition, cycloaddition reactions could be studied and characterized by UV-vis and FT-IR spectroscopy,

which provide more tools to monitor and calculate the efficiency of coupling reaction of PDEAm homopolymer with PEO-PLA diblock polymer.

Reference (Chapter 4)

1. Grubbs, R. B.; Sun, Z., Shape-changing polymer assemblies. *Chem. Soc. Rev.* **2013,** *42* (17), 7436-7445. (doi: 10.1039/c3cs60079c)

2. Sureshbabu, V. V.; Venkataramanarao, R.; Naik, S. A.; Narendra, N., Synthesis of Ureido-Linked Glycosylated Amino Acids from N-alpha-Fmoc-Asp/Glu-5-oxazolidinones and Their Application to Neoglycopeptide Synthesis. *Synth. Commun.* **2008,** *38* (21), 3640-3654. (doi: 10.1080/00397910802213711)

3. Lohmeijer, B. G. G.; Pratt, R. C.; Leibfarth, F.; Logan, J. W.; Long, D. A.; Dove, A. P.; Nederberg, F.; Choi, J.; Wade, C.; Waymouth, R. M.; Hedrick, J. L., Guanidine and amidine organocatalysts for ring-opening polymerization of cyclic esters. *Macromolecules* **2006,** *39* (25), 8574-8583. (doi: 10.1021/ma0619381)

4. Kiesewetter, M. K.; Scholten, M. D.; Kirn, N.; Weber, R. L.; Hedrick, J. L.; Waymouth, R. M., Cyclic guanidine organic catalysts: what is magic about triazabicyclodecene? *J. Org. Chem.* **2009,** *74* (24), 9490-9496. (doi: 10.1021/jo902369g)

5. Allen, A. L.; Tan, K. J.; Fu, H.; Batteas, J. D.; Bergbreiter, D. E., Solute- and temperature-responsive "smart" grafts and supported membranes formed by covalent layer-by-layer assembly. *Langmuir* **2012,** *28* (11), 5237-5242. (doi: 10.1021/la204626e)

6. Perrier, S.; Takolpuckdee, P.; Westwood, J.; Lewis, D. M., Versatile chain transfer agents for reversible addition fragmentation chain transfer (RAFT) polymerization to synthesize functional polymeric architectures. *Macromolecules* **2004,** *37* (8), 2709-2717. (doi: 10.1021/ma035468b)

7. Chan, J. W.; Yu, B.; Hoyle, C. E.; Lowe, A. B., Convergent synthesis of 3-arm star polymers from RAFT-prepared poly(N,N-diethylacrylamide) via a thiol-ene click reaction. *Chem Commun (Camb)* **2008,** (40), 4959-4961. (doi: 10.1039/b813438c)

8. Wang, Z. M.; He, J. P.; Tao, Y. F.; Yang, L.; Jiang, H. J.; Yang, Y. L., Controlled chain branching by RAFT-based radical polymerization. *Macromolecules* **2003,** *36* (20), 7446-7452. (doi: 10.1021/ma025673b)

9. Fournier, D.; Hoogenboom, R.; Schubert, U. S., Clicking polymers: a straightforward approach to novel macromolecular architectures. *Chem. Soc. Rev.* **2007,** *36* (8), 1369-1380. (doi: 10.1039/b700809k)

10. Tasdelen, M. A., Diels-Alder "click" reactions: recent applications in polymer and material science. *Polymer Chemistry* **2011,** *2* (10), 2133-2145. (doi: 10.1039/c1py00041a)

Chapter 5 Conclusion and Outlook

In this thesis, a new class of thermally responsive ABC PEO-*b*-PDEAm-*b*-PDBAm triblock copolymers has been synthesized by RAFT polymerization. The fast transformation rate (within several minutes) from small spherical micelles to large aggregates, including worm micelles, vesicles and large compound micelles, was confirmed by DLS and TEM. The enhanced rate supports our hypothesis that the absence of strong interchain hydrogen bonding in the middle thermally responsive block of hydrophilic-responsive-hydrophobic ABC triblock copolymers could accelerate aggregate rearrangement. In addition, we have also designed a rapidly reversible thermoresponsive ABC triblock copolymer worm gel, which results from a sphere-to-worm transition at temperatures above the LCST of the PDEAm block. A preliminary experiment was also conducted, confirming the successful encapsulation of a hydrophilic dye Rhodamine B into the large compound micelles formed upon heating. These thermally morphological transitions and solution behavior may potentially be used in a range of applications such as drug delivery, molecular actuators and biosensors.[1-8]

Although we successfully characterized and investigated the fast thermally induced behavior of PEO-*b*-PDEAm-*b*-PDBAm triblock copolymers in water, there are still some aspects require further study.

Firstly, the rate of thermally induced morphological transition is fast (within 10 minutes), but the LCST of our PEO-*b*-PDEAm-*b*-PDBAm triblock copolymers in water (>45°C) is a bit higher than is desirable for biological applications. It is possible to lower this transition

temperature by increasing the molecular weight of the thermally responsive PDEAm block [9-12]or copolymerization with other hydrophobic monomers[13-15].

Secondly, three different thermally induced transitions from small spherical micelles to large aggregates including wormlike micelles, vesicles, or large compound micelles—were observed. Spherical micelle to vesicle or large compound micelle transitions can be explained by the new thermodynamically favorable structures with their small hydrophilic mass fractions (f<0.3) at 55 °C. We do not fully understand the spherical micelle to wormlike micelle transition. Further experiments including modeling studies and construction of more detailed phase diagram could help understand the formation and stability of wormlike micelles.

Thirdly, in our TEM experiment, we used uranyl acetate as a negative staining to preserve the structure and polymer samples are dried out on the TEM grids before imaging. It is possible that drying these samples can cause some changes in their sizes or morphologies.[16] Cryo-TEM or *in situ* cell TEM and SAXS may provide useful information about the aggregate morphologies, because their sample preparation process can keep the polymer solvated during measurement.

Last but not least, a preliminary experiment confirmed the successful encapsulation of a hydrophilic dye Rhodamine B into the large compound micelles. Further studies in this direction may include encapsulation of different types of particles/molecules using different methods and modification of the triblock polymers to optimized encapsulation efficiency.

Reference (Chapter 5)

1. Schmaljohann, D., Thermo- and pH-responsive polymers in drug delivery. *Adv Drug Deliv Rev* **2006,** *58* (15), 1655-1670. (doi: 10.1016/j.addr.2006.09.020)

2. Li, C.; Gunari, N.; Fischer, K.; Janshoff, A.; Schmidt, M., New perspectives for the design of molecular actuators: thermally induced collapse of single macromolecules from cylindrical brushes to spheres. *Angew. Chem. Int. Ed. Engl.* **2004,** *43* (9), 1101-1104. (doi: 10.1002/anie.200352845)

3. Pietsch, C.; Hoogenboom, R.; Schubert, U. S., Soluble polymeric dual sensor for temperature and pH value. *Angew. Chem. Int. Ed. Engl.* **2009,** *48* (31), 5653-5656. (doi: 10.1002/anie.200901071)

4. Meng, F.; Zhong, Z.; Feijen, J., Stimuli-responsive polymersomes for programmed drug delivery. *Biomacromolecules* **2009,** *10* (2), 197-209. (doi: 10.1021/bm801127d)

5. de Las Heras Alarcon, C.; Pennadam, S.; Alexander, C., Stimuli responsive polymers for biomedical applications. *Chem. Soc. Rev.* **2005,** *34* (3), 276-285. (doi: 10.1039/b406727d)

6. Ganta, S.; Devalapally, H.; Shahiwala, A.; Amiji, M., A review of stimuli-responsive nanocarriers for drug and gene delivery. *J Control Release* **2008,** *126* (3), 187-204. (doi: 10.1016/j.jconrel.2007.12.017)

7. Stuart, M. A.; Huck, W. T.; Genzer, J.; Muller, M.; Ober, C.; Stamm, M.; Sukhorukov, G. B.; Szleifer, I.; Tsukruk, V. V.; Urban, M.; Winnik, F.; Zauscher, S.; Luzinov, I.; Minko, S., Emerging applications of stimuli-responsive polymer materials. *Nat Mater* **2010,** *9* (2), 101-113. (doi: 10.1038/nmat2614)

8. Gil, E. S.; Hudson, S. M., Stimuli-reponsive polymers and their bioconjugates. *Prog. Polym. Sci.* **2004,** *29* (12), 1173-1222. (doi: 10.1016/j.progpolymsci.2004.08.003)

9. Freitag, R.; Baltes, T.; Eggert, M., A Comparison of Thermoreactive Water-Soluble Poly-N,N-Diethylacrylamide Prepared by Anionic and by Group-Transfer Polymerization. *J Polym Sci Pol Chem* **1994,** *32* (16), 3019-3030. (doi: DOI 10.1002/pola.1994.080321603)

10. Rieger, J.; Grazon, C.; Charleux, B.; Alaimo, D.; Jerome, C., Pegylated Thermally Responsive Block Copolymer Micelles and Nanogels via In Situ RAFT Aqueous Dispersion Polymerization. *J Polym Sci Pol Chem* **2009,** *47* (9), 2373-2390. (doi: 10.1002/pola.23329)

11. Lessard, D. G.; Ousalem, M.; Zhu, X. X.; Eisenberg, A.; Carreau, P. J., Study of the phase transition of poly(N,N-diethylacrylamide) in water by rheology and dynamic light scattering. *J Polym Sci Pol Phys* **2003,** *41* (14), 1627-1637. (doi: 10.1002/polb.10517)

12. Watanabe, R.; Takaseki, K.; Katsumata, M.; Matsushita, D.; Ida, D.; Osa, M., Characterization of poly(N,N-diethylacrylamide) and cloud points in its aqueous solutions. *Polym. J.* **2016,** *48* (5), 621-628. (doi: 10.1038/pj.2015.120)

13. Feil, H.; Bae, Y. H.; Feijen, J.; Kim, S. W., Effect of Comonomer Hydrophilicity and Ionization on the Lower Critical Solution Temperature of N-Isopropylacrylamide Copolymers. *Macromolecules* **1993,** *26* (10), 2496-2500. (doi: DOI 10.1021/ma00062a016)

14. Park, J. S.; Kataoka, K., Precise control of lower critical solution temperature of thermosensitive poly(2-isopropyl-2-oxazoline) via gradient copolymerization with 2-ethyl-2-oxazoline as a hydrophilic comonomer. *Macromolecules* **2006,** *39* (19), 6622-6630. (doi: 10.1021/ma0605548)

15. Cunningham, V. J.; Ratcliffe, L. P. D.; Blanazs, A.; Warren, N. J.; Smith, A. J.; Mykhaylyk, O. O.; Armes, S. P., Tuning the critical gelation temperature of thermo-responsive diblock copolymer worm gels. *Polymer Chemistry* **2014,** *5* (21), 6307-6317. (doi: 10.1039/c4py00856a)

16. Patterson, J. P.; Robin, M. P.; Chassenieux, C.; Colombani, O.; O'Reilly, R. K., The analysis of solution self-assembled polymeric nanomaterials. *Chem. Soc. Rev.* **2014,** *43* (8), 2412-2425. (doi: 10.1039/C3CS60454C)

Appendix

A1. Selected NMR Spectra (All spectra in d-chloroform unless otherwise stated)

A1.1 α-Bromophenylacetate terminated poly(ethylene oxide)

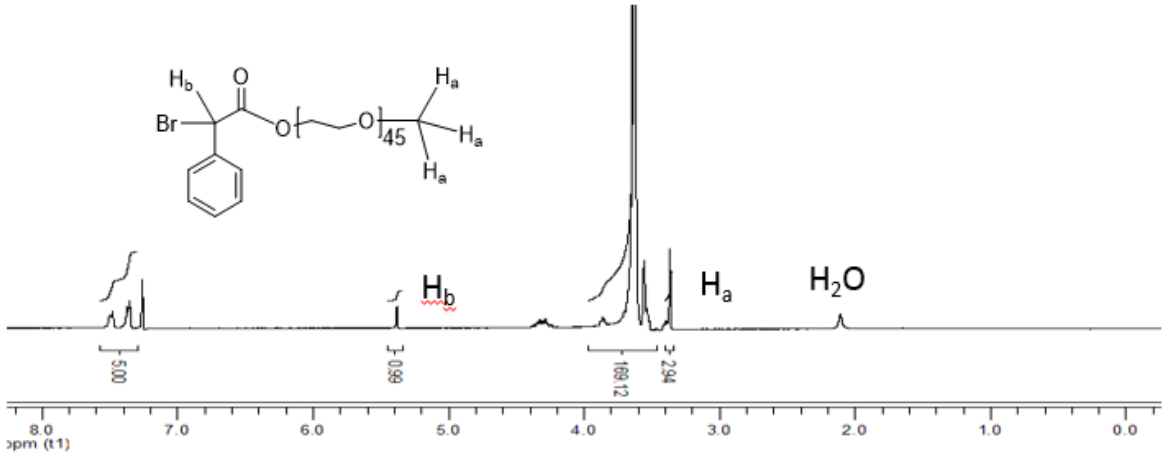

A1.2 PEO_{45} Macro-CTA

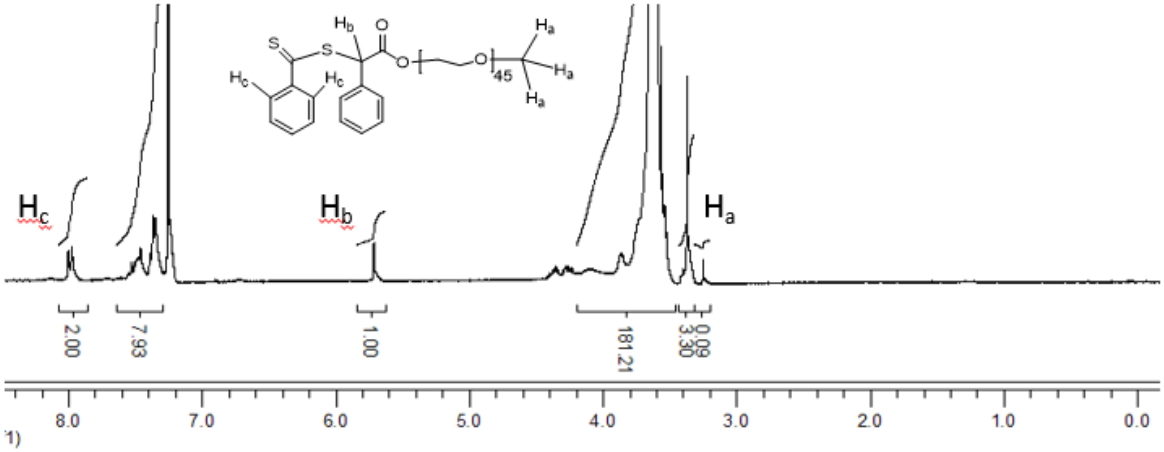

A1.3 *N,N*-Diethylacrylamide

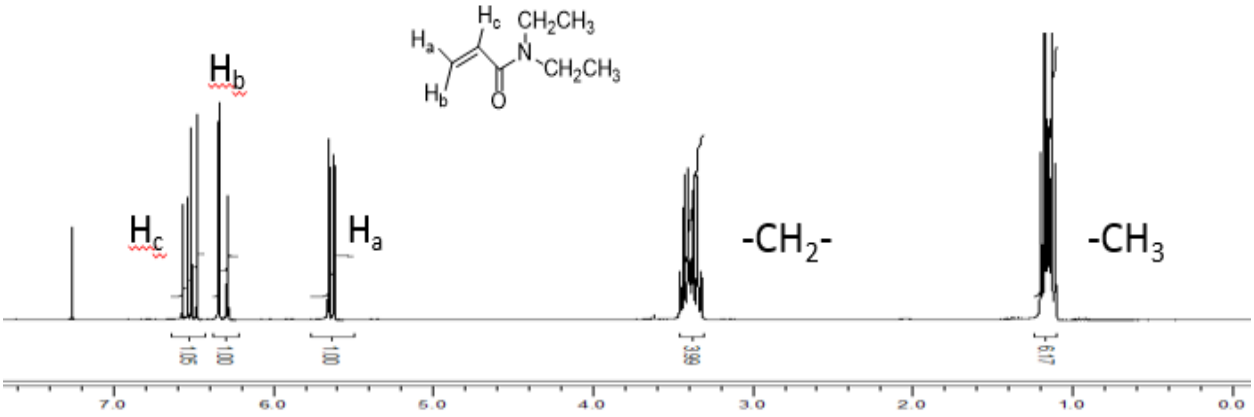

A1.4 *N*, *N*-Dibutylacrylamide

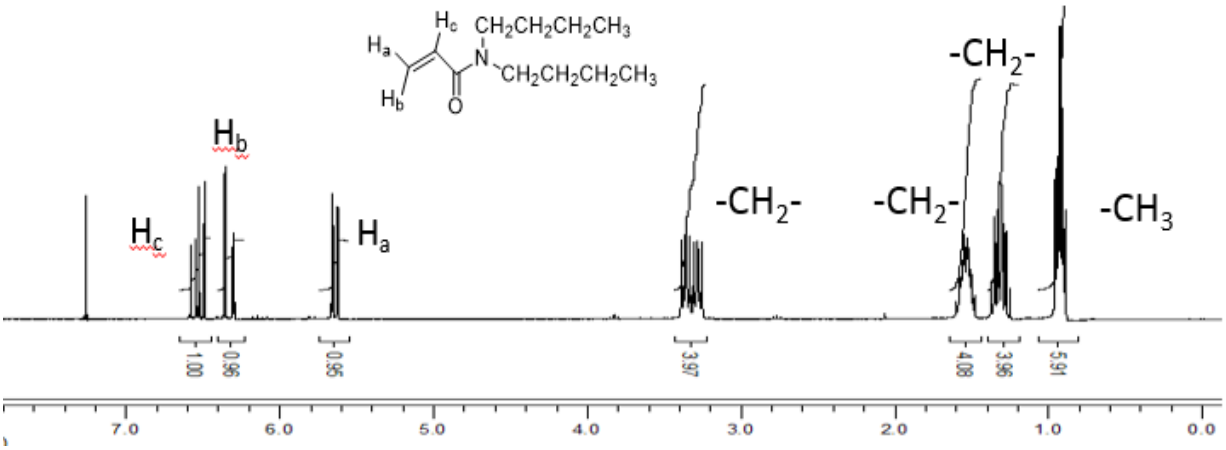

A1.5 3-Azidopropylamine

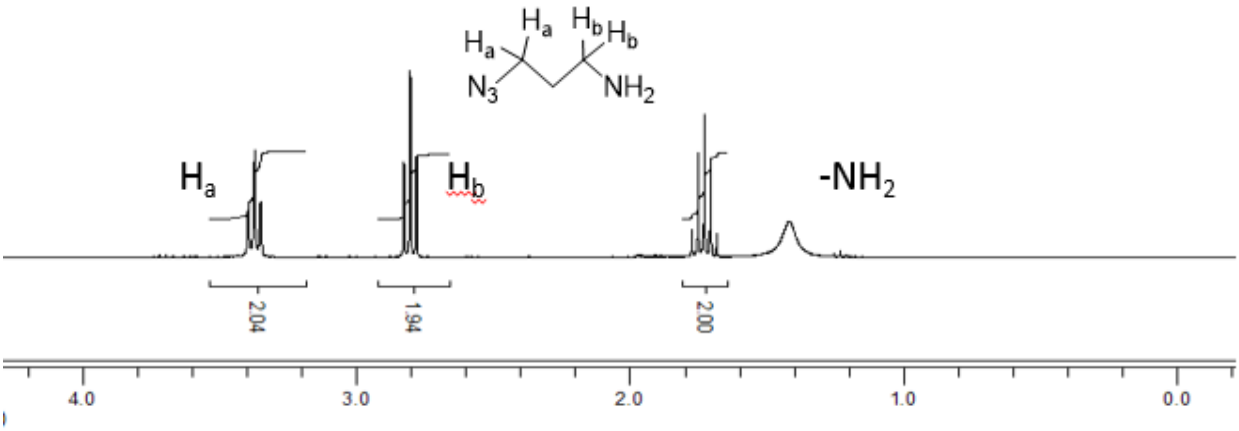

A1.6 3-azidopropylacrylamide

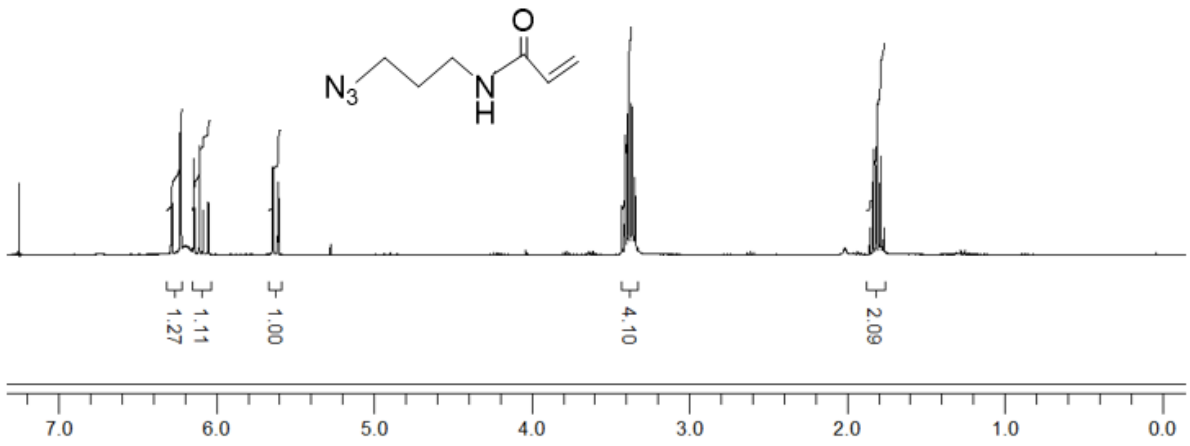

A1.7 *p*-Toluidine

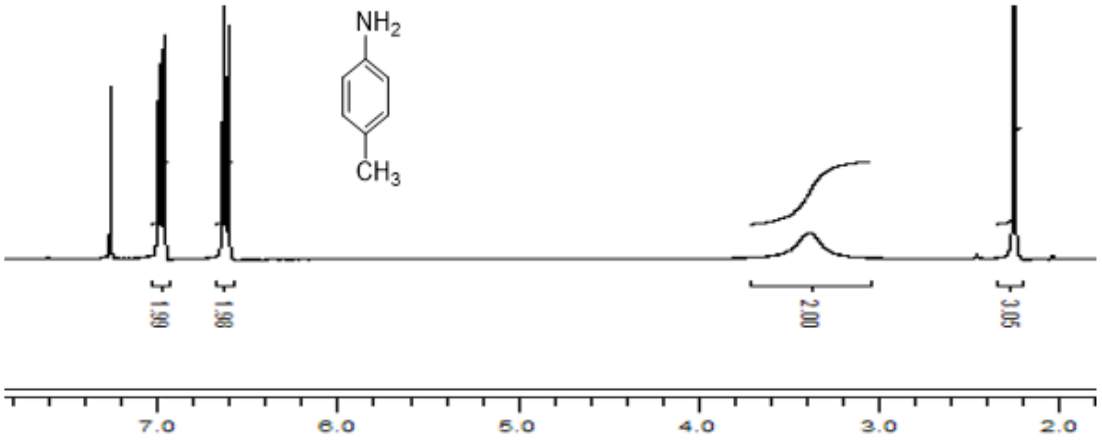

A1.8 4-azidotoluene

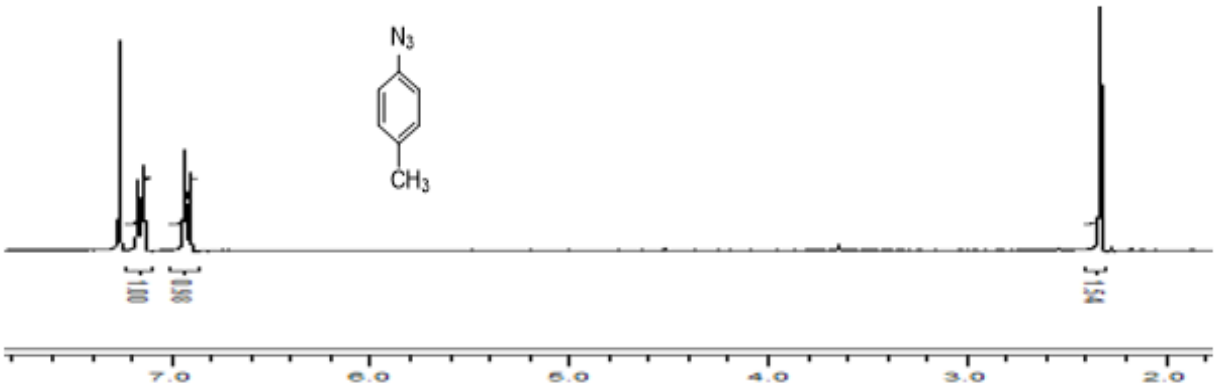

A1.9 4-azidobenzyl bromide

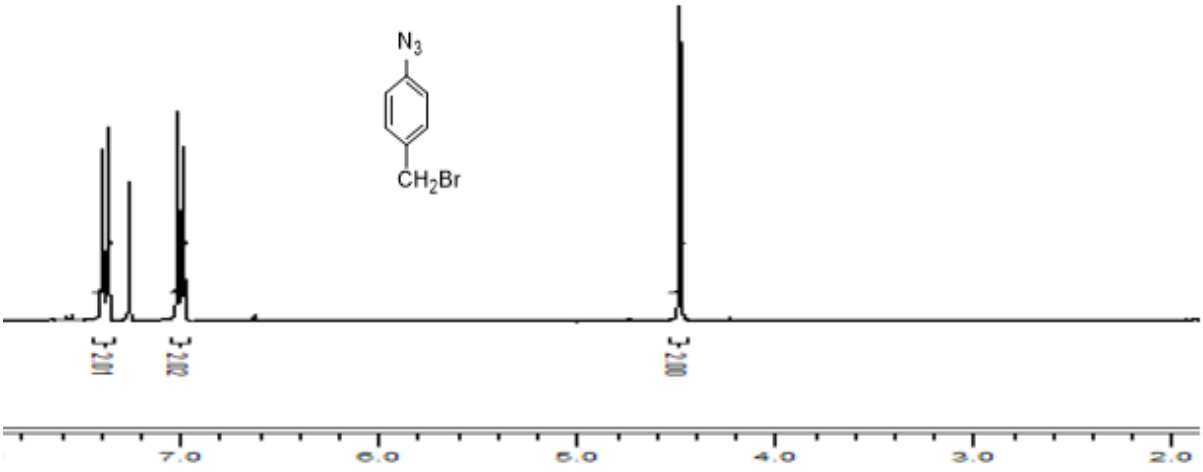

A1.10 *N*-(4-azidophenyl)phthalimide

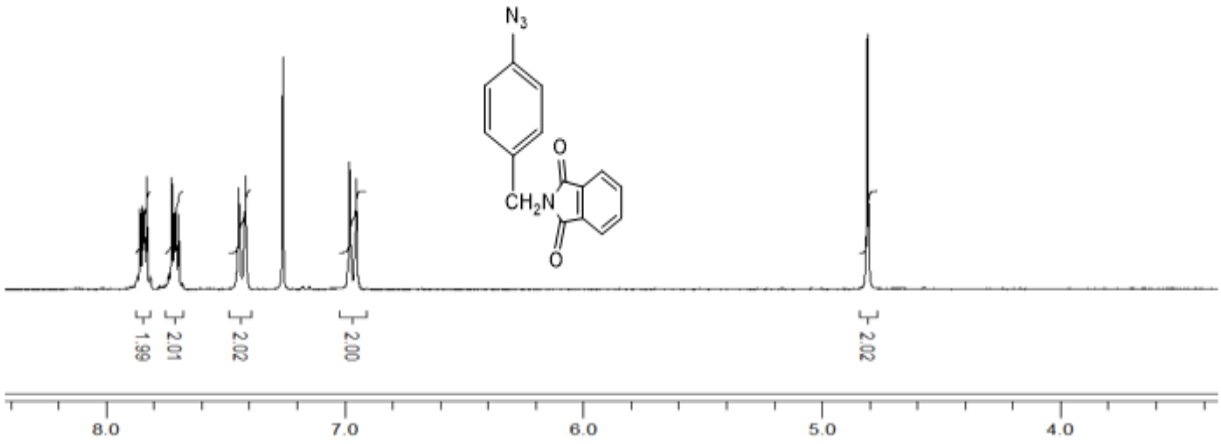

A1.11 4-azidobenzylamine

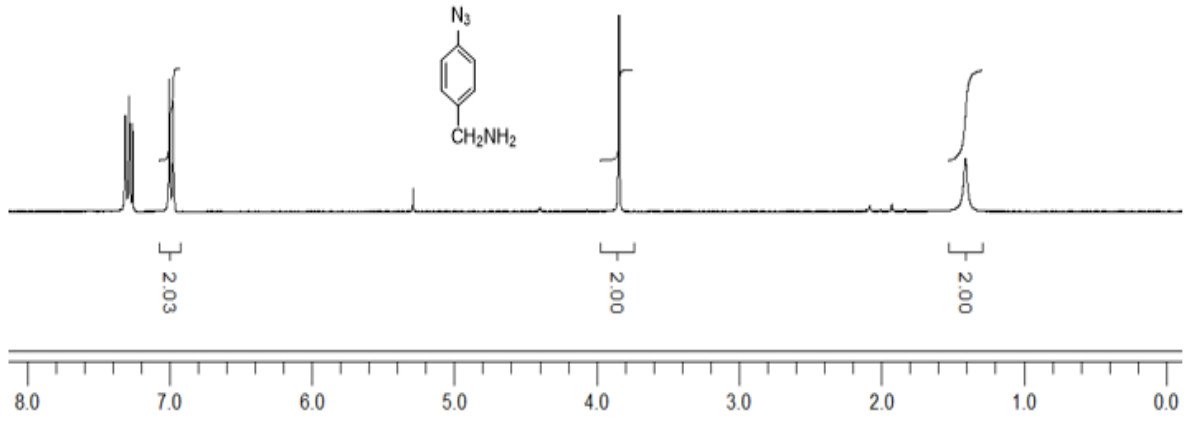

A1.12 *N*-(4-azidobenzyl)acrylamide

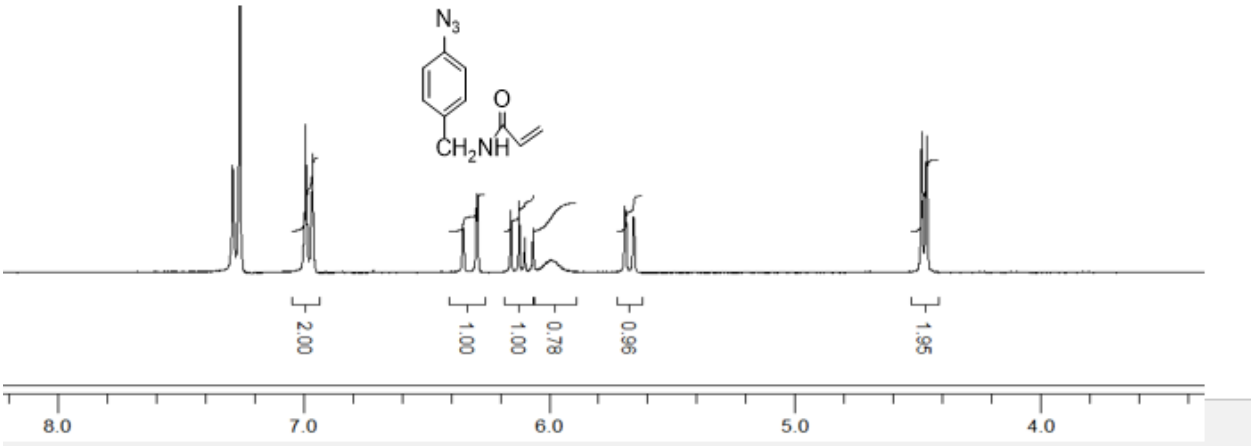

A1.13 *S*-methoxycarbonylphenylmethyl dithiobenzoate

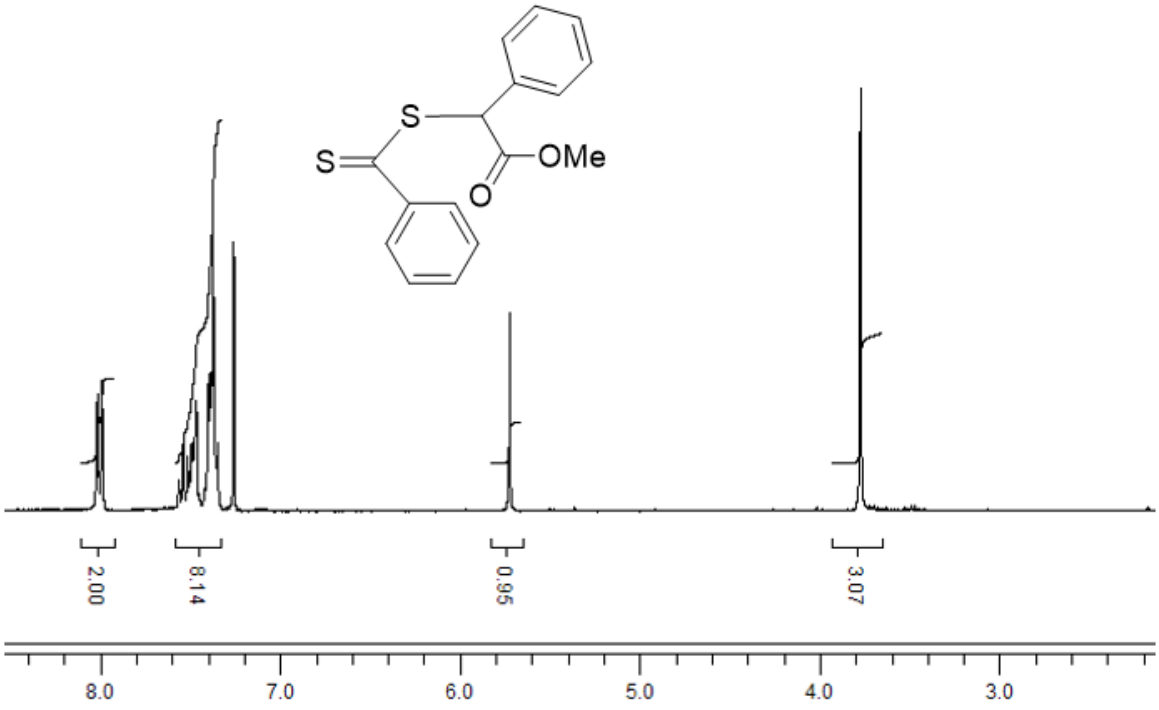

A1.14 *N*-acryloxysuccinimide

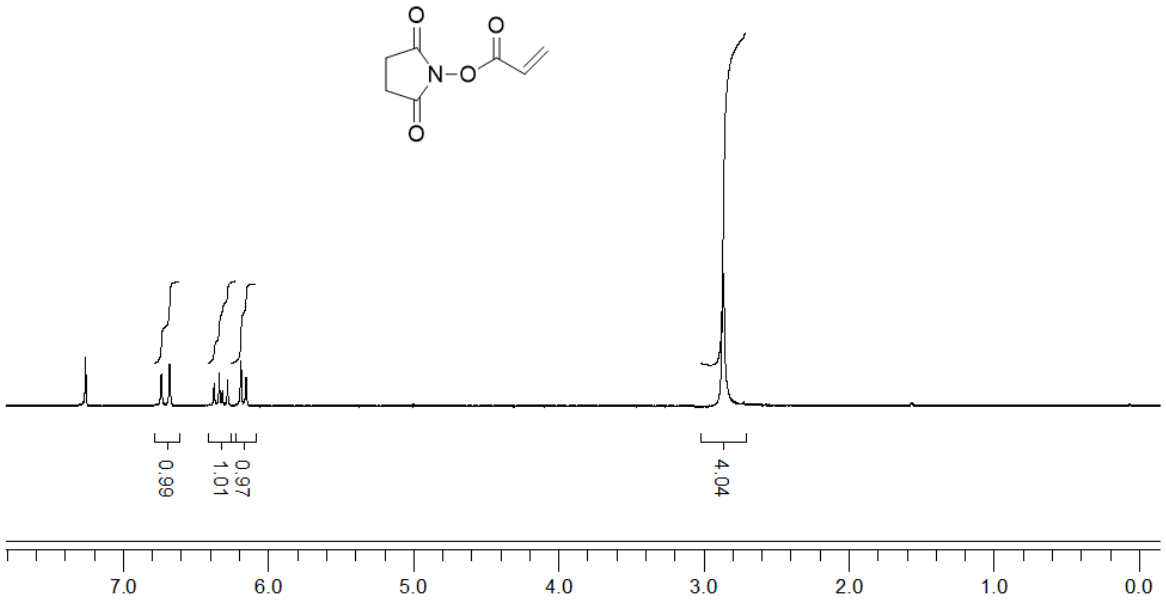

A1.15 PEO-*b*-PDEAm$_{41}$-*b*-PDBAm$_{12}$* triblock copolymers

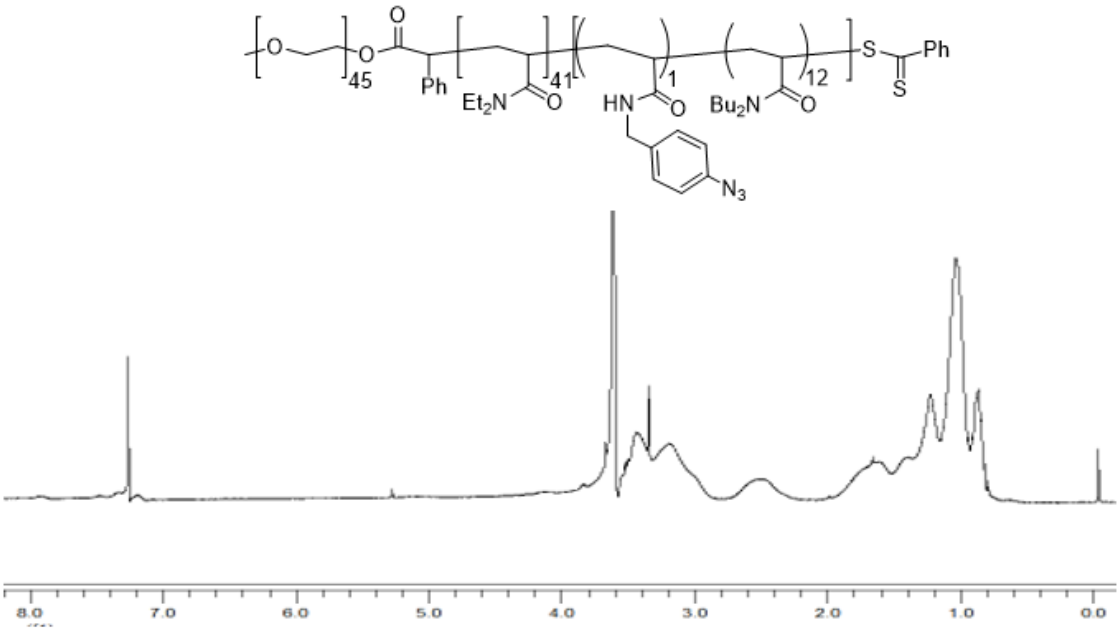

A2. Selected DLS raw data from Malvern Zetasizer NanoZS instrument

A2.1 DLS raw data of one measurement of PEO_{45}-*b*-$PDEAm_{41}$-*b*-$PDBAm_{12}$ in water at 25 °C.

Z-Average (nm):	25.57964	Derived Count Rate (kcps):	4960.94064799...
Standard Deviation:	0	Standard Deviation:	0
%Std Deviation:	0	%Std Deviation:	0
Variance:	0	Variance:	0

Size d.nm	Mean Intensity Percent	Std Dev Intensity Percent
0.4000	0.0	
0.4632	0.0	
0.5365	0.0	
0.6213	0.0	
0.7195	0.0	
0.8332	0.0	
0.9649	0.0	
1.117	0.0	
1.294	0.0	
1.499	0.0	
1.736	0.0	
2.010	0.0	
2.328	0.0	
2.696	0.0	
3.122	0.0	
3.615	0.0	
4.187	0.0	
4.849	0.0	

Size d.nm	Mean Intensity Percent	Std Dev Intensity Percent
5.615	0.0	
6.503	0.0	
7.531	0.0	
8.721	0.0	
10.10	0.0	
11.70	0.0	
13.54	1.9	
15.69	6.0	
18.17	10.7	
21.04	14.6	
24.36	16.5	
28.21	16.1	
32.67	13.7	
37.84	10.0	
43.82	6.0	
50.75	2.7	
58.77	0.7	
68.06	0.0	

Size d.nm	Mean Intensity Percent	Std Dev Intensity Percent
78.82	0.0	
91.28	0.0	
105.7	0.0	
122.4	0.0	
141.8	0.0	
164.2	0.0	
190.1	0.0	
220.2	0.0	
255.0	0.0	
295.3	0.0	
342.0	0.0	
396.1	0.0	
458.7	0.0	
531.2	0.0	
615.1	0.0	
712.4	0.0	
825.0	0.0	
955.4	0.0	

Size d.nm	Mean Intensity Percent	Std Dev Intensity Percent
1106	0.0	
1281	0.0	
1484	0.0	
1718	0.0	
1990	0.0	
2305	0.0	
2669	0.0	
3091	0.0	
3580	0.1	
4145	0.2	
4801	0.3	
5560	0.4	
6439	0.0	
7456	0.0	
8635	0.0	
1.000e4	0.0	

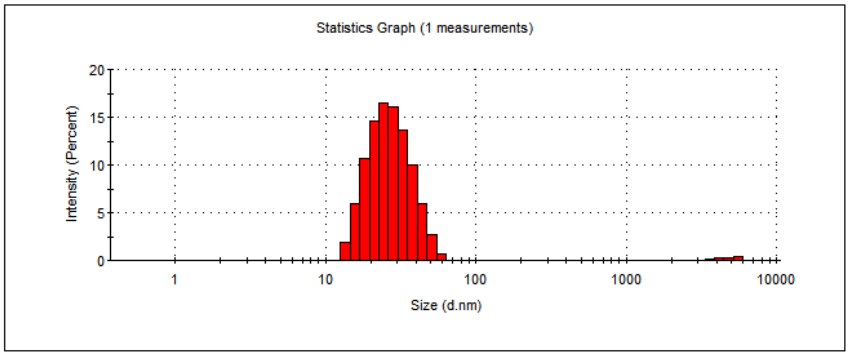

A2.2 DLS raw data of 3 measurements of PEO_{45}-*b*-$PDEAm_{89}$-*b*-$PDBAm_{109}$ in water at 25 °C

Z-Average (nm):	123.3047	**Derived Count Rate (kcps):**	12104.5727271...
Standard Deviation:	1.48324	**Standard Deviation:**	418.006275465...
%Std Deviation:	1.202906	**%Std Deviation:**	3.45329227959...
Variance:	2.2	**Variance:**	174729.246328...

Size d.nm	Mean Intensity Percent	Std Dev Intensity Percent
0.4000	0.0	0.0
0.4632	0.0	0.0
0.5365	0.0	0.0
0.6213	0.0	0.0
0.7195	0.0	0.0
0.8332	0.0	0.0
0.9649	0.0	0.0
1.117	0.0	0.0
1.294	0.0	0.0
1.499	0.0	0.0
1.736	0.0	0.0
2.010	0.0	0.0
2.328	0.0	0.0
2.696	0.0	0.0
3.122	0.0	0.0
3.615	0.0	0.0
4.187	0.0	0.0
4.849	0.0	0.0

Size d.nm	Mean Intensity Percent	Std Dev Intensity Percent
5.615	0.0	0.0
6.503	0.0	0.0
7.531	0.0	0.0
8.721	0.0	0.0
10.10	0.0	0.0
11.70	0.0	0.0
13.54	0.0	0.0
15.69	0.0	0.0
18.17	0.0	0.0
21.04	0.0	0.0
24.36	0.0	0.0
28.21	0.0	0.0
32.67	0.0	0.0
37.84	0.0	0.0
43.82	0.0	0.0
50.75	0.1	0.1
58.77	0.6	0.6
68.06	2.9	0.9

Size d.nm	Mean Intensity Percent	Std Dev Intensity Percent
78.82	6.8	0.6
91.28	11.1	0.5
105.7	14.5	1.1
122.4	16.2	1.3
141.8	15.7	1.1
164.2	13.3	0.6
190.1	9.7	0.4
220.2	5.8	0.8
255.0	2.6	0.8
295.3	0.7	0.5
342.0	0.0	0.1
396.1	0.0	0.0
458.7	0.0	0.0
531.2	0.0	0.0
615.1	0.0	0.0
712.4	0.0	0.0
825.0	0.0	0.0
955.4	0.0	0.0

Size d.nm	Mean Intensity Percent	Std Dev Intensity Percent
1106	0.0	0.0
1281	0.0	0.0
1484	0.0	0.0
1718	0.0	0.0
1990	0.0	0.0
2305	0.0	0.0
2669	0.0	0.0
3091	0.0	0.0
3580	0.0	0.0
4145	0.0	0.0
4801	0.0	0.0
5560	0.0	0.0
6439	0.0	0.0
7456	0.0	0.0
8635	0.0	0.0
1.000e4	0.0	0.0

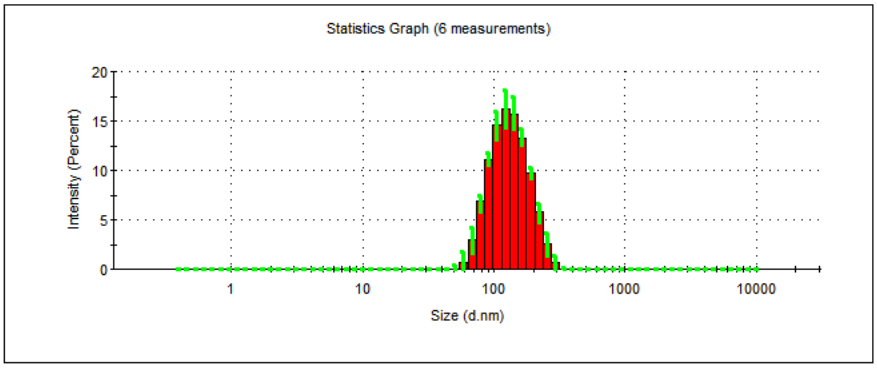

A3. Selected unprocessed TEM images

A3.1 PEO_{45}-$PDEAm_{41}$-$PDBAm_{12}$ in water at 25 °C

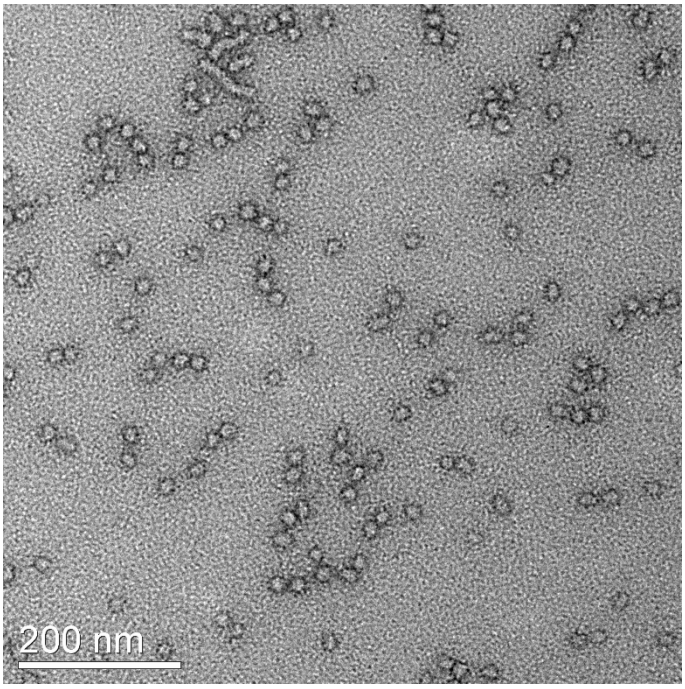

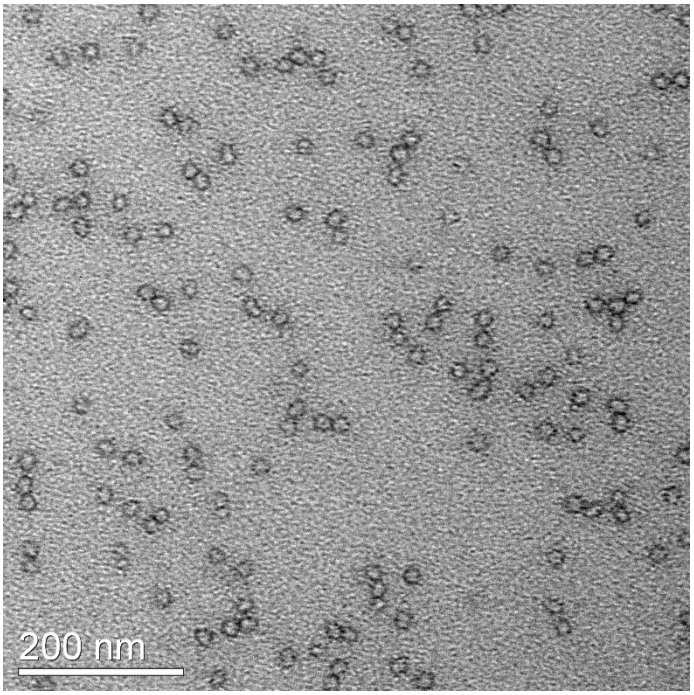

A3.2 PEO_{45}-$PDEAm_{41}$-$PDBAm_{16}$ in water at 25 °C

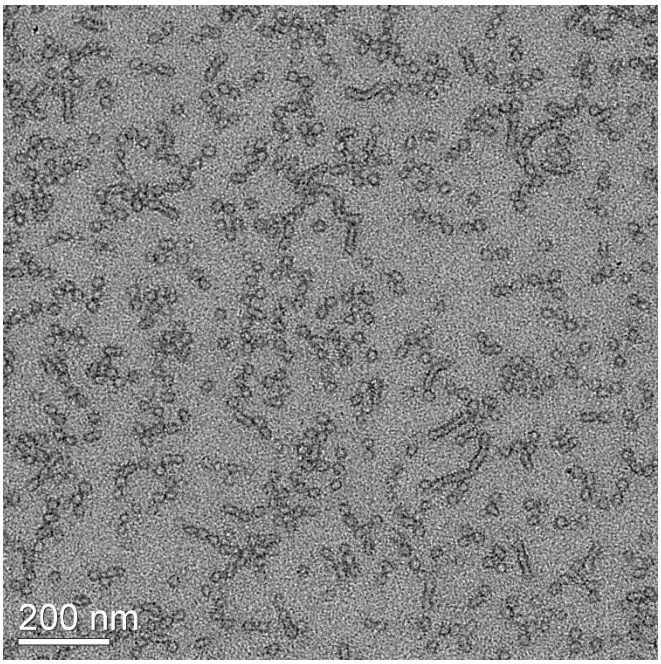

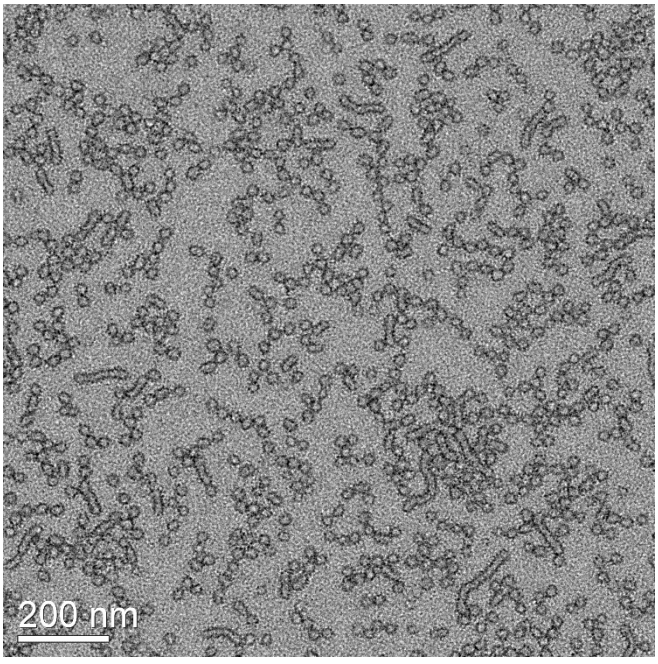

A3.3 PEO_{45}-$PDEAm_{41}$-$PDBA_{22}$ in water at 25 °C

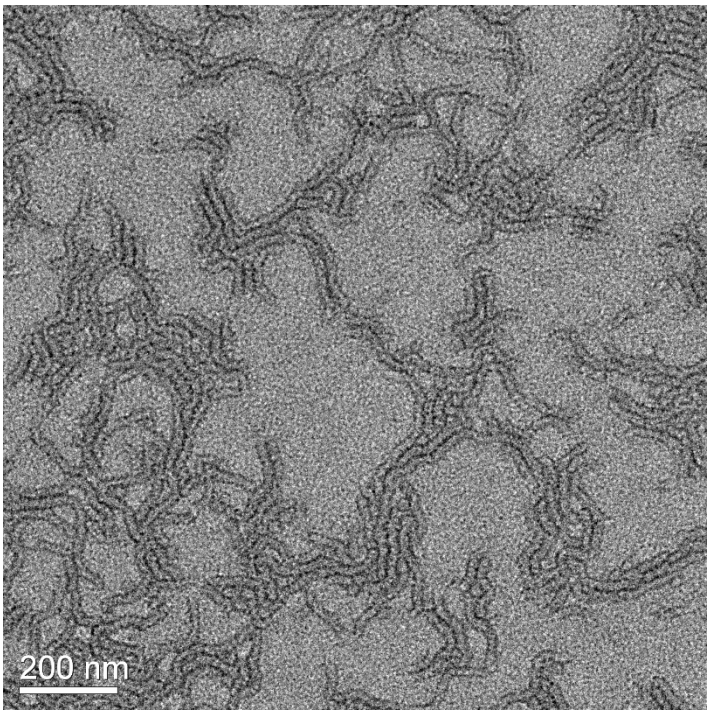

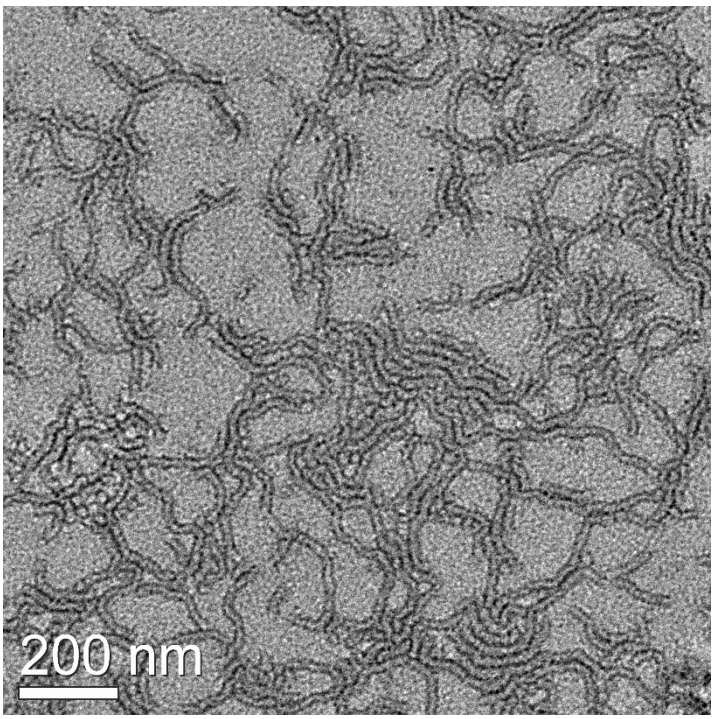

A3.4 PEO_{45}-$PDEAm_{41}$-$PDBAm_{50}$ in water at 25 °C

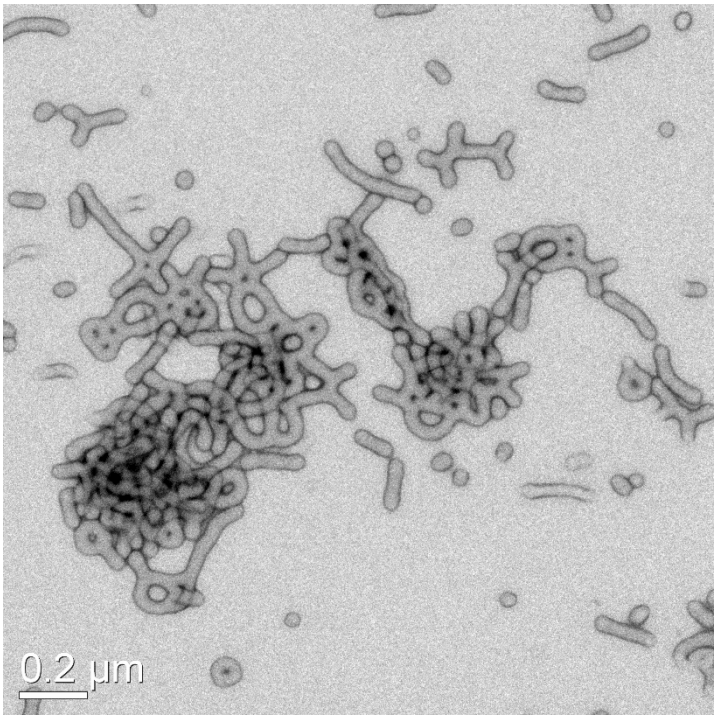

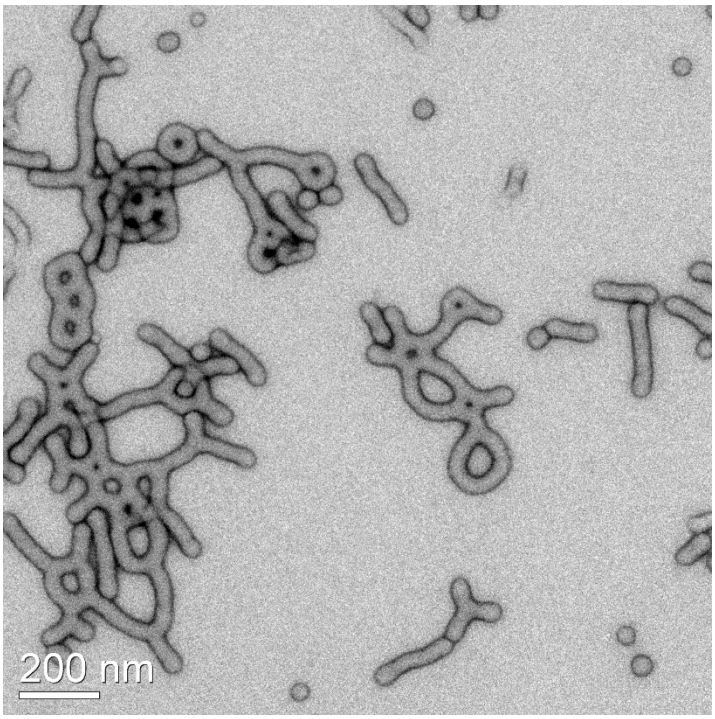

A3.5 PEO_{45}-$PDEAm_{41}$-$PDBAm_{92}$ in water at 25 °C

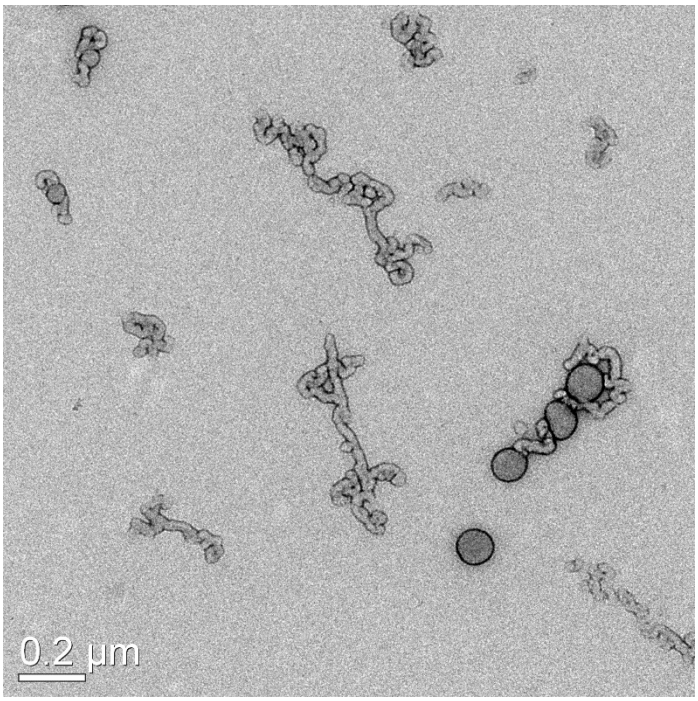

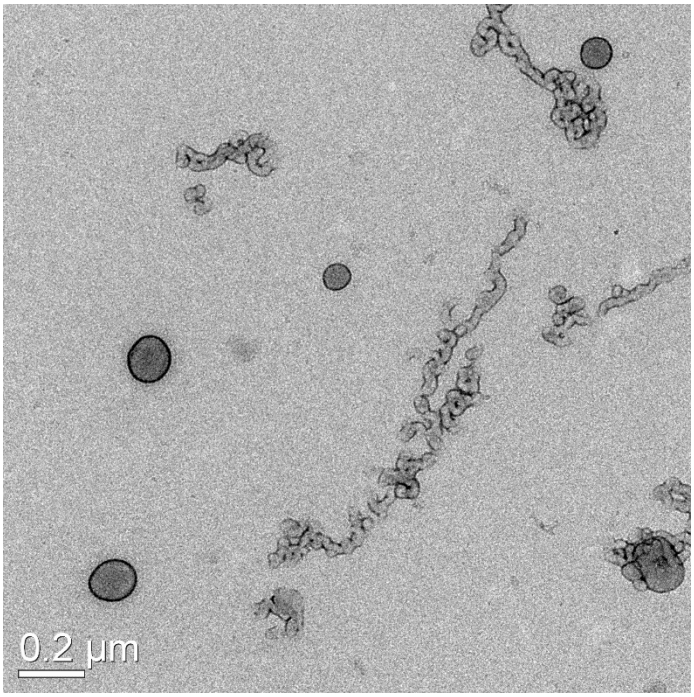

A3.6 PEO_{45}-$PDEAm_{41}$-$PDBAm_{176}$ in water at 25 °C

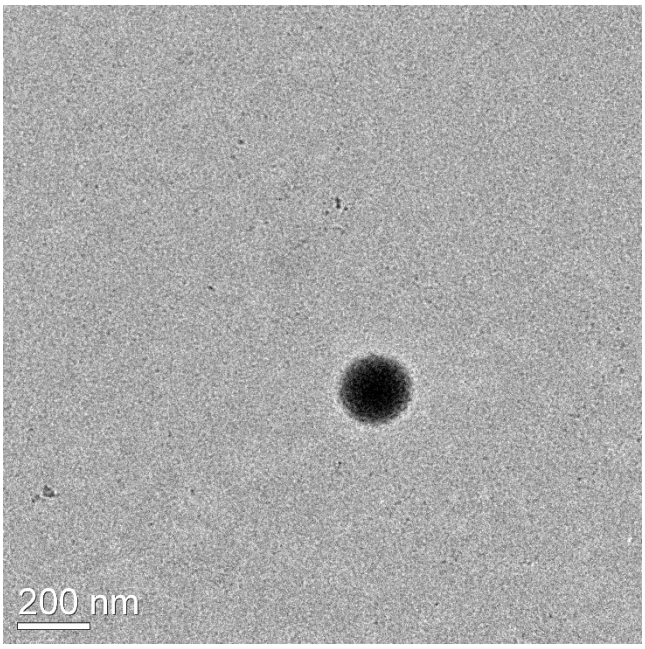

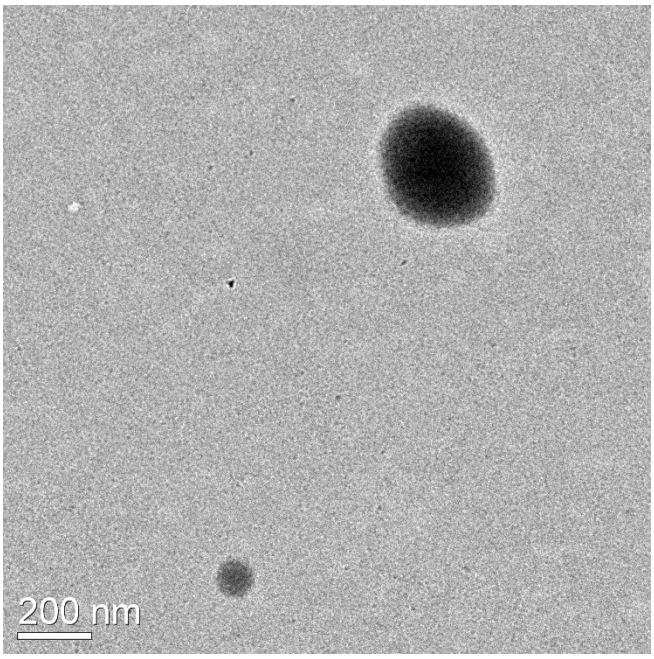

A3.7 PEO_{45}-$PDEAm_{89}$-$PDBAm_{12}$ in water at 25 °C

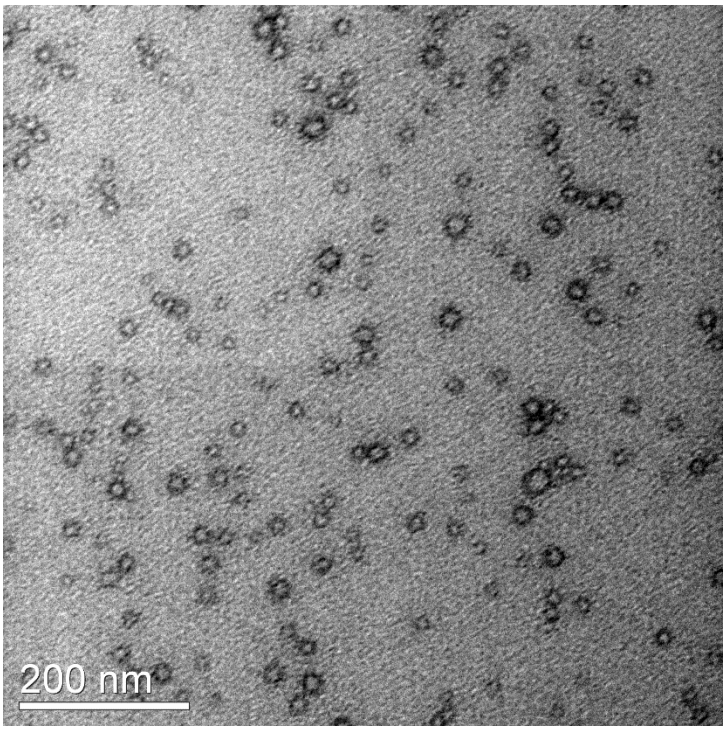

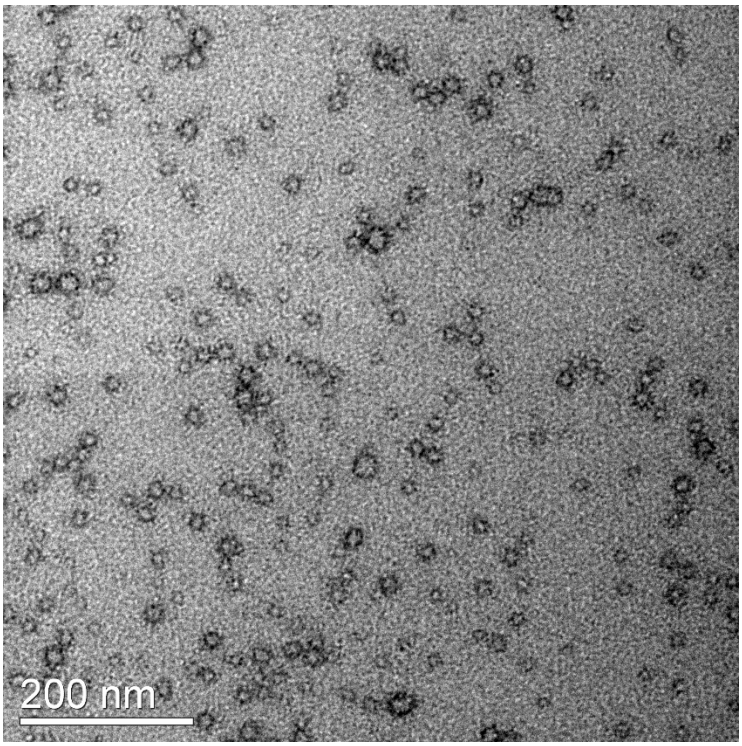

A3.8 PEO_{45}-$PDEAm_{89}$-$PDBAm_{24}$ in water at 25 °C

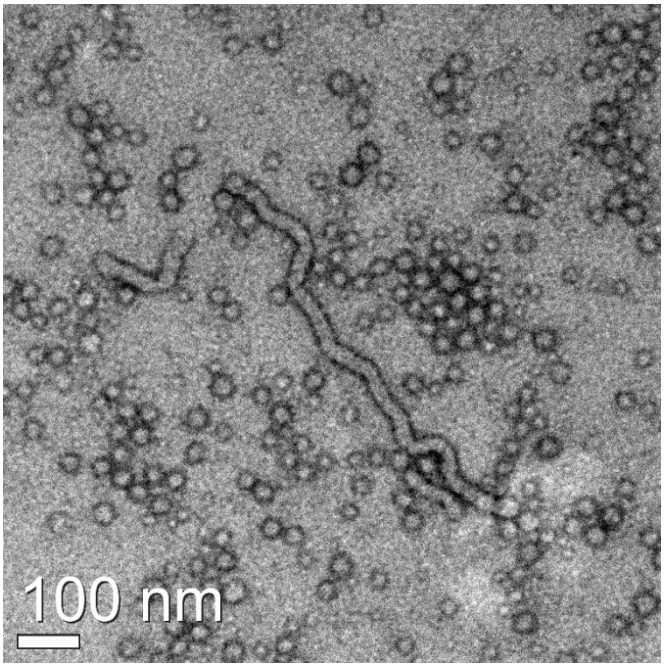

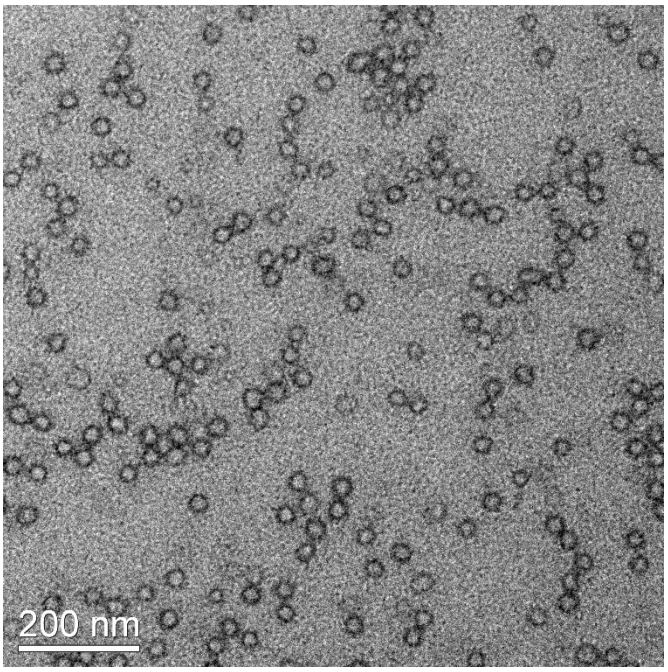

A3.9 PEO_{45}-$PDEAm_{89}$-$PDBAm_{32}$ in water at 25 °C

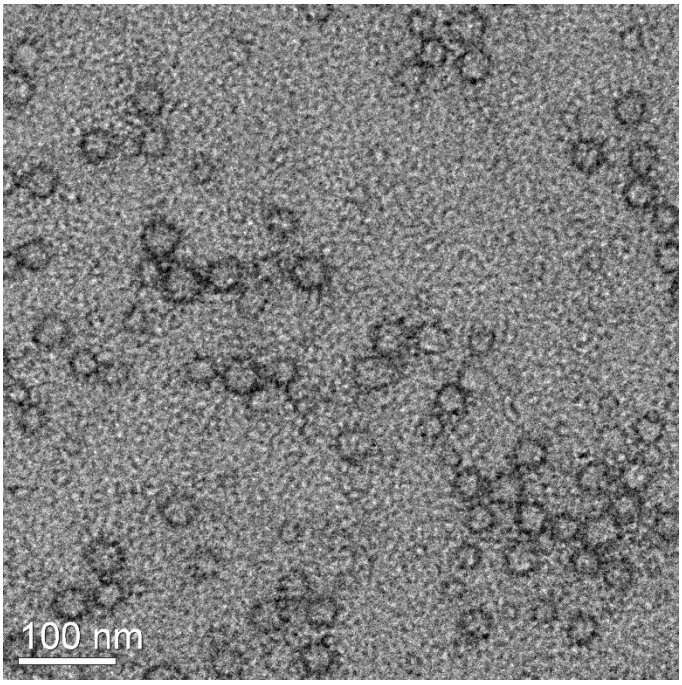

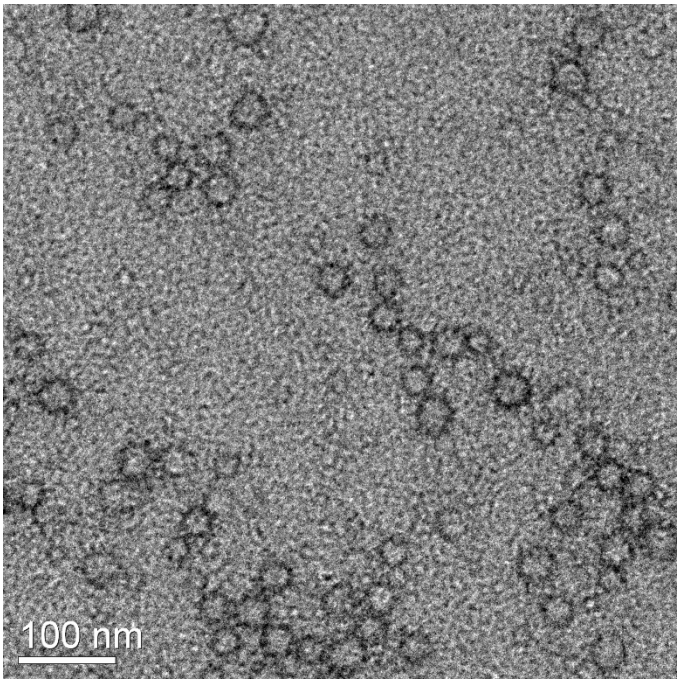

A3.10 PEO_{45}-$PDEAm_{89}$-$PDBAm_{37}$ in water at 25 °C

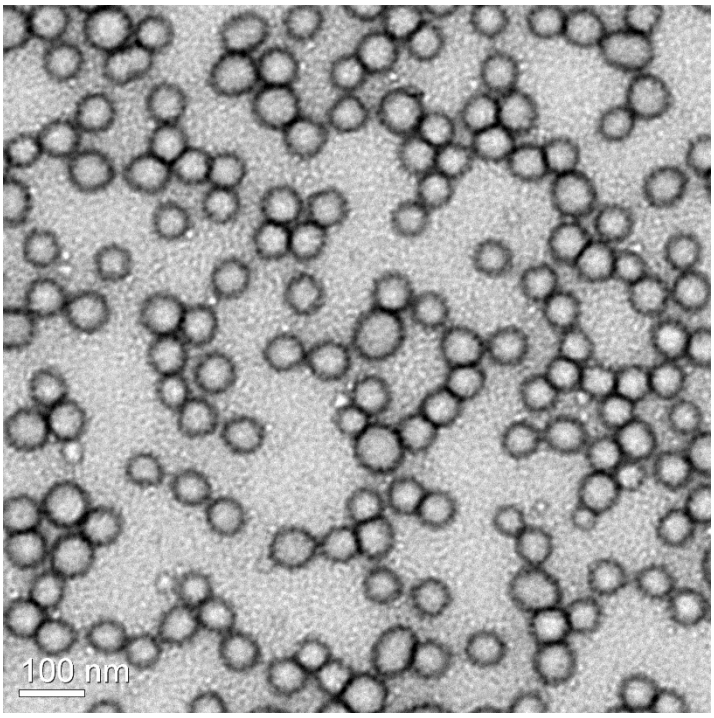

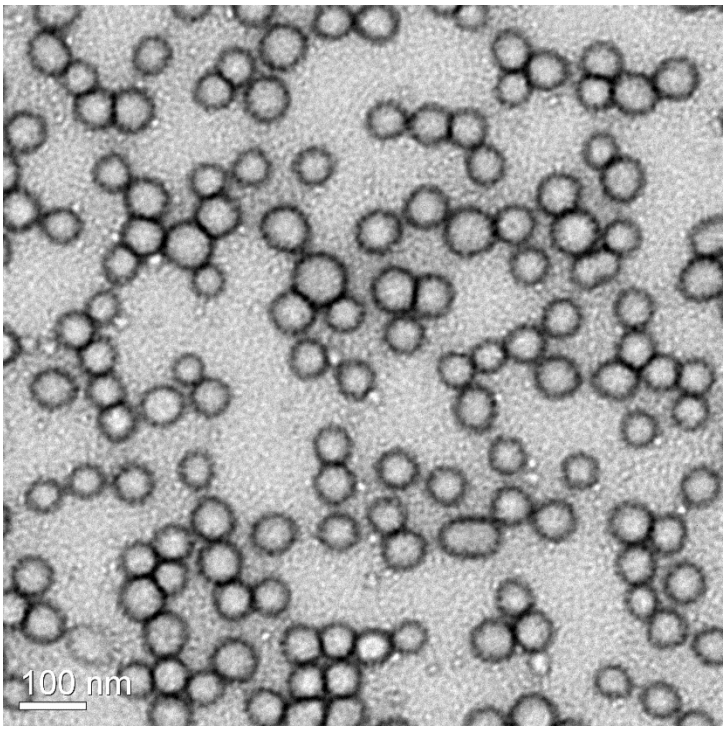

A3.11 PEO_{45}-$PDEAm_{89}$-$PDBAm_{74}$ in water at 25 °C

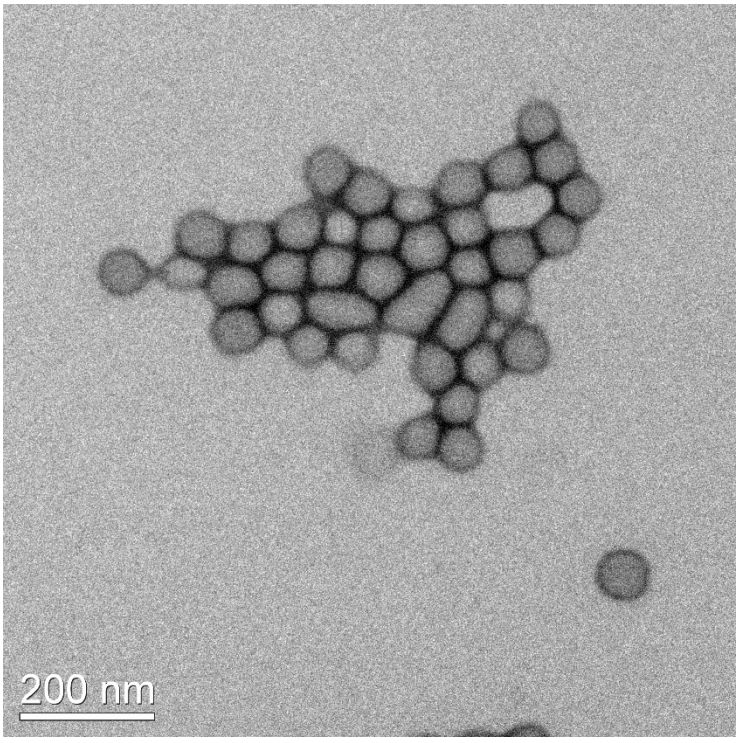

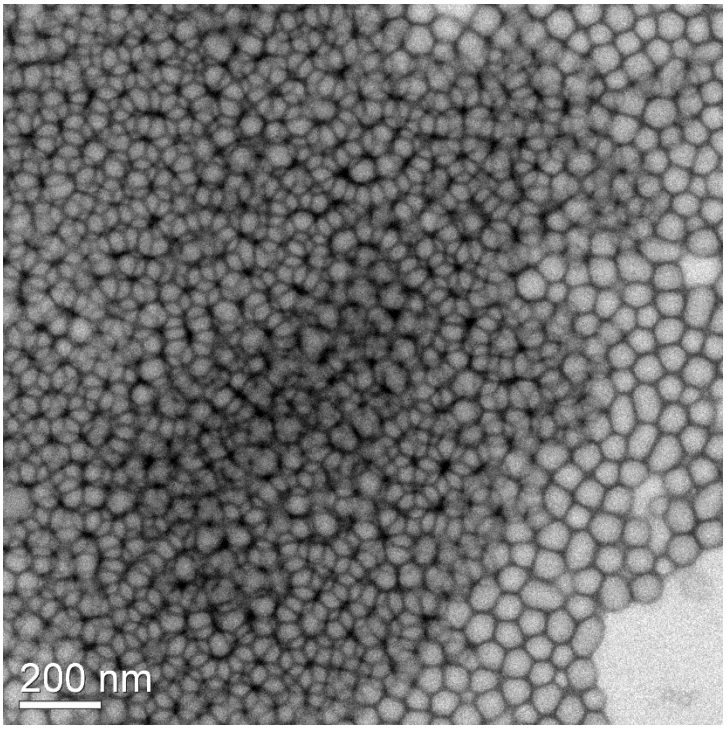

A3.12 PEO_{45}-$PDEAm_{89}$-$PDBAm_{109}$ in water at 25 °C

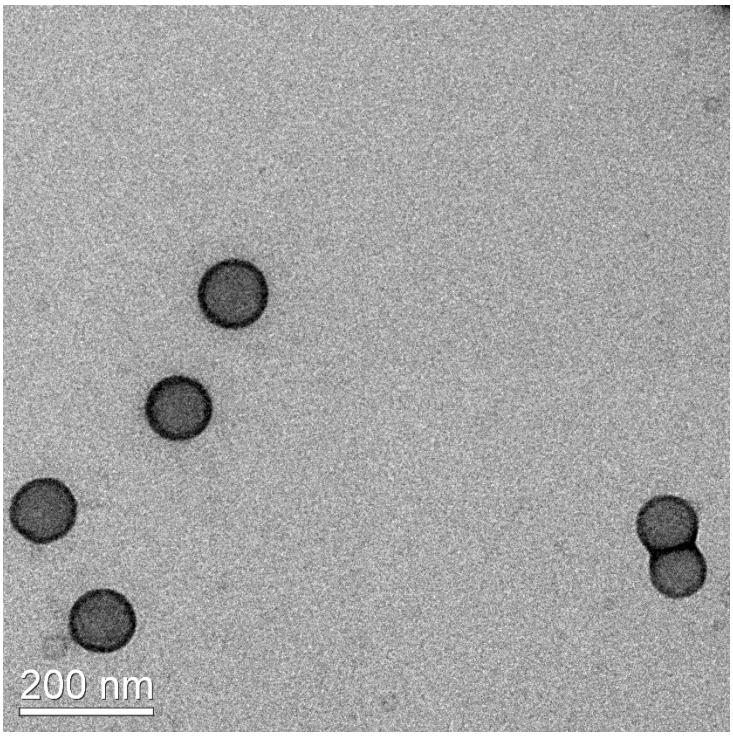

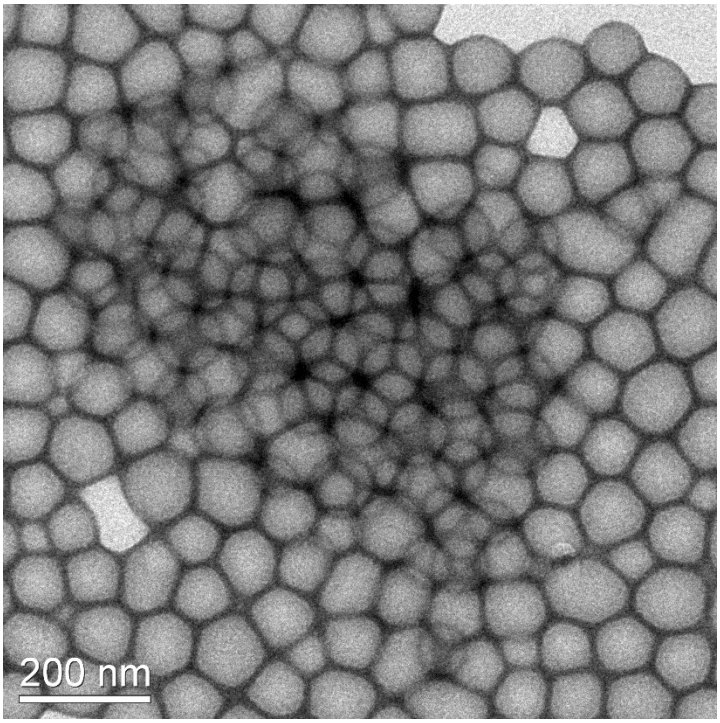

A3.13 PEO_{45}-$PDEAm_{89}$-$PDBAm_{173}$ in water at 25 °C

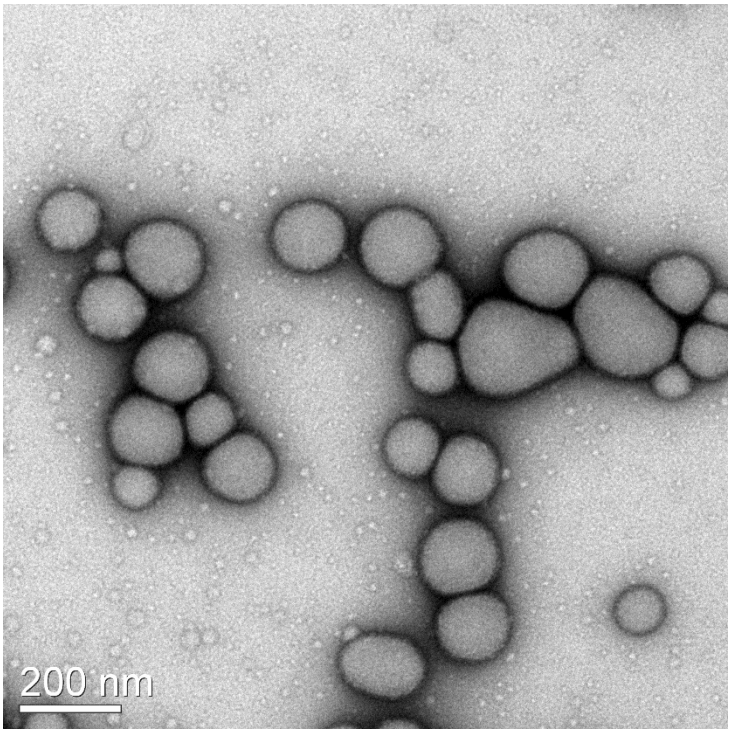

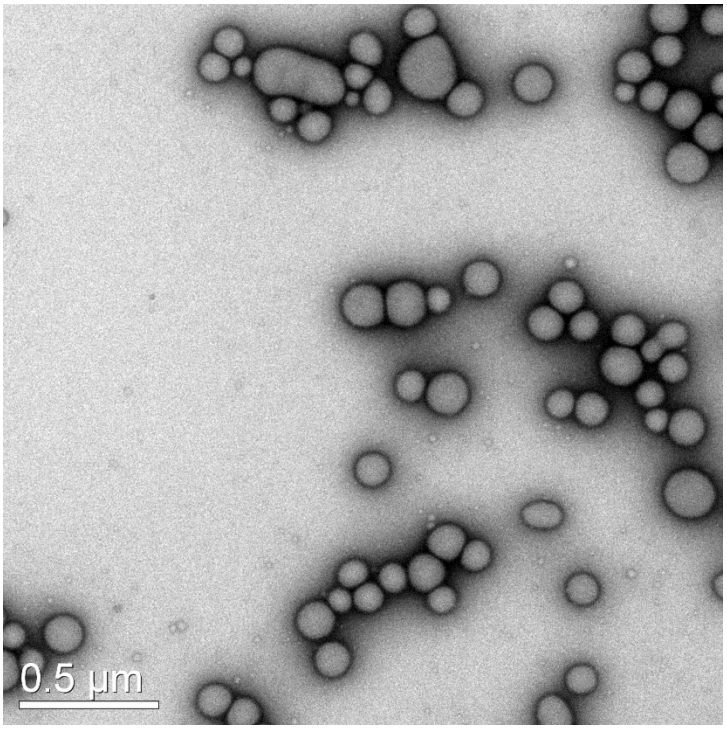

A3.14 PEO_{45}-$PDEAm_{89}$-$PDBAm_{296}$ in water at 25 °C

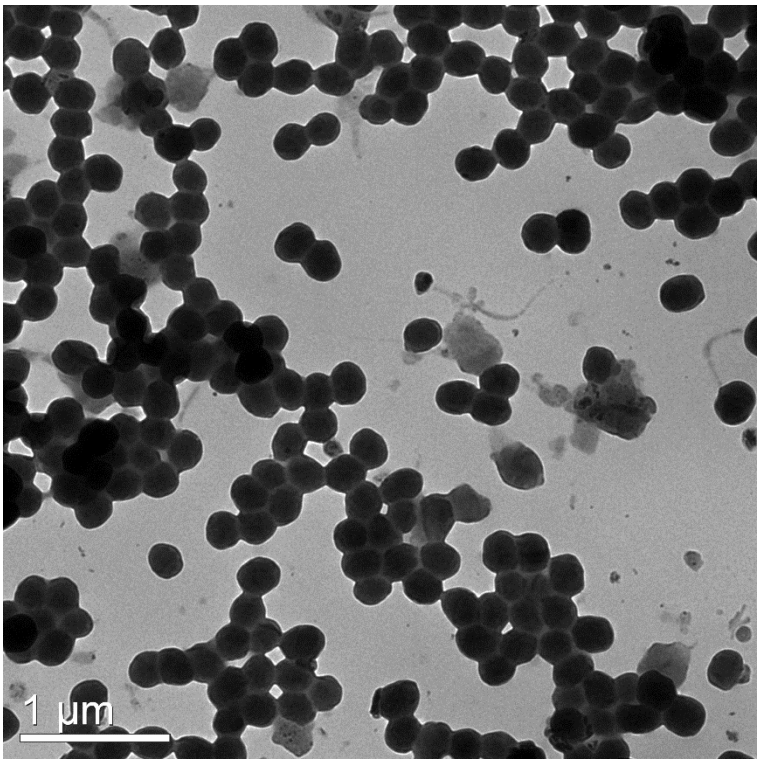

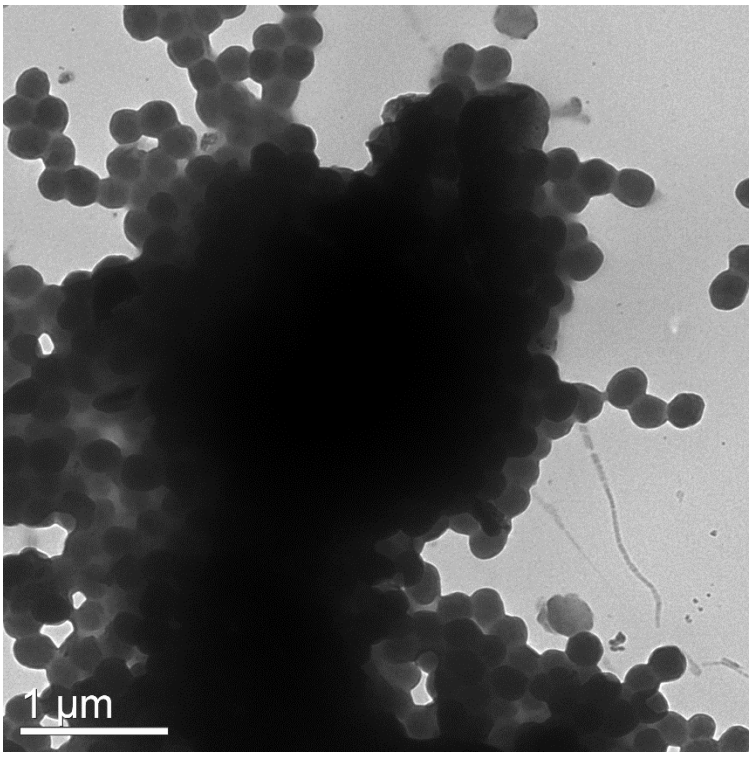

A3.15 PEO_{45}-$PDEAm_{57}$-$PDBAm_{26}$ in water at 25 °C

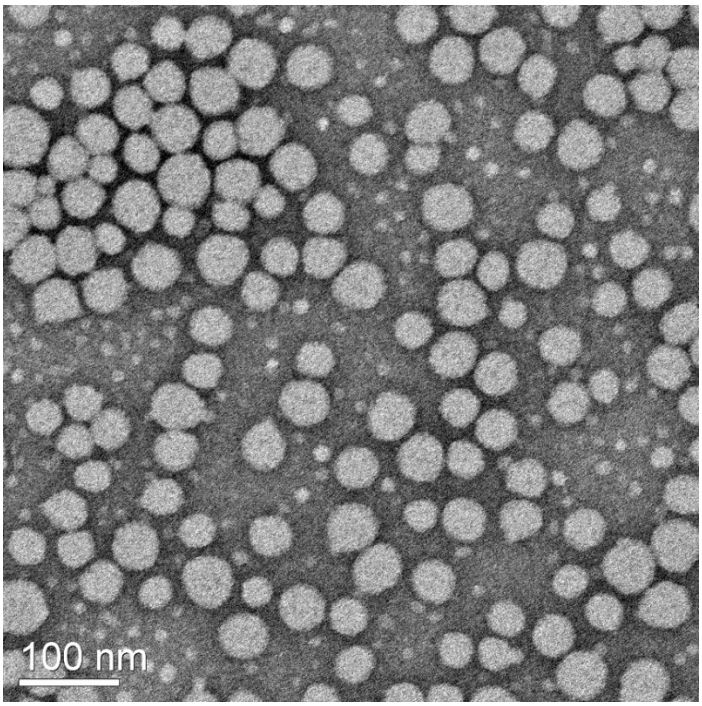

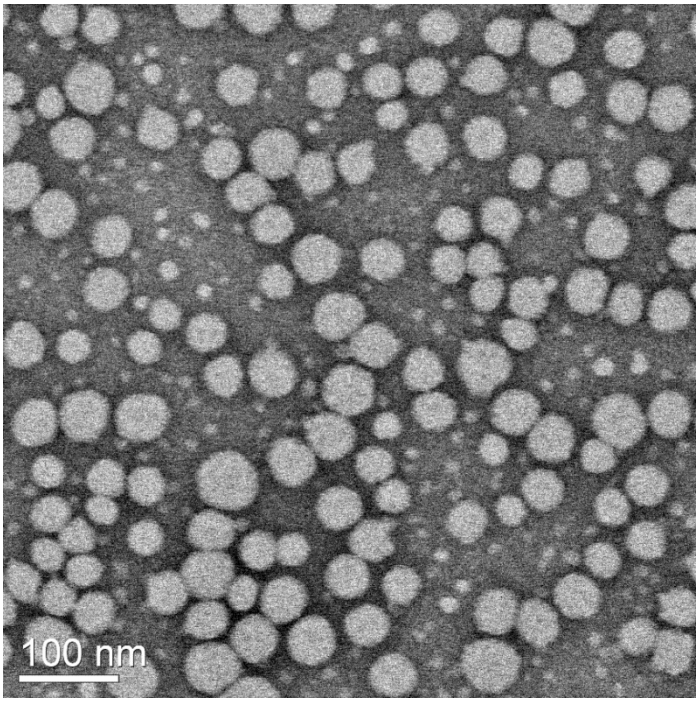

A3.16 PEO_{45}-$PDEAm_{57}$- $PDBAm_{52}$ in water at 25 °C

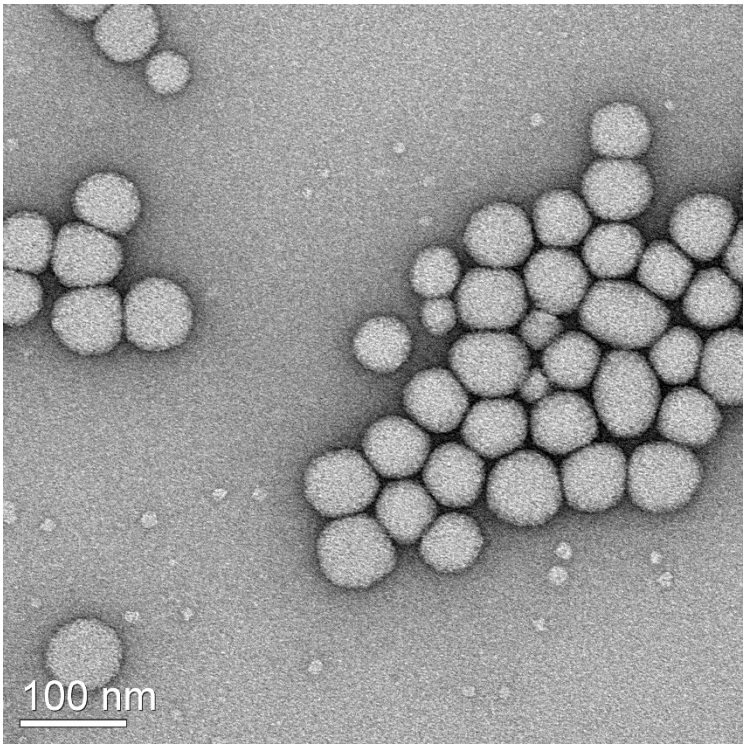

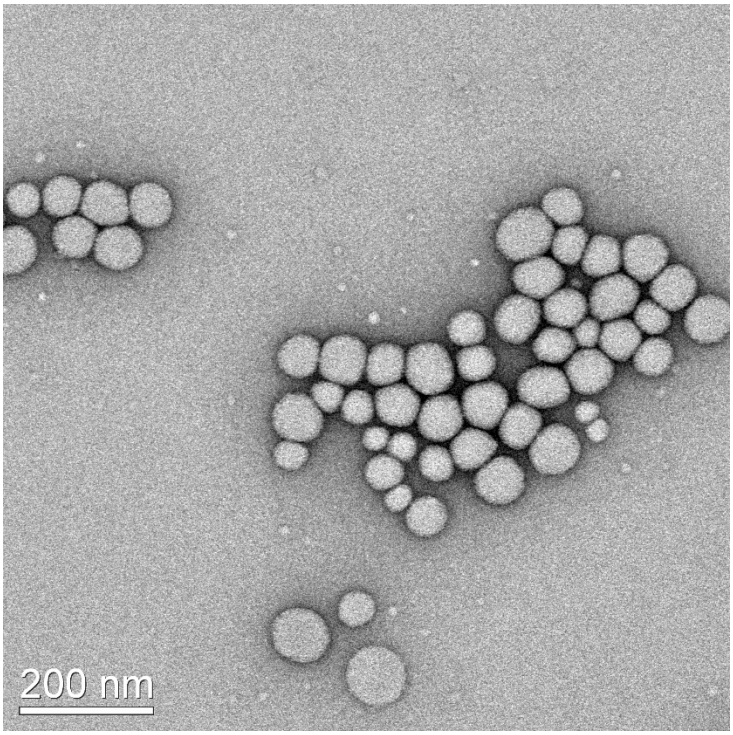

A3.17 PEO_{45}-$PDEAm_{89}$-$PDBAm_{12}$ in water after heating 10 min at 55 °C

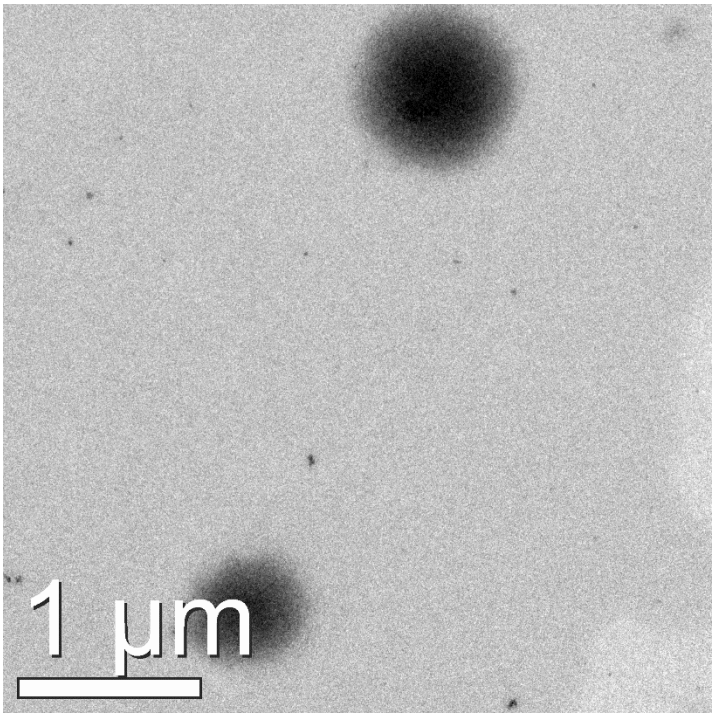

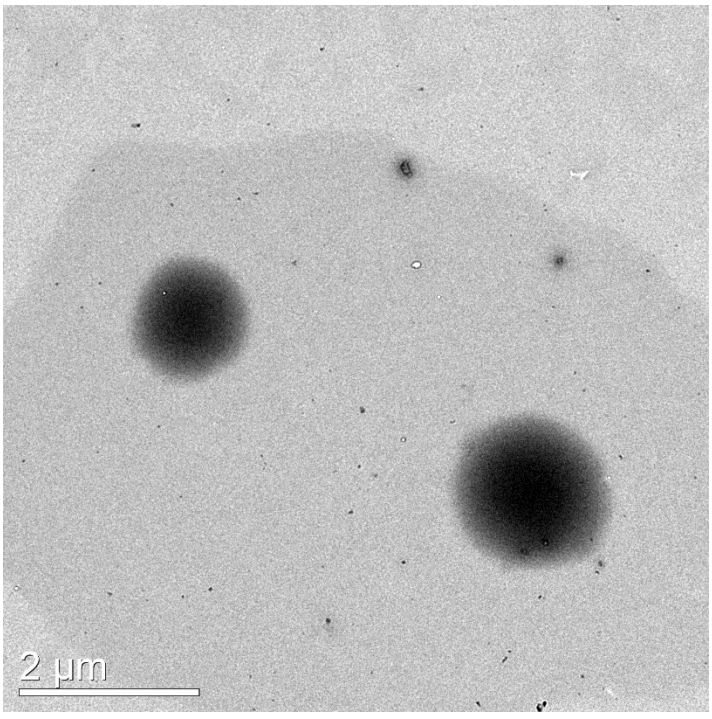

A3.18 PEO_{45}-$PDEAm_{41}$-$PDBAm_{12}$ in water after heating 10 min at 55 °C

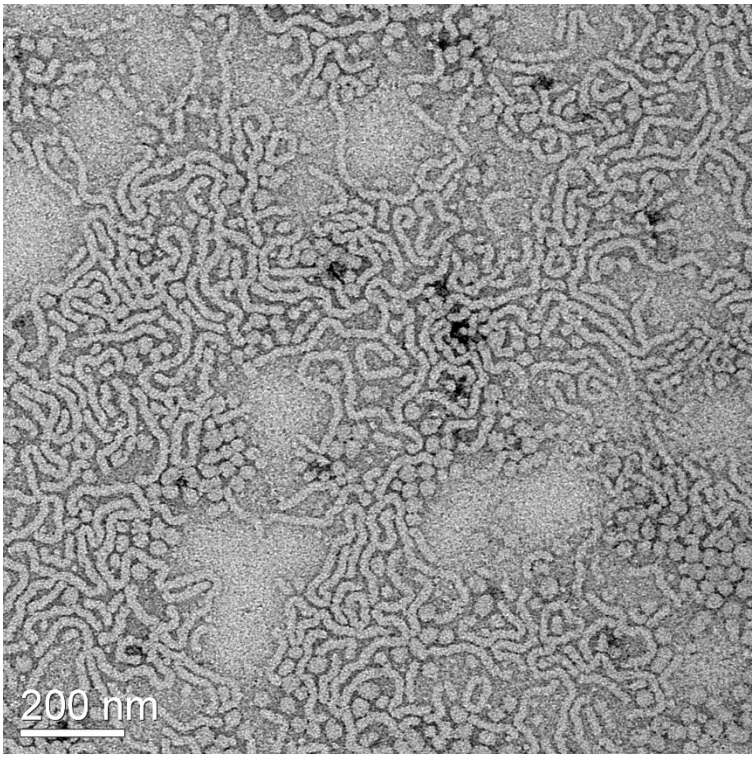

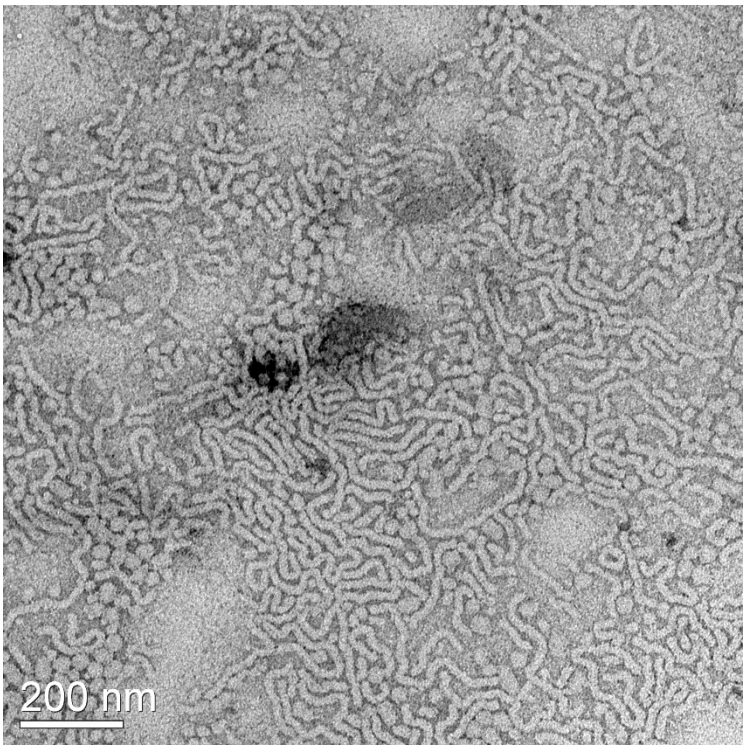

A3.19 PEO_{45}-$PDEAm_{33}$-$PDBAm_6$ in water after heating 10 min at 60 °C.

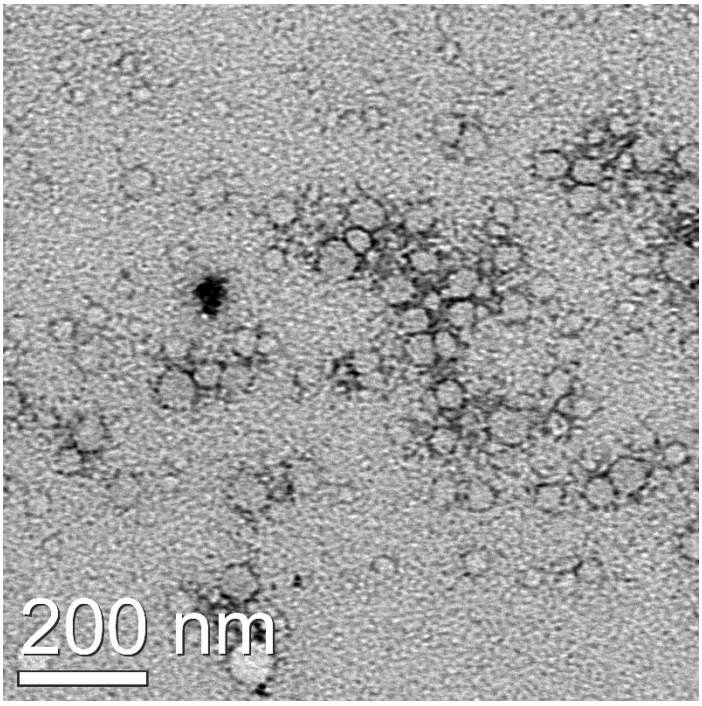

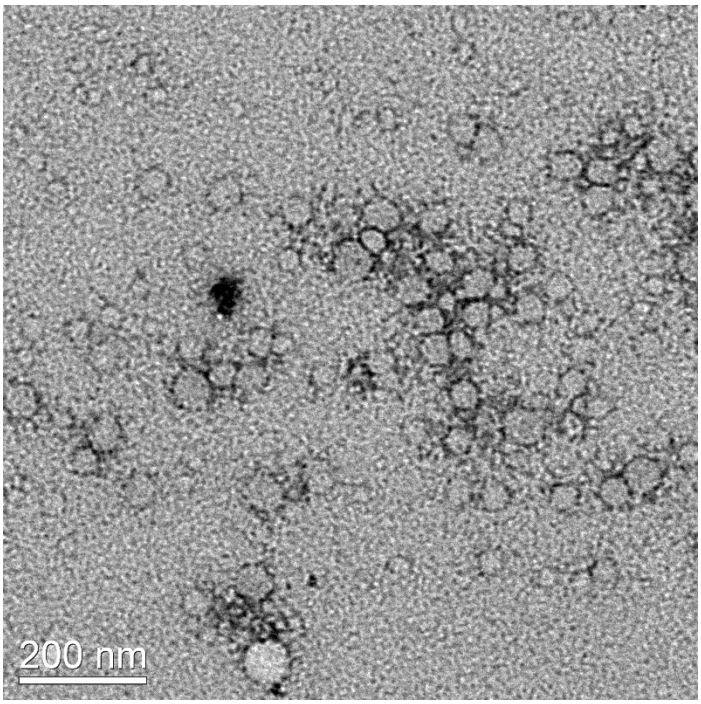

A3.20 PEO_{45}-$PDEAm_{41}$-$PDBAm_{12}$ in water after heating 3 weeks at 55 °C

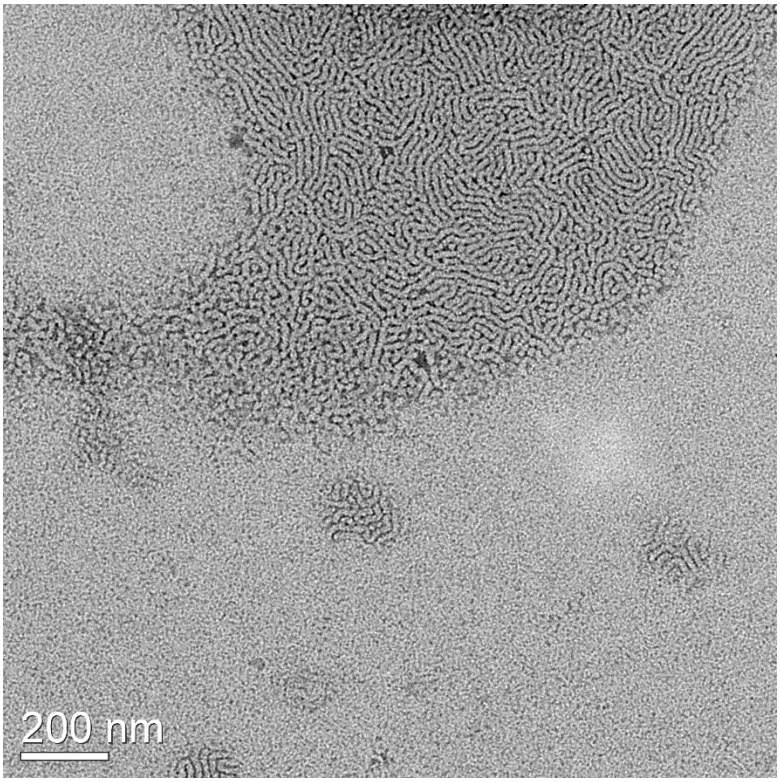

.